

**Ring-width and $\delta^{13}\text{C}$ chronologies from *Thuja occidentalis* L. trees
growing at the northwestern limit of their distribution, central Canada**

By

Robert C.F. Au

A thesis submitted to the
Faculty of Graduate Studies of the University of Manitoba
In Partial Fulfillment of the Requirements for the Degree of

MASTER OF SCIENCE

Department of Biological Sciences

University of Manitoba

Winnipeg, Manitoba, Canada

R3T 2N2

© Robert C.F. Au 2009

Abstract

Stable carbon isotope ratios ($\delta^{13}\text{C}$) in tree-ring cellulose are modified by environmental conditions occurring during carbon fixation. Researchers have however not reached a consensus as to whether extractives, lignin and/or hemicelluloses, all with specific isotopic signatures, should be removed prior to dendroisotopic analysis. The topic of the first paper dealt with the comparison of *Thuja occidentalis* L. wood components and their suitability for subsequent dendroisotopic analyses. It was recommended that holocellulose be isolated since an alpha-cellulose yield may be too low for subsequent mass spectrometer analysis, especially when narrow rings are encountered and multiple stable isotope analyses are to be performed per sample.

The second paper investigated the associations between the ring-width and $\delta^{13}\text{C}$ chronologies with climate variables. The $\delta^{13}\text{C}$ chronology spanned from 1650 to 2006 A.D. and incorporated dead and living *T. occidentalis* trees selected from two sites in central Manitoba, Canada. Compared to the $\delta^{13}\text{C}$ values, ring width was more often associated with climate conditions in the year prior to ring formation. However, moisture stress was limiting for both radial growth and carbon assimilation. During the year of ring-formation, ring width was associated with spring and early summer conditions whereas, $\delta^{13}\text{C}$ was more indicative of overall summer conditions. Nonetheless, each of ring width and $\delta^{13}\text{C}$ contained individualistic climate information which could be used in tandem for long-term climate reconstruction.

Acknowledgements

Many people have contributed to this project in various ways throughout its course. I thank Dr. Jacques Tardif, my supervisor, for his guidance and pertinent comments which have developed my appreciation for science. Special thanks go to France Conciatori for her invaluable experience in Dendrochronology and to Derrick Ko Heinrichs for his great help in the field. Valuable suggestions came from my committee members, Drs. Bill Buhay and Sylvie Renault. Dr. Martin Girardin was especially kind in calculating the Canadian Drought Code and for useful discussions on statistical techniques. In addition, I have benefited from the presence and assistance of numerous colleagues which have helped maintain a lively atmosphere in and around our workspace. Thanks are also due to the laboratory assistants, Justin Waito, Stephen Gietz and Anton Zavialov. Useful advice came from Tim Davis, Brock Epp, Candice Grant, Susanne Kames and Jeff Renton. I thank Dr. Chris Eastoe of the Environmental Isotope Laboratory, University of Arizona, for his expertise in operating the mass spectrometer. The Mettler Toledo AX26 electrical balance was generously provided by the Department of Geography, University of Winnipeg. Kind support was provided by the biology technicians at the University of Winnipeg, notably, Brenda Van Dekerkhove, Tara Powell and Susan Wiste. Our biology secretary, Pamela Delorme, was also very helpful. I thank Dr. Steven W. Leavitt of the Laboratory of Tree-Ring Research, University of Arizona, and Dr. Benjamin Harlow of the Stable Isotope Core Laboratory, Washington State University, for several useful discussions regarding chemical pretreatment. I am indebted to my parents for their support in my interest of biology and eventually in the field of Dendrochronology. Financial assistance was provided by the Canada Research Chairs

Program, the Faculty of Science Graduate Studentship from the University of Manitoba, the National Sciences and Engineering Research Council of Canada and the University of Winnipeg.

Dedication

This work is dedicated to the memory of Karl Au, my father, who passed away in December 2006.

Table of Contents

Abstract.....	ii
Acknowledgements.....	iii
Dedication.....	v
List of Figures.....	ix
List of Tables.....	xii
List of Appendices.....	xiv
1.0 General Introduction.....	1
1.1. Introduction.....	1
1.1.1. Stable isotopes.....	1
1.1.2. Stable isotopes in environmental studies.....	3
1.1.3. Stable isotopes in tree-ring studies.....	4
1.1.4. Stable carbon isotope discrimination.....	6
1.1.5. Stomatal conductance and photosynthetic rate as limiting factors.....	8
1.1.6. Tree-ring $\delta^{13}\text{C}$ values and water-use efficiency.....	12
1.1.7. Dendroisotopic studies in the North American Boreal Forest.....	15
1.1.8. Ecology of <i>Thuja occidentalis</i> L.....	17
1.1.9. Selecting a wood component to analyze in tree rings.....	21
1.1.10. Objectives and hypotheses.....	22
2.0 Chemical pretreatment of <i>Thuja occidentalis</i> tree rings: implications for dendroisotopic studies.....	24
2.1. Abstract.....	24
2.2. Introduction.....	25
2.3. Materials and Methods.....	29
2.3.1. Study area.....	29
2.3.2. Sample preparation.....	29
2.3.3. Chemical extraction.....	30
2.3.4. Statistical analysis.....	32
2.4. Results/Discussion.....	32
2.4.1. Enriched <i>Thuja occidentalis</i> tree-ring cellulose.....	32
2.4.2. Comparison of wood tissue fractions.....	34

2.4.3. Carbon isotopic change from extractive, lignin and hemicellulose removal	35
2.5. Conclusion	39
2.6. Acknowledgments	40
2.7. References	41
3.0 Ring-width and $\delta^{13}\text{C}$ chronologies from <i>Thuja occidentalis</i> L. trees as recorders of drought	52
3.1. Abstract	52
3.2. Introduction	54
3.3. Methods	58
3.3.1. Study area	58
3.3.2. Site selection	61
3.3.3. $\delta^{13}\text{C}$ chronology development	63
3.3.3.1. Sample preparation	63
3.3.3.2. Chemical extraction	65
3.3.3.3. $\delta^{13}\text{C}$ standard & residual chronologies	67
3.3.3.4. $\delta^{13}\text{C}$ discrimination	68
3.3.4. Ring-width chronology development	70
3.3.5. Temporal stability of the <i>Thuja occidentalis</i> ring width and $\delta^{13}\text{C}$ relationship	71
3.3.6. Dendroclimatic analysis	73
3.3.7. <i>Thuja occidentalis</i> cross-species comparisons	76
3.4. Results	77
3.4.1. <i>Thuja occidentalis</i> ring-width and $\delta^{13}\text{C}$ site statistics	77
3.4.2. Cross-correlations between <i>Thuja occidentalis</i> ring-width and $\delta^{13}\text{C}$ series	78
3.4.3. Low frequency trends in $\delta^{13}\text{C}$ series	78
3.4.4. Signal strength in <i>Thuja occidentalis</i> ring-width and $\delta^{13}\text{C}$ residual chronologies	80
3.4.5. Low-frequency trends in regional chronologies	81
3.4.6. Temporal stability of <i>Thuja occidentalis</i> ring-width and $\delta^{13}\text{C}$ residual chronologies	82

3.4.7. <i>Thuja occidentalis</i> ring-width association with climate	84
3.4.8. <i>Thuja occidentalis</i> $\delta^{13}\text{C}$ association with climate	85
3.4.9. Temporal stability of ring width and $\delta^{13}\text{C}$ – climate associations	86
3.4.10. Comparing <i>Thuja occidentalis</i> $\delta^{13}\text{C}$ with previous $\delta^{13}\text{C}$ chronologies from Manitoba	88
3.5. Discussion	89
3.5.1. Ring width and $\delta^{13}\text{C}$ association/ common signal	89
3.5.2. Site differences in soil moisture influence the climatic information contained in <i>Thuja occidentalis</i> $\delta^{13}\text{C}$	91
3.5.3. Ring-width and $\delta^{13}\text{C}$ sensitivity to drought periods on the Boreal Plains ..	94
3.5.4. <i>Thuja occidentalis</i> ring width and $\delta^{13}\text{C}$ display individualistic climatic windows	98
3.5.5. Temporal stability of ring width and $\delta^{13}\text{C}$ – climate associations	103
3.5.6. Tree-ring $\delta^{13}\text{C}$ chronologies in Manitoba show different limitations to carbon assimilation	105
3.6. Conclusion	107
3.7. Acknowledgements	109
3.8. References	110
4.0 General Conclusions	149
5.0 Bibliography	152

List of Figures

Figure 2.1. *Thuja occidentalis* decadal whole wood (WW), extractive-free wood (EF), holocellulose (HC) and α -cellulose (AC) samples showing a) % yield (EF, n=24; HC, n=16; AC, n=8), b) % carbon (n=8), and c) $\delta^{13}\text{C}$ values (n=8).

.....49

Figure 2.2. Mean absolute difference (offset) of paired wood components as indicated from paired t-tests. The text above each bar lists the wood fraction(s) theoretically removed between the two wood components. All comparisons were found to be statistically significant ($p \leq 0.001$, n=8); the 95% confidence intervals are also shown.

.....50

Figure 3.1. Map of the study area showing the location of sampling sites -A (red triangle) and -B (red square).

.....130

Figure 3.2. Monthly average temperature and total precipitation for Grand Rapids Hydro from January to December and during the reference period of 1971-2000.

.....131

Figure 3.3. Example of the standardization procedure for *Thuja occidentalis* tree number B-6. a) the carbon isotope series ($\delta^{13}\text{C}$ values) is represented by a thin line and the 60-year cubic spline curve is indicated by the thick line. b) the resultant dimensionless indices after each $\delta^{13}\text{C}$ value was divided by its corresponding value estimated by the spline curve.

.....132

Figure 3.4. Carbon isotope series ($\delta^{13}\text{C}$ values) for the period 1650 to 2006. The live (black lines) and dead (colored lines) *Thuja occidentalis* trees are shown. The decline in atmospheric $\delta^{13}\text{C}$ (scale on right y-axis) since 1850 AD is also superimposed over the lower sub-figure as reported by McCarroll and Loader (2006).

.....133

Figure 3.5. The standard (*left panel*) and residual (*right panel*) *Thuja occidentalis* chronologies for both $\delta^{13}\text{C}$ and ring-width: ab) A-RWL, cd) B-RWL, ef) A- $\delta^{13}\text{C}$, gh) B- $\delta^{13}\text{C}$, ij) AB- $\delta^{13}\text{C}$, kl) AB-RWL and mn) REG-RWL. All chronologies were also smoothed with an 11-year un-weighted moving average (black line) to highlight the low-frequency trends.

.....134

Figure 3.6. *Thuja occidentalis* REG-RWL, $\delta^{13}\text{C}$ discrimination (Δ) and AB- $\delta^{13}\text{C}$ standard chronologies. The regime shift detection (solid red line) for each chronology verified that changes in the mean from one period to another did not emerge from a red noise process.

.....135

Figure 3.7. Principal components analyses (PCA) performed on correlation matrices conducted for the period 1681-2005 (a), five overlapping 100-year periods beginning in 1700 and ending in 1999 (b-f) and for the periods: 1900-1959 (g) and 1960-2005 (h) illustrating the relationships among the seven *T. occidentalis* residual chronologies.

.....136

Figure 3.8. Pearson correlation coefficients between A) PC1, B) REG-RWL, C) PC2 and D) AB- $\delta^{13}\text{C}$ and monthly climate variables from May of the year prior to ring formation (large caps) to September of the year of ring formation (small caps).

.....137

Figure 3.9. Pearson correlation coefficients between REG-RWL (*top panel*) A) during 1900-1959 and B) during 1960-2005 and AB- $\delta^{13}\text{C}$ (*bottom panel*) C) during 1900-1959 and D) 1960-2005 and monthly climate variables from May of the year prior to ring formation (large caps) to September of the year of ring formation (small caps).

.....139

Figure 3.10. First-differenced $\delta^{13}\text{C}$ chronologies of *Thuja occidentalis* (ab- $\delta^{13}\text{C}$), *Picea glauca* (pgl- $\delta^{13}\text{C}$) and *Pinus banksiana* (pba- $\delta^{13}\text{C}$).

.....141

List of Tables

Table 2.1. $\delta^{13}\text{C}$ and % C for each decadal tree segment of whole wood (WW), extractive-free wood (EF), holocellulose (HC) and α -cellulose (AC).	51
Table 3.1. Descriptive statistics for dead and living <i>Thuja occidentalis</i> ring-width (RWL) measurement series.	142
Table 3.2. Descriptive statistics for dead and living <i>Thuja occidentalis</i> $\delta^{13}\text{C}$ series.	143
Table 3.3. Pearson correlation matrix between standardized <i>Thuja occidentalis</i> $\delta^{13}\text{C}$ series from live and dead trees at sites-A and -B.	144
Table 3.4. Pearson correlation matrix between standardized <i>Thuja occidentalis</i> ring-width and $\delta^{13}\text{C}$ series from dead trees at sites-A and -B.	145
Table 3.5. Pearson correlation matrix between standardized <i>Thuja occidentalis</i> ring-width and $\delta^{13}\text{C}$ series from live trees at sites-A and -B.	146
Table 3.6. Descriptive statistics for the $\delta^{13}\text{C}$, ring-width (RWL) and discrimination (Δ) <i>Thuja occidentalis</i> chronologies for each individual-site (A and B), both sites (AB) and regional ring-width (REG-RWL).	147

Table 3.7. Correlation matrix of the seven *Thuja occidentalis* residual chronologies for the common period 1681-2005.

.....148

List of Appendices

Appendix 1

Figure A1.1. The a) mean distance and b) weighted distance of the three nearby meteorological stations at the mid-point of sites-A and -B from which the BioSIM climate data were interpolated.
.....173

Figure A1.2. Eleven-year moving interval Pearson correlations between standard REG-RWL and AB- $\delta^{13}\text{C}$ chronologies whereby each successive segment advanced one year in time from 1650-2006.
.....174

Figure A1.3. Principal components analyses (PCA) performed on correlation matrices conducted over six 50-year periods beginning in 1700 and ending in 1999 (a-f) and illustrating the relationships among the seven *T. occidentalis* residual chronologies.
.....175

Table A1.1. Pearson correlation matrix between standardized *Thuja occidentalis* $\delta^{13}\text{C}$ series from dead trees at sites-A and -B.
.....176

Table A1.2. Pearson correlation matrix between standardized *Thuja occidentalis* $\delta^{13}\text{C}$ series from live trees at sites-A and -B.
.....177

Appendix 2

Table A2.1. Matrix of Pearson correlation coefficients between the A- $\delta^{13}\text{C}$ chronology and monthly climate variables.

.....178

Table A2.2. Matrix of Pearson correlation coefficients between the B- $\delta^{13}\text{C}$ chronology and monthly climate variables.

.....179

Table A2.3. Matrix of Pearson correlation coefficients between the AB- $\delta^{13}\text{C}$ chronology and monthly climate variables.

.....180

Table A2.4. Matrix of Pearson correlation coefficients between the A-RWL chronology and monthly climate variables.

.....181

Table A2.5. Matrix of Pearson correlation coefficients between the B-RWL chronology and monthly climate variables.

.....182

Table A2.6. Matrix of Pearson correlation coefficients between the AB-RWL chronology and monthly climate variables.

.....183

Table A2.7. Matrix of Pearson correlation coefficients between the REG-RWL chronology and monthly climate variables.

.....	184
Table A2.8. Matrix of Pearson correlation coefficients between the PC1 scores and monthly climate variables.	
.....	185
Table A2.9. Matrix of Pearson correlation coefficients between the PC2 scores and monthly climate variables.	
.....	186
Table A2.10. Matrix of Pearson correlation coefficients between the AB- $\delta^{13}\text{C}$ scores and monthly climate variables from 1900-1959.	
.....	187
Table A2.11. Matrix of Pearson correlation coefficients between the AB- $\delta^{13}\text{C}$ scores and monthly climate variables from 1960-2005.	
.....	188
Table A2.12. Matrix of Pearson correlation coefficients between the REG-RWL scores and monthly climate variables from 1900-1959.	
.....	189
Table A2.13. Matrix of Pearson correlation coefficients between the REG-RWL scores and monthly climate variables from 1960-2005.	
.....	190

Appendix 3

Figure A3.1. Pearson correlation coefficients between A) A-RWL, B) B-RWL, C) A- $\delta^{13}\text{C}$ and D) B- $\delta^{13}\text{C}$ and monthly climate variables from May of the year prior to ring formation (large caps) to September of the year of ring formation (small caps).

.....191

Figure A3.2. Pearson correlation coefficients between PC1 (*top panel*) A) during 1900-1959 and B) during 1960-2005 and PC2 (*bottom panel*) C) during 1900-1959 and D) during 1960-2005 and monthly climate variables from May of the year prior to ring formation (large caps) to September of the year of ring formation (small caps).

.....193

1.0 General Introduction

1.1. Introduction

1.1.1. Stable isotopes

Earth's biota contains organic compounds which commonly consist of carbon, hydrogen, oxygen and nitrogen elements (Leuenberger et al. 1998). The atoms within these organic compounds are essential to living organisms as well as to ecosystem processes. Atoms of an element are unique from those of other elements in that they possess inherent chemical and physical properties which allow them to be easily identified and placed on the Periodic Table of Elements based on the number of protons found within their nuclei (Petrucci et al. 2002; Faure and Mensing 2005). Within each nucleus, however, the number of neutrons may also vary in addition to the protons so that each variation in neutron number of an element is termed an isotope. Each isotope of an element is therefore defined by the same number of protons in its nucleus but a different number of neutrons resulting in an inherent subtlety in mass (Hoefs 1987). Isotopes whose nuclei do not decay with time are termed stable while those which are unstable are categorized as radioactive isotopes (Faure and Mensing 2005; Sharp 2007). The advantage of examining stable isotopes is that their nuclei do not alter in configuration over time resulting in the preservation of their isotopic signatures.

Some of the common stable isotopes found in living organisms include the two stable isotopes of carbon (^{12}C and ^{13}C), the two of hydrogen (^1H and $^2\text{H}(\text{D})$), the three of oxygen (^{16}O , ^{17}O and ^{18}O) and the two of nitrogen (^{14}N and ^{15}N). Isotopes which contain the fewest number of neutrons in their nuclei are commonly referred to as the lighter

isotopes while those containing more are referred to as the heavier isotopes (Sternberg 1989). The inherent slight differences in mass among isotopes result in different bond strengths (Sharp 2007) with the more abundant lighter isotope being more reactive as it forms bonds more easily broken compared to the heavier isotope (Hoefs 1987). As a result of their intrinsically higher reactivity, lighter isotopes are less discriminated against in biochemical reactions and are therefore more concentrated in organic matter (Melander and Saunders 1979; Kendall and McDonnell 1998; Dawson and Brooks 2001). This change in partitioning of heavy to light isotopes from source to product is known as isotope fractionation and the tendency of stable isotopes to undergo this process throughout the environment allows for high resolution examination of ecological processes (Dawson et al. 2002). Since lighter isotopes tend to be synthesized more readily into organic material than heavier isotopes, organic material will always be depleted in the latter compared to the source. Furthermore, the isotopic value which is measured as less negative compared to that from another sample is termed as enriched since it contains a higher abundance of the heavier isotope.

In stable isotope studies, the current procedure is to express the heavy to light isotope ratio with reference to that of a known standard as it is often more reliable and convenient than measuring the absolute isotopic composition (Ehleringer and Rundel 1989). This international standard also allows researchers to make cross-study comparisons. The delta (δ) notation is shown below as the isotopic difference between a sample and standard and is expressed in parts per thousand (‰):

$$\delta = (R_{\text{sample}}/R_{\text{standard}} - 1)1000, \quad [1]$$

where R is the abundance of heavy to light isotopes. All standards have a δ value of 0‰. For carbon, $^{13}\text{C}/^{12}\text{C}$ represents the molar fraction of R and its current standard is Vienna-PDB (VPDB) (Coplen 1995).

1.1.2. Stable isotopes in environmental studies

The stable isotopic composition of organic material has been analyzed to answer many environmental questions ranging from cellular to ecosystem levels (Dawson et al. 2002). For example, stable carbon isotopes have been used to identify shifts in food sources of animals and the carbon turnover rates within their tissues (Fry and Arnold 1982; Tieszen et al. 1983) as well as changes in human diets to reveal past social structure and agricultural practices (Peterson and Fry 1987). Moreover, carbon isotopes have been traced across trophic levels to identify the resources most important in an ecosystem (Peterson et al. 1986; Bowling et al. 2002). The analysis of the stable carbon isotopic composition of soil organic matter characteristic of both woodland (C3) and grassland (C4) species have revealed a transition from grassland to forest during the last 40-120 years in a subtropical Savanna (Boutton et al. 1999). During this vegetation change, additional analysis of the stable oxygen and hydrogen isotopic composition of plant and soil water confirmed that grassland and tree species utilized water from the upper half meter and from the upper four meters of the soil profile, respectively. Leaf $\delta^{13}\text{C}$ variation was also found to be a robust indicator of life form groups (deciduous or evergreen trees, shrubs, forbs and mosses) related to carbon and water fluxes within boreal ecosystems (Brooks et al. 1997).

Stable isotope ratios preserved within the minerals, fluids and gases of terrestrial and ocean sediment cores have also been used to model the climate of the last several million years (Leuenberger et al. 1998; Sharp 2007). Much work on stable hydrogen and oxygen isotope analysis has focused on ice and firn as well as marine fauna cored from the ocean floor (Bradley 1999). In Antarctica, surface temperatures over the past 150,000 years have been reconstructed from measurements of oxygen isotopes in ice cores (Lorius et al. 1985) and a 1000-year high precision record of atmospheric $\delta^{13}\text{C}$ was extracted from CO_2 trapped in ice cores (Francey et al. 1999). Although ocean sediment cores can provide intra-annual, annual and centennial scale resolutions (Maslin and Swann 2006) it is often difficult to absolutely date every year reliably and ice core records tend to be concentrated close to the poles (McCarroll et al. 2003).

1.1.3. Stable isotopes in tree-ring studies

Tree rings provide precisely dated annual resolution and offer some of the most high resolution climatic information from continental temperate regions (Fritts 1976; Schweingruber 1996; Hughes 2002). Dendrochronological studies have traditionally focused on the development of ring-width chronologies (Fritts 1976; Schweingruber 1996), some of which have extended back for millennia and were used to calibrate radiocarbon dating (Stuiver and Reimer 1993). Since radial growth is often associated with dominant environmental conditions, overlapping ring-width measurements can be replicated with many series and cross-checked with established chronologies from surrounding areas to provide absolute dating. However, varying limiting factors to radial

growth could result in anomalous annual growth increments throughout a growing season whereas, stable isotope variability is usually dominated through stomatal restrictions to photosynthesis (McCarroll and Loader 2006). Yet another advantage in dendroisotopic research is that isotope chronologies require less replication than the traditional ring-width chronologies to achieve adequate signal strength (i.e. Long 1982; Leavitt and Long 1988; Robertson et al. 1997a; McCarroll and Pawellek 1998; Gagen et al. 2004; Tardif et al. 2008). Several researchers in the field of dendrochronology have also stated that the biosynthesis and physiological controls governing stable isotope ratios in tree-ring cellulose are better understood than those governing radial growth (Loader et al. 2003; McCarroll and Loader 2006).

More recently, there has been growing interest in using multiple tree-ring proxies including ring width, maximum latewood density and stable isotopes which could provide additional information regarding a climatic parameter unavailable from any single proxy (McCarroll and Pawellek 1998; McCarroll et al. 2003; McCarroll and Loader 2006). For example, McCarroll et al. (2003) have reported a correlation coefficient of 0.73 between mean actual and estimated July temperature reconstructed from ring-width, latewood density and tree-ring $\delta^{13}\text{C}$ chronologies. Additionally, the combined $\delta^{13}\text{C}$ and ring-width proxies were shown to provide a strong calibration with respect to May-September precipitation (Gagen et al. 2006). Examination of multiple proxies from common samples of Scots pine (*Pinus sylvestris* L.) in the French Alps have shown that stable carbon isotope series shared a stronger common signal than those of radial growth proxies, i.e. latewood width, maximum density, implying greater site

dependency for the latter (Gagen et al. 2004). Gagen et al. (2004) have found that the common signal in their stable carbon isotope chronology of *P. sylvestris* was enhanced when stable carbon isotope series were combined from two sites separated by 400m elevation but the common signal of either ring-width or latewood density chronology was weakened when the same procedure was applied. The expansion of dendroclimatology to include stable isotope research and new approaches thereof has broadened our understanding of climate phenomena (Sharp 2007). Since dendroisotopic climate reconstructions require detailed insight into tree physiology, it is essential to review the main processes involved in the carbon fixation of trees.

1.1.4. Stable carbon isotope discrimination

Carbon-12 and carbon-13 have near identical chemical properties as a result of their extra-nuclear structure but a difference in mass results in the differential discrimination between them during carbon fixation (Farquhar et al. 1982; Faure and Mensing 2005). Two constant isotopic fractionations occur during photosynthesis: 1) fractionation by diffusion and 2) fractionation by carboxylation. Once the CO₂ has diffused through the stomata and has been incorporated into the leaf tissue, the internal CO₂ reacts with the primary carboxylating enzyme, ribulose-1,5-bisphosphate carboxylase (RuBisCO) (Park and Epstein 1960). Leaf sugars, primary photosynthates, are then fixed into plant tissues. Subsequent isotopic fractionations affect the carbon isotope composition only to a slight degree (Craig 1954; Park and Epstein 1960) and contribute little to the ¹³C/¹²C ratio of organic carbon (Raven and Farquhar 1990). Plants are separated into three groups based on their photosynthetic pathways, C3, C4 and

CAM. Farquhar et al. (1982) expressed the isotopic composition of C3 plants (‰) in relation to the concentration of CO₂ inside the leaf to that outside the leaf according to the equation:

$$\delta^{13}\text{C}_p = \delta^{13}\text{C}_a - a - (b - a)(c_i / c_a), \quad [2]$$

where $\delta^{13}\text{C}_a$ and $\delta^{13}\text{C}_p$ are the isotopic values of atmospheric CO₂ and plant, respectively, a is discrimination against ¹³C during diffusion (~ -4.4‰), b is discrimination against ¹³C during carboxylation (~ -27‰) and c_i and c_a are the intercellular leaf and ambient air CO₂ concentrations, respectively. This model has been validated using gas exchange measurements (Evans et al. 1986) and $\delta^{13}\text{C}_a$ may now be extrapolated based on a long high-precision ice core record from the Antarctic (Francey et al. 1999). Whereas gas exchange techniques provide measurements of photosynthetic rate at a point in time, $\delta^{13}\text{C}$ values indicate photosynthetic activity throughout the period the tissue was synthesized (Dawson et al. 2002). From equation 2 above, the ¹³C concentration within plant matter depends on metabolic processes that drive the synthesis of carbon. Although these fractionation rates are relatively constant, the intercellular composition of CO₂ does vary within the leaf due to fluctuations of entry and utilization of CO₂ controlled by stomatal conductance and photosynthesis, respectively, which determine tree-ring $\delta^{13}\text{C}$ values (McCarroll and Loader 2006).

Most trees belong to the C3 group and heavily discriminate (Δ) against ¹³C during carbon uptake (Leavitt 1993a). As a result, organic matter is always depleted in ¹³C compared to that of ambient air. According to Farquhar et al. (1982) and later reinforced

by others (Farquhar et al. 1988, 1989; Duquesnay et al. 1998; Saurer et al. 2004), discrimination against ^{13}C (‰) during photosynthesis in C3 plants can be approximated by the equation:

$$\Delta = \frac{(\delta^{13}\text{C}_a - \delta^{13}\text{C}_p)}{(1 + \delta^{13}\text{C}_p/1000)}, \quad [3]$$

See equation 2 for term definitions. The extent of ^{13}C discrimination within the plant depends on the rate of CO_2 supply that is available to the sites of carbon fixation at any given time (Gillon et al. 1998). During periods when the CO_2 supply is not restricted, discrimination will reflect the fractionation rate of RuBisCO. That is, when conditions are moist, stomatal conductance does not limit the photosynthetic rate resulting in greater discrimination by RuBisCO (Gillon et al. 1998). Alternatively, the fractionation rate will reflect that due to diffusion as stomatal closure interrupts and limits the supply of CO_2 . During hot, dry conditions photosynthesis depletes the internal CO_2 more quickly than it is replenished through stomatal conductance. This diminished internal CO_2 supply results in little discrimination of ^{13}C by RuBisCO resulting in more ^{13}C becoming assimilated to maintain continued carbon fixation (Leavitt and Long 1989; McCarroll and Loader 2006). In the natural environment, however, the CO_2 supply is usually only partially limiting and therefore, discrimination values generally vary between the diffusive and carboxylation fractionations.

1.1.5. Stomatal conductance and photosynthetic rate as limiting factors

Tree-ring $\delta^{13}\text{C}$ signatures vary in response to the prevailing balance between stomatal conductance and photosynthetic rate during the growing season (Hemming et al.

2001; McCarroll and Loader 2006). Moisture stress and thus, stomatal conductance has usually been cited as the major limiting factor controlling carbon assimilation in stable carbon dendroisotopic studies. Stomatal resistance is affected by water availability, relative humidity and air temperature (Welker et al. 1993; Panek and Waring 1997; Boettger et al. 2002; McCarroll and Loader 2006). Consequently, many researchers have identified an inverse relationship between tree-ring $\delta^{13}\text{C}$ values and moisture availability (Leavitt and Long 1989; Lipp et al. 1991; Robertson et al. 1997a; Brooks et al. 1998; Leuenberger et al. 1998; Gagen et al. 2004; Kirilyanov et al. 2008). Differences between humid and dry sites were shown to influence tree-ring $\delta^{13}\text{C}$ for Common beech (*Fagus sylvatica* L.) in the Swiss Central Plateau, Switzerland (Saurer et al. 1995). Tree-ring $\delta^{13}\text{C}$ at the dry sites were inversely correlated to precipitation during May, June and July while this association was much less pronounced at the humid site suggesting that site conditions should not be neglected when interpreting tree-ring $\delta^{13}\text{C}$ variations.

Waterhouse et al. (2000) have found a strong inverse correlation between $\delta^{13}\text{C}$ values and river flow in the tree-rings of *P. sylvestris* in western Siberia. A stronger sensitivity in tree-ring $\delta^{13}\text{C}$ to moisture conditions was shown for trees farther away from the river. Hence, the authors speculated that the increase in river flow allowed for more area around the river bank to be flooded. A rise in available soil moisture would thus lower vapor pressure deficit thereby resulting in depleted $\delta^{13}\text{C}$. Warren et al. (2001) have reviewed an extensive range of conifer $\delta^{13}\text{C}$ values in leaves and wood tissue from varying environmental conditions. The authors indicated that carbon isotope data may only reflect drought stress in seasonally dry climates where precipitation is less than evaporation. For example, $\delta^{13}\text{C}$ values of Pinon pine (*Pinus edulis* Engelm.) tree-rings

from southwestern United States have been used to successfully reconstruct the July Palmer Drought Severity Indices (Leavitt and Long 1989) and obtain a better understanding of the water and carbon cycle of this region (Leavitt et al. 2007). Moisture stress signals may, therefore, be readily observed in tree-ring $\delta^{13}\text{C}$ since trees interact with environmental conditions (high temperatures, low precipitation, high evaporation, increased radiation and low relative humidity) related with drought (Leavitt 1993a).

Lipp et al. (1991) have shown that tree-ring cellulose $\delta^{13}\text{C}$ values in Silver fir (*Abies alba* Mill.) were positively correlated with temperature and negatively correlated with relative humidity and precipitation during August. Their results also indicated that δD values, in comparison with $\delta^{13}\text{C}$, were a much weaker tracer for climate variations. In eastern Siberia, the number of frost days and minimum temperatures during the summer had a much greater influence on Cajander larch (*Larix cajanderi* Mayr.) tree growth, i.e. ring-width and maximum latewood density, than on carbon assimilation (Kirilyanov et al. 2008). Instead, $\delta^{13}\text{C}$ variations were positively associated with June-July maximum temperature and negatively with July precipitation during the year of ring formation. Likewise, the sensitivity of Pedunculate oak (*Quercus robur* L.) $\delta^{18}\text{O}$ and $\Delta^{13}\text{C}$ chronologies to summer drought deficit (relative humidity, summer temperature, water stress) enabled a reconstruction of these variables explaining between 45 to 60% of year-to-year variability (Raffalli-Delercq 2004). Robertson et al. (1997b) have also found a positive correlation with temperature and negative correlations with relative humidity and rainfall using *Q. robur* tree-ring $\delta^{13}\text{C}$ values during current-year July-August. Hemming et al. (1998) have addressed whether a tree-ring $\delta^{13}\text{C}$ chronology containing a coherent

climate signal could be constructed from the $\delta^{13}\text{C}$ series of three different tree species; *F. sylvatica*, *Q. robur* and *P. sylvestris* on the estate of Woburn Abbey, Bedfordshire, England. Isotope series from the three tree species were combined and yielded negative correlations with current June-September relative humidity and positive correlations with mean July-October maximum temperature.

Aside from stomatal conductance, other tree-ring $\delta^{13}\text{C}$ studies of *P. sylvestris* at their northern distributional limit in northern Finland (McCarroll and Pawellek 2001; McCarroll et al. 2003; Gagen et al. 2007) and of White spruce (*Picea glauca* (Moench) Voss) in subarctic Manitoba, Canada (Tardif et al. 2008) have reported photosynthetic rate as the limiting factor to carbon assimilation which, in turn, is determined by temperature and sunshine. The researchers from northern Finland have reported *P. sylvestris* tree-ring $\delta^{13}\text{C}$ values to be positively correlated with the combined mean daily sunshine hours and mean temperature during current-year July and August, while correlations with summer precipitation were of secondary importance (McCarroll and Pawellek 2001; McCarroll et al. 2003; Gagen et al. 2007). The authors suggested that these results could reflect the influence of sunshine on photosynthetic rate. Saurer et al. (2004) also have found that $\delta^{13}\text{C}$ values measured in *Larix*, *Pinus* and *Picea* tree-rings sampled from eastern Siberian sites were positively correlated with mean April-September temperature of the year of growth.

1.1.6. Tree-ring $\delta^{13}\text{C}$ values and water-use efficiency

Atmospheric CO_2 is the substrate of photosynthesis for terrestrial plants and therefore fluctuations in CO_2 concentrations directly affect plant physiological function (Marshall and Monserud 1996). These fluctuations may be observed as the CO_2 concentration partial pressure gradient between the intercellular spaces of the leaf and the ambient air. Since photosynthetic rate depletes and stomatal conductance replenishes the concentration of leaf intercellular CO_2 , the overall balance between the two act as a measure of water-use efficiency (carbon gain per unit of water loss). Intrinsic water-use efficiency (iWUE), the ratio of net photosynthesis (A) to stomatal conductance of water vapor (gH_2O) is given by Saurer et al. (2004) as follows:

$$\frac{c_i}{c_a} = \frac{\Delta - a}{b - a}, \quad [4]$$

where the values for a, b and c_a are obtained through the literature to calculate c_i , intercellular leaf CO_2 concentration. See equation 2 for term definitions. Subsequently, iWUE may be estimated using the equation:

$$\text{iWUE} = \frac{A}{\text{gH}_2\text{O}} = (c_a - c_i) \frac{1}{1.6}, \quad [5]$$

Since transpiration rate is dependant upon evaporation and thus soil moisture availability, discrimination against ^{13}C is associated with decreased water-use efficiency in C3 plants (Farquhar et al. 1982; Hubick et al. 1986; Hubick and Farquhar 1989; Farquhar et al. 1989; Valentini et al. 1992; Guehl et al. 1995; Leuenberger et al. 1998). For example, lower water-use efficiency was indicated by greater discrimination in *Larix*

spp. leaves than compared to those of co-occurring evergreen conifers where moisture was limiting for tree growth below 3000-4000m elevation (Kloeppel et al. 1998). According to this rationale, more water stress should reflect higher $\delta^{13}\text{C}$ values in organic matter as plants regulate their stomata for optimal water-use efficiency.

Furthermore, the effect of long-term variations in atmospheric CO_2 concentration on intrinsic water-use efficiency may contain important implications for the application of $\delta^{13}\text{C}$ values in C_3 plants for climate reconstruction (Polley et al. 1993; Bert et al. 1997). The increase in atmospheric CO_2 during the last 100 years could have increased water-use efficiency from 17% to 22% in *Larix*, *Pinus* and *Picea* trees (Saurer et al. 2004), by 44% in dense, even-aged *F. sylvatica* (Duquesnay et al. 1998) and by 30% in mature *A. alba* from the 1930s to 1980s which were found to be consistent with strong increases in radial growth over the same period (Bert et al. 1997). Similar long-term increases in water-use efficiency have been found in tree-rings from arid environments during this period (Feng and Epstein 1995). However, Kienast and Luxmoore (1988) have reported that increased growth observed in their tree-ring chronologies was greater than the paralleled elevations in atmospheric CO_2 concentrations and therefore could not be solely explained by them.

Since the onset of the industrial revolution, fossil fuel emissions have offset the relationship between tree-ring cellulose $\delta^{13}\text{C}$ values and water-use efficiency. In recent decades, a shift in association between tree-ring $\delta^{13}\text{C}$ and $\delta^{18}\text{O}$ values from the first half of the 20th century provided evidence of an increase in stomatal control of photosynthesis

in White Cypress-pine (*Callitris columellaris* F. Muell.) due to an increase in rainfall in northwestern Australia (Cullen et al. 2008). Beerling (1994) simulated leaf gas exchange responses to the increase in atmospheric CO₂ concentration from 280 to 350 ppm during the last 150 years following the onset of the industrial revolution. The water-use efficiency of temperate trees was shown to have increased via a 20% decline in stomatal conductance and coincided with very little rise in photosynthetic rate. Moreover, increased water-use efficiency through lowered transpiration from elevated CO₂ concentrations may decrease the likelihood and/or magnitude of moisture stress and could also result in increased growth under moisture-limited environments (Eamus and Jarvis 1989; Mooney et al. 1991; Pitelka 1994). Alternatively, a homeostasis of water-use efficiency in three coniferous species in western United States was reported by Marshall and Monserud (1996) who have found that ambient to leaf intercellular CO₂ concentration has remained constant as c_i adjusted according to the rise of c_a . Nonetheless, elevated CO₂ concentrations will likely produce a constant c_i/c_a response in some species and vary in others (Ehleringer and Cerling 1995).

Differences in water-use within the same environmental conditions may also be prominent between the genders of a species. Males of Manitoba maple (*Acer negundo* L.) were found to be more conservative in their water-use compared to females during years where moisture was plentiful (Ward et al. 2002). Moreover, nitrogen fertilization (Mitchell and Hinckley 1993; Guehl et al. 1995) and decreased leaf stomatal density over the past 150-200 years observed from herbarium leaves (Woodward 1993) could have also stimulated the increase of water-use efficiency. It is thus important to establish

whether relationships among environmental parameters remain temporally stable over the long-term, especially over the last century. Multiple stable isotope chronologies may give insight into the temporal stability of physiological response. Scheidegger et al. (2000) have developed a conceptual model based on the $\delta^{18}\text{O}$ and $\delta^{13}\text{C}$ values in leaves of C3 plants that attempts to distinguish whether differences in intercellular CO_2 concentration are controlled predominantly by either stomatal conductance or photosynthetic capacity. The model draws on the association between $\delta^{18}\text{O}$ and $\delta^{13}\text{C}$ values as a response to change in environmental conditions.

1.1.7. Dendroisotopic studies in the North American Boreal Forest

Few dendroisotopic studies have been conducted within the North American Boreal Forest (Gray and Thompson 1977; Gray and Song 1984; Brooks et al. 1998; Barber et al. 2000; Bukata and Kyser 2007; Simard et al. 2008a; 2008b; Buhay et al. 2008; Tardif et al. 2008) and these have focused largely on *P. glauca* and Jack pine (*Pinus banksiana* Lamb.). In the Edmonton area, *P. glauca* cellulose $^{18}\text{O}/^{16}\text{O}$ (Gray and Thompson 1977) and cellulose nitrate δD values (Gray and Song 1984) were found to be highly positively associated with mean annual temperature of the region. Tree-ring cellulose $\delta^{18}\text{O}$ indices of *P. glauca* were positively and significantly correlated with mean autumn and winter seasonal temperatures prior to the growing season (Gray and Thompson 1977). In Thompson, Manitoba, only precipitation variables were found to be significant in a regression model aimed at explaining the temporal variation in *P. banksiana* carbon isotope ratios (Brooks et al. 1998). Growing season precipitation was positively correlated with depleted $\delta^{13}\text{C}$ values whereas, winter precipitation was

positively associated with enriched $\delta^{13}\text{C}$ values. Brooks et al. (1998) concluded that the seasonal distribution of precipitation was important for the growth of *P. banksiana* as a high snow load may reduce soil temperatures and thereby prevent the early resumption of photosynthesis in the spring.

Furthermore, $\delta^{13}\text{C}$ composition in *P. glauca* growing at the northern tree-line in Manitoba have been suggested to be primarily controlled by photosynthetic rate and not stomatal conductance as moisture stress was not shown to be a major determinant of either photosynthesis or radial growth (Tardif et al. 2008). The authors hypothesized that if stomatal conductance had a major influence on $^{13}\text{CO}_2$ assimilation, $\delta^{13}\text{C}$ values would be greater during those years where warm and dry conditions prevailed than it would in those where warm and wet conditions dominated. However, statistical analysis did not reveal any difference between warm/ dry and warm/ wet conditions with regard to $\delta^{13}\text{C}$ indices. Instead, $\delta^{13}\text{C}$ enrichment was observed during years with warmer summer months regardless of prevailing moisture conditions. They concluded that years with warmer summer months maximize photosynthesis and therefore $^{13}\text{CO}_2$ uptake in *P. glauca*.

The analysis of *P. glauca* ring-width, maximum latewood density and $\delta^{13}\text{C}$ chronologies developed from the Alaskan boreal forest indicated that temperature induced drought stress could have weakened the positive association between temperature and radial growth during the late 20th century (Barber et al. 2000). Moisture stress was observed by consistently negative correlations between discrimination of

holocellulose ^{13}C and spring and summer monthly mean temperatures during the year of growth. Aside from studies examining the tree-ring $\delta^{13}\text{C}$ –climate association, other studies have reported a relationship between tree-ring $\delta^{13}\text{C}$ and Spruce budworm (*Choristoneura fumiferana* Clem.) defoliation events on its host species, Balsam fir (*Abies balsamea* (L.) Mill.) and Black spruce (*Picea mariana* (Mill.) BSP.) 100 km north of Chicoutimi, Quebec, Canada (Simard et al. 2008a; 2008b). In addition, temporal trends in Red and White oak (*Quercus rubra* L. and *Quercus alba* L., respectively) and White and Yellow birch (*Betula papyrifera* Marsh. and *Betula alleghaniensis* Britt., respectively) tree-ring $\delta^{13}\text{C}$ and $\delta^{15}\text{N}$ values were found to record the regional extent of pollution across Ontario and in New Brunswick since isotopic values were consistent with increasing anthropogenic influence on the carbon and nitrogen cycles since the mid-1900s (Bukata and Kyser 2007). Stable isotopes in tree-rings of different species within the North American boreal forest, therefore, require more attention. No dendroisotopic studies have been reported regarding stable carbon isotope analysis of modern Northern white-cedar (*Thuja occidentalis* L.) and little of its range have been sampled by dendrochronologists (Sheppard and Cook 1988).

1.1.8. Ecology of *Thuja occidentalis* L.

Thuja occidentalis is a shade tolerant, monoecious conifer that ranges from southeastern Manitoba, down throughout Minnesota and then eastward to both the Canadian maritime provinces and the northeastern states (Johnston 1990; Sims et al. 1990). The limit of the northwestern continuous distribution of the species is reached in Manitoba (Johnston 1990) and is located south of Lake Winnipeg and east of the Red

River (Scoggan 1957). However, disjunct populations also occur in the Cedar Lake Region, adjacent to the northern end of Lake Winnipegosis, central Manitoba (Scoggan 1957; Tardif and Stevenson 2001). These populations are located at about 300 km northwest of the limit of its continuous distribution in southeastern Manitoba (Ko Heinrichs and Tardif 2006). The extent of these populations is believed to be the result from the minimization of fire frequency, size and/or intensity due to the presence of the surrounding three lakes (Tardif and Stevenson 2001; Ko Heinrichs and Tardif 2006).

Thuja occidentalis belongs to the *Cupressaceae* and are usually found in moist, temperate environments with annual precipitation generally ranging from 710 to 1170mm (Johnston 1990). Average temperatures within its distribution vary from -4 to -12°C in January and from 16 to 22°C in July (Johnston 1990).

Thuja occidentalis possesses broad physiological tolerances to extremes in moisture regimes (Collier and Boyer 1989; Matthes-Sears and Larson 1991) prevailing in lowlands consisting of cool, moist, nutrient-rich sites on organic or calcareous mineral soils (Scoggan 1957; Johnston 1990) to well-drained elevated uplands (Curtis 1946; Habeck 1958; Musselman et al. 1975). Growth is usually reduced in moisture-saturated lowlands (Johnston 1990) and becomes extremely impeded on limestone cliffs of the Niagara Escarpment, Ontario (Larson and Kelly 1991; Matthes-Sears and Larson 1991). Johnston (1990) has noted the susceptibility to fire of *T. occidentalis* as a result of its shallow root system and the high oil content of its foliage and bark. As a result, *T. occidentalis* dominated stands generally increase with time following fire (Bergeron and Debuc 1989). The maximum ages of *T. occidentalis* growing in xeric conditions were

reported to exceed 900 years in the Northwestern Québec boreal forest (Archambault and Bergeron 1992a) and almost 1600 years on the cliffs of the Niagara Escarpment, Ontario (Larson and Kelly 1991; Kelly et al. 1994; Larson and Melville 1996; Buckley et al. 2004; Kelly and Larson 2007). In Manitoba, maximum ages were found to be in excess of 450 years in agreement with those found by Case (2000) and the oldest living *T. occidentalis* began growth in 1613 at a hydric site (F. Conciatori personal communication 2007). *Thuja occidentalis* reaching such great ages appear as gnarled, stunted and possess sparse foliage with frequent apical mortality (Archambault and Bergeron 1992a, b). Indeed, great longevity appears to largely coincide with growth-stunted *T. occidentalis* inhabiting extreme environments (Johnston 1990).

In central and eastern Canada, ring-width chronologies have been used to model the relationship between radial growth and climate in *T. occidentalis* (Larson and Kelly 1991; Archambault and Bergeron 1992b; Kelly et al. 1994; Case 2000; Tardif and Stevenson 2001; Buckley et al. 2004). Water stress was shown to be particularly important for *T. occidentalis* radial growth during June of the current growing season (Tardif and Stevenson 2001). Additionally, St. George and Nielsen (2001) have developed ring-width and maximum density chronologies of *T. occidentalis* dating back to the mid-1600s from southeastern Manitoba. The authors found lower inter-series correlations with maximum density than compared to ring width and speculated that the former parameter was more strongly affected by local environmental factors relative to ring width. Therefore, *T. occidentalis* ring width but not maximum density could be useful for further development of paleoclimatic records in southeastern Manitoba.

Early summer water stress may limit *T. occidentalis* growth (Larson and Kelly 1991; Archambault and Bergeron 1992a; Tardif and Stevenson 2001) and extremely hot summers in the year prior to ring formation were negatively associated with *T. occidentalis* radial growth during the following year in southern Ontario (Kelly et al. 1994). In central Manitoba, the radial growth of *T. occidentalis* was found to be negatively associated to August maximum temperature of the year prior to ring formation and positively to June and July precipitation during the year of ring formation indicating a response to drought (Tardif and Stevenson 2001). Case (2000) also conducted a dendroclimatological reconstruction of precipitation using *T. occidentalis* in the same area and observed drought periods throughout the 18th to 20th centuries. In the Niagara Escarpment, Southern Ontario, hot and dry conditions during the growing season were related to moisture stress of *T. occidentalis* which was interpreted to have caused a decrease in growth during the following year (Buckley et al. 2004). Similarly, Archambault and Bergeron (1992b) have reported a close correspondence between the Canadian Drought Code and radial growth which indicated that water availability was a limiting factor to *T. occidentalis* growth. Furthermore, researchers have suggested that *T. occidentalis* was suitable for the long-term reconstruction of drought events (Archambault and Bergeron 1992b; Tardif and Stevenson 2001; Buckley et al. 2004). These researchers have observed the positive effect of June precipitation coupled with the negative effect of June temperature on radial growth of *T. occidentalis* during the year of ring formation. Given that this is the first dendroisotopic analysis of *T. occidentalis*, it is speculated that the climate controls governing ring width will contrast with those

controlling tree-ring $\delta^{13}\text{C}$ variation. However, since certain wood components are formed at different times throughout the year, consideration should be given to ascertain which component is analyzed to best capture climatic variation.

1.1.9. Selecting a wood component to analyze in tree rings

The isotopic ratios of carbon, hydrogen and oxygen within wood cellulose can be determined by mass spectrometry (Long 1982) and these parameters are commonly analyzed in dendroisotopic research. Alpha (α)-cellulose, hemicelluloses and lignin are the wood components which constitute the majority (~70-90%) of whole plant tissues (Benner et al. 1987; Macfarlane et al. 1999). The structure of α -cellulose and hemicellulose components is referred to as hollocellulose. Alpha-cellulose occurs as microfibrils, hemicelluloses fill the spaces adjacent to the microfibrils while lignin is present throughout the cell wall and intercellular regions (Core et al. 1976). These components vary in the isotopic composition (Wilson and Grinsted 1977; Mazany et al. 1980) which may change from year-to-year (Leavitt 1993a; Loader et al. 2002) and may be different according to species (Timell 1967; Benner et al. 1987). Therefore, analysis of the proper wood component is a crucial step in dendroisotopic research. However, the selection of the particular wood component to analyze often still rests on time constraints, available laboratory equipment and expertise. Although advances to sample processing and stable isotope mass spectrometry have made analysis much less time consuming (Hughes 2002; McCarroll and Loader 2006), the selection of a standard wood component to isolate and analyze remains unresolved among dendroisotopic researchers.

The analysis of one wood component is usually preferred over whole wood because the composite nature of whole wood contains multiple isotopic signatures and mobile organic substances such as oils, lipids and resins transferable among tree-rings (Freyer 1986; Schweingruber 1996; Warren et al. 2001). For example, although lignin is non-mobile throughout woody tissue, it was found to be $\delta^{13}\text{C}$ depleted by 2-6‰ relative to the whole plant (Benner et al. 1987). Loader et al. (2003) have shown a close correspondence in tree-ring $\delta^{13}\text{C}$ variation between cellulose and lignin in *Q. robur* but have noted that differential decay between cellulose and lignin would likely affect these variations preserved in sub-fossil wood. Either α -cellulose or holocellulose are usually isolated from whole wood for stable isotope analysis (Leavitt 1993a; Borella et al. 1998; Leuenberger et al. 1998; Macfarlane et al. 1999). According to Borella et al. (1998), differences between the $\delta^{13}\text{C}$ values of α -cellulose and holocellulose among tree species vary from -0.34 to 1.03‰. However, α -cellulose requires an additional chemical treatment after holocellulose has been extracted which results in greater sample loss. Previous dendroisotopic studies have reported holocellulose $\delta^{13}\text{C}$ composition as an adequate environmental proxy (Leavitt 1993b; Barber et al. 2000; Gagen et al. 2006) and reproducibility was shown to be within ~0.1‰ from sample preparation to mass spectrometry (Leavitt and Long 1984).

1.1.10. Objectives and hypotheses

The aim of this study is to improve our understanding of the environmental factors limiting the growth of *T. occidentalis* trees at their northwestern limit of distribution in Manitoba. The potential of this species as a recorder of drought has been

highlighted by several studies which have examined its radial growth. However, there have been no dendroisotopic studies of *T. occidentalis* throughout its modern range of distribution in North America. The development of *T. occidentalis* tree-ring $\delta^{13}\text{C}$ chronologies will provide greater insight into *T. occidentalis* physiological response to climate and to climate change dynamics prominent throughout the last century. Moreover, consensus has not been reached among researchers as to the particular wood component to isolate for dendroisotopic study. The subject of the first paper involves the comparison of various wood components of *T. occidentalis* for dendroisotopic analysis. The second paper addresses the main objectives of the study which include 1) the investigation of the association between tree-ring $\delta^{13}\text{C}$ values and ring width in addition to the response of these variables to climate and 2) provide a multi-century inference of drought events based on tree-ring $\delta^{13}\text{C}$ and ring width analyses. Previous dendroisotopic studies have reported that ring-width indices were not correlated with tree-ring $\delta^{13}\text{C}$ indices derived from the same tree (Mazany et al. 1980; Brooks et al. 1998; Tardif et al. 2008), the same is hypothesized for our study. The nature of these unassociated indices may indicate that the stable isotope and ring-width chronologies respond to entirely different climatic factors which may also vary through time. Since the onset and cessation of radial growth and carbon fixation do not take place simultaneously, both tree-ring $\delta^{13}\text{C}$ and ring width analyses could provide complementary information to yield a more robust climate signal resulting in a better representation of pre-instrumental climate (McCarroll et al. 2003; Gagen et al. 2006; Kirilyanov et al. 2008; Tardif et al. 2008).

2.0 Chemical pretreatment of *Thuja occidentalis* tree rings: implications for dendroisotopic studies ¹

2.1. Abstract

There is currently still debate as to whether extractives, lignin and/or hemicelluloses, all with specific isotopic signatures, should be removed prior to dendroisotopic analysis. This study reports the range of modern tree-ring $\delta^{13}\text{C}$ values of cellulose from *Thuja occidentalis* L., a species that has been under-utilized in dendroisotopic research despite its broad range and great longevity in North America. The main objective of this study was to recommend a *T. occidentalis* wood component to isolate for future $\delta^{13}\text{C}$ dendroisotopic analysis. Annually resolved tree-ring decades common among eight *T. occidentalis* trees were excised from cross-sections and homogenized. The tree-ring decade from each tree was then chemically processed from untreated whole wood (WW) to extractive-free wood (EF), to holocellulose (HC) and to α -cellulose (AC). Sub-samples were analyzed for $\delta^{13}\text{C}$, % carbon and % yield after each stage of chemical treatment. We recommend that HC be extracted for *T. occidentalis* as an AC yield may be too low in instances where tree-ring samples are very small. *Thuja occidentalis* tree-ring $\delta^{13}\text{C}$ values were found to be enriched with respect to needle-leaved conifers but in close agreement with those of other scale-leaved evergreens reported in the literature.

Keywords: Northern white-cedar; stable carbon isotope; cellulose extraction; wood chemistry; dendrochronology; scale-leaved evergreen

¹ This chapter was published in the Canadian Journal of Forest Research: Au, R. and Tardif, J.C. 2009. Chemical pretreatment of *Thuja occidentalis* tree-rings: implications for dendroisotopic studies. Canadian Journal of Forest Research 39: 1777-1784.

2.2. Introduction

Tree-ring isotope analysis provides some of the highest resolution climatic information from continental temperate forests and is of great interest to climate modelers who develop scenarios to model climate change (Switsur and Waterhouse 1998). Recent improvements in batch chemical processing and stable isotope mass spectrometry have made isotopic analysis much more efficient and possible for increasingly smaller sample sizes (Hughes 2002; McCarroll and Loader 2006). In addition to ring-width chronologies, tree-rings can provide other proxies such as earlywood and latewood density as well as stable carbon, oxygen and hydrogen isotope inter-annual variation (Hughes 2002). The development of chronologies from these proxies complements and adds complexity to existing knowledge of environmental factors controlling tree physiological response.

In dendroisotopic analysis, there has been considerable debate regarding the particular wood component to isolate for determination of isotopic composition especially since cellulose separation has become the rate-limiting step (McCarroll and Loader 2006). Researchers remain divided regarding the particular wood component to analyze and furthermore, the precise extraction techniques necessary. Either α -cellulose (AC) or holocellulose (HC) are generally isolated from whole wood (WW) for stable isotope analyses (Leavitt and Danzer 1993; Van de Water 2002). Restricting analysis to cellulosic compounds assures that mobile oils, lipids, waxes, organic acids and resins, collectively termed as extractives, do not cross-contaminate among annual $\delta^{13}\text{C}$ values

(Leavitt and Danzer 1993; McCarroll and Loader 2006; Harlow et al. 2006). In some studies, both WW and cellulose were found to exhibit a close correspondence in $\delta^{13}\text{C}$ values (Livingston and Spittlehouse 1996; Loader et al. 2003). Therefore, the analysis of WW was preferred over cellulose since chemical processing was not required for the former. Analyzing WW, however, requires careful consideration as each wood component within contains a distinct isotopic signature due to differences in biosynthetic assimilation (Park and Epstein 1961). The isotopically depleted non-cellulose components (extractives, lignin) produced from secondary metabolic pathways (Wilson and Grinstead 1977) present in WW may also vary in proportion among samples (Leavitt and Long 1982) and according to species (Hoper et al. 1998). In fact, lignin and cellulose were shown to be laid down during different times in the growing season (Wilson and Grinstead 1977). Furthermore, since lignin may be susceptible to differential decay in relation to cellulose (Loader et al. 2003), $\delta^{13}\text{C}$ measurements of WW from trees that had died long ago would have to be scrutinized against those from WW of live trees. Borella et al. (1998) have indicated that a residual 5% lignin remaining with cellulose may lower the $\delta^{13}\text{C}$ of cellulose by as much as 0.15‰. The $\delta^{13}\text{C}$ measurements of WW are therefore likely to result in weaker and more variable correlations with climate through time compared to those of HC (Cullen and Grierson 2006).

Hoper et al. (1998) have indicated that the wood component isolated for analyses may depend entirely on the species under investigation i.e. resinous versus non-resinous species. Harlow et al. (2006) have suggested that extraction to HC is largely unnecessary for tree-ring $\delta^{13}\text{C}$ analyses based on a wide range of 44 angiosperm and gymnosperm

species sampled from contrasting environmental conditions. Instead, extractive removal may be the only necessary chemical procedure since a relatively consistent $\delta^{13}\text{C}$ offset of about 1.00‰ was observed between extractive-free wood (EF) and extracted HC. In contrast, extractive removal was deemed unnecessary in both pine and oak standards by other researchers as long as AC was extracted as the end product (Rinne et al. 2005; Boettger et al. 2007). It may be that researchers need to adjust extraction procedures according to the tree species of interest and nature of study. More studies that examine the effects of chemical processing on the $\delta^{13}\text{C}$ values of annually resolved common tree-ring segments among individual tree species, such as Leavitt and Long (1982), Loader et al. (2003) and Taylor et al. (2008), are needed. Such studies are particularly important to determine whether the effects of chemical processing are homogenous among all trees within and between sites prior to chronology building.

Despite the extensive range of *Thuja occidentalis* L. in North America which includes the southern portion of eastern Canada and adjacent northern portion of the United States (Johnston 1990) and a longevity in excess of 1600 years (Larson and Melville 1996), only a scarce number of studies have analyzed the stable carbon isotope ratios of the species. Studies have referred to the isotopic composition of *T. occidentalis* leaf litter i.e. Rosenfeld and Roff (1992) while others have reported the isotopic values of sub-fossil wood submerged in Lake Huron and Lake Michigan (Hunter et al. 2006; Leavitt et al. 2006). The longevity of *T. occidentalis* along with findings from recent studies suggests that it may be an invaluable species for paleoenvironmental reconstruction (Archambault and Bergeron 1992; Tardif and Stevenson 2001; Buckley et

al. 2004). For example, the longest ring-width chronology (2787 years) from eastern North America was developed using *T. occidentalis* from the Niagara Escarpment, southern Ontario, Canada and used to infer hydroclimatic conditions for the past 1400 years (Buckley et al. 2004). The sensitivity of *T. occidentalis* radial growth to moisture availability during the year of ring formation further accents the suitability of this species for long-term reconstruction of drought events (Archambault and Bergeron 1992; Tardif and Stevenson 2001; Buckley et al. 2004). Tree-ring stable carbon isotopic variations are a reflection of current photosynthate influenced by both stomatal resistance and photosynthetic assimilation (Francey and Farquhar 1982). In central Canada, only two $\delta^{13}\text{C}$ tree-ring chronologies have been published (Brooks et al. 1998; Tardif et al. 2008). The *Picea glauca* (Moench) Voss $\delta^{13}\text{C}$ chronology constructed by Tardif et al. (2008) was found to be influenced by climatic parameters over a longer period throughout the growing season than those that affected the ring-width chronology. Additionally, the importance of the seasonal distribution of precipitation for the growth of *Pinus banksiana* (Lamb.) was also revealed by annual carbon isotope analysis (Brooks et al. 1998). However, no studies have explored the potential of *T. occidentalis* in stable isotope dendroclimatology. Long *T. occidentalis* stable carbon isotope chronologies may reveal previously undocumented environmental responses of this species.

Given that dendroisotopic studies only give passing reference to the stable isotopic composition of *T. occidentalis* and that a lack of consensus exists as to whether cellulose extraction is necessary, the objectives of this study were i) to report on the range of modern tree-ring $\delta^{13}\text{C}$ values of *T. occidentalis* in whole wood, extractive-free wood,

holocellulose and α -cellulose; ii) to compare modern $\delta^{13}\text{C}$ values of *T. occidentalis* with published values of sub-fossil *T. occidentalis* wood and iii) to recommend a wood component to isolate for future $\delta^{13}\text{C}$ analysis of *T. occidentalis* tree-rings.

2.3. Materials and Methods

2.3.1. Study area

Disjunct populations of *T. occidentalis* are found northwest of the species' continuous range in the inter-lake region of central Manitoba along The Pas end moraine (53°00'N, 99°50'W) between Cedar Lake and Lake Winnipeg (Scoggan 1957). In this region, old-growth *T. occidentalis* stands occur at both hydric and xeric sites (Tardif and Stevenson 2001). For this study, eight dead trees 279-459 years of age growing in hydric conditions were selected from two sites (02 and 17). The $\delta^{13}\text{C}$ values of progressively purified cellulose were examined from cross-dated *T. occidentalis* cross-sections. Site-02 contains trees with concentric radial growth whereas, eccentric radial growth characterizes the majority of trees at site-17.

2.3.2. Sample preparation

On each wood cross-section of the eight *T. occidentalis* trees, two 1.2cm by 1.2cm radial blocks of variable length containing the tree-ring segment formed from 1901 to 1910 AD were separated using a band saw followed by a scalpel. These segments were all extracted from the heartwood. These radial blocks were excised at approximately ninety-degrees in relation to one another whenever possible. The radial blocks were then sanded with progressively finer sandpaper on all sides and wood dust

was vacuumed in between the sandings. To ensure homogeneity, both ten-year segments of each tree were pooled and ground with a Wiley Intermediate Mill (Thomas Scientific, Swedesboro, NJ) to pass through a 20-mesh screen. It is possible that the 20-mesh size used during the milling of samples could have resulted in sample inhomogeneity as noted by Borella et al. (1998). However, a fineness of 115-mesh as proposed by Borella et al. (1998) would have increased sample processing time and may not be easily feasible for projects requiring many samples to be analyzed. The ground wood material from each tree-ring decade was then equally separated into four vials. Of the four vials, the wood in one vial was retained for WW analysis while wood in the remaining three vials were transferred into F57 filter pouches (ANKOM Technology, Macedon, NY) and heat sealed. This resulted in three filter pouches per tree containing the tree-rings formed from 1901 to 1910. Of these three pouches per tree, each underwent one of three treatments to result in EF, HC or AC.

2.3.3. Chemical extraction

Gaudinski et al. (2005) have shown that the Jayme-Wise method of cellulose extraction was the most reliable compared to the other methods they had studied. Correspondingly, batch extraction of samples to HC followed the Jayme-Wise method as modified by Leavitt and Danzer (1993). For treatment-1 resulting in EF, extractives were removed from the samples of all three pouches from each tree using the soxhlet extraction process with the reservoir flask filled with 2:1 toluene:ethanol and run for 24 hours. Afterwards, this mixture was replaced with 100% ethanol and run for another 24 hours. For treatment-2 resulting in HC, two pouches containing EF from each tree were

placed in an acidified sodium chlorite solution for 48 hours at 70°C to remove the lignin. Samples were then rinsed with deionized water until conductivity reached < 5µmho/cm. Following treatment-2, one pouch was set aside while the remaining pouch went to treatment-3 where hemicelluloses were separated from HC to yield AC. The remaining pouch continued through a 17.5% sodium hydroxide (NaOH) wash for 1 hour (Pettersen 1984). Following the NaOH wash, the pouch was rinsed with deionized water and stirred in a 10% glacial acetic acid solution for one hour and rinsed again. Pouches were oven-dried at 70°C for 12 hours and weighed prior to and after each chemical extraction to calculate the percentage of sample remaining following processing.

Subsequently, the % yield of each sample was calculated following each treatment as the ratio of dry weight remaining relative to that of WW. For each sample, this resulted in three, two and one % yield replicate(s) for EF, HC and AC, respectively. The mean % yield of EF, HC and AC was then calculated. It should be noted that the weight of each individual pouch, which was weighed prior to any chemical extraction, was subtracted from the measurement at each weighing. All samples were weighed using a Mettler Toledo AX26 electrical balance (resolution of 2 µg). For each sample, approximately 0.5mg of WW, EF, HC or AC was weighed and encased in a tin foil capsule. Samples were measured for $^{13}\text{C}/^{12}\text{C}$ composition and percent carbon (% C) using a continuous flow stable isotope mass-spectrometer at the Environmental Isotope Laboratory, Department of Geosciences, University of Arizona. The $\delta^{13}\text{C}$ values are expressed in ‰ relative to the Vienna PeeDee belemnite (VPDB) standard. The

analytical precision was 0.10‰ and ~1.2‰ for all $\delta^{13}\text{C}$ and % C measurements, respectively.

2.3.4. Statistical analysis

From the decadal tree-ring segments, the mean and standard deviation of all samples was determined for each wood component. To compare the effect of extractive, lignin and hemicellulose removal, paired t-tests were used to test whether $\delta^{13}\text{C}$ values differed among wood fractions (WW, EF, HC and AC) originating from the same tree. All statistical analyses were conducted with Systat (v. 11) for Windows (SYSTAT 2004a) and SigmaPlot (v. 9.01) for Windows (SYSTAT 2004b).

2.4. Results/Discussion

2.4.1. Enriched *Thuja occidentalis* tree-ring cellulose

The leaves of evergreen species are usually more water-use efficient than those of deciduous species and hence contain enriched $\delta^{13}\text{C}$ values (Marshall and Zhang 1994). Compared to other evergreen species, *T. occidentalis* was found to have much more enriched $\delta^{13}\text{C}$ values (Table 2.1) and exceeded the positive extreme of the typical C_3 plant $\delta^{13}\text{C}$ range for whole tissue (-33 to -23‰) reported by Sharp (2007). In this study, *T. occidentalis* $\delta^{13}\text{C}$ values obtained for HC from the decadal tree-ring segments ranged from -22.1 to -19.8‰. Sample 17-5 consistently showed the most enriched $\delta^{13}\text{C}$ values relative to those of other samples (Table 2.1). Some examples of more typical $\delta^{13}\text{C}$ values were found in the AC of *P. glauca* and HC of *P. banksiana* $\delta^{13}\text{C}$ chronologies from central Canada which were shown to have ranges of -25.3 to -22.6‰ and -25.3 to -

22.3‰, respectively (Brooks et al. 1998; Tardif et al. 2008). Enriched $\delta^{13}\text{C}$ values of HC within or close to the range of those observed in our study appear to be characteristic of scale-leaved evergreen species and have been reported for *Juniperus monosperma* (Engelm.) Sarg. (Leavitt and Long 1982), *Callitris glaucophylla* J. Thompson and L.A.S. Johnson (Cullen and Macfarlane 2005) and *Thuja plicata* Donn ex D.Don (Harlow et al. 2006). Hence, similar $\delta^{13}\text{C}$ values to *T. occidentalis* are also observed in other plants within *Cupressaceae* or in those evergreen species with comparatively similar leaf morphology.

Thuja occidentalis was also found to be the most $\delta^{13}\text{C}$ -enriched when HC was analyzed among different tree species sampled from the remains of a submerged Holocene coniferous forest in Lake Huron and Lake Michigan (Hunter et al. 2006; Leavitt et al. 2006). In support of these findings, *Thuja plicata* (western red-cedar) leaves were found to exhibit the highest mean $\delta^{13}\text{C}$ values among those of many native coniferous and deciduous tree species in the north-central Rockies (Marshall and Zhang 1994) and in Montana and Idaho (Korol 2001). Differences in the $\delta^{13}\text{C}$ values of samples at a particular location varied according to species and leaf morphology (i.e. deciduous versus evergreen) as well as within and among altitudes (Marshall and Zhang 1994). Moreover, the scale-leaves of *Juniperus* spp. have been shown to contain many xeric adaptations including reduced surface area, thick cuticle, overlapping leaves, and reduced stomata density and sunken stomata, all of which minimize evapotranspiration (Johnsen 1963; Miller and Shultz 1987). It is possible that the distinct scale-leaf compared to

needle-leaf architecture in conifers may predispose the former for enhanced water-use efficiency (Zhang and Cregg 1996; Korol 2001).

In our study, the *T. occidentalis* $\delta^{13}\text{C}$ values obtained for HC (Table 2.1) were similar to those reported by Hunter et al. (2006) for HC from submerged sub-fossil *T. occidentalis* wood which ranged from -23.8 to -20.8‰. Our values also remained in the same range after the depletion of $\delta^{13}\text{C}$ associated with the increase in atmospheric CO_2 from fossil fuel emissions since 1850 AD was taken into account. During the decade 1901 to 1910, atmospheric $\delta^{13}\text{C}$ values were reported to deviate from -0.28 to -0.24‰ with respect to the pre-industrial standard of -6.4‰ (McCarroll and Loader 2006). Larson and Melville (1996) have also shown that the wood anatomy of annual rings in early Holocene *T. occidentalis* trees was similar to that in modern specimens from the Niagara Escarpment, Canada. Although no chemical analysis was conducted, scanning electron microscope photographs of the cross- and radial-sections of Holocene-age *T. occidentalis* wood tissue showed remarkably little microbial decay. The similarity in range of $\delta^{13}\text{C}$ values between HC from modern (this study) and HC from sub-fossil *T. occidentalis* wood 6420-7095 ^{14}C years before present (Hunter et al. 2006) further stress the high water-use efficiency of *T. occidentalis* relative to needle-leaved conifers.

2.4.2. Comparison of wood tissue fractions

The % yield of all samples decreased consistently relative to WW with successive chemical treatment (sample % yield means: EF, 85.5±4.0, n=24; HC, 66.3±4.0, n=16; AC, 34.1±8.2, n=8; Figure 2.1a). Similar % yields of 59 and 44 for HC and AC,

respectively, were reported by Pettersen (1984) for *T. occidentalis* wood. Increased processing up to HC progressively enriched $\delta^{13}\text{C}$ values and progressively decreased % C (Table 2.1). The most pronounced successive $\delta^{13}\text{C}$ enrichment and decrease in % C were recorded in HC after lignin removal (Figure 2.1bc; Table 2.1). However, processing from HC to AC led to depletion in $\delta^{13}\text{C}$ values of samples and yield but to an increase of % C of samples (Table 2.1). These results are consistent with those reported for *C. glaucophylla* (Cullen and Macfarlane 2005). We presume that this rise in % C is a result of decreased carbon contents of hemicelluloses, low molecular-weight polysaccharides, that when removed, consequently increase % C of AC. The transition from HC to AC was also marked by relatively low yield of AC that was almost two times lower than HC and representing as little as a quarter of the original WW. Similarly, Timell (1967) found that hemicelluloses accounted for 26% of EF in *T. occidentalis*. Loader et al. (2002) have reported the yield of AC to be 30% while that of HC retained a yield of 50%. Since samples frequently contain extremely narrow tree-rings, particular caution should be taken regarding the treatment type.

2.4.3. Carbon isotopic change from extractive, lignin and hemicellulose removal

Isotopic offsets among all wood components were found to be statistically significant following paired t-tests (Figure 2.2). The largest mean offset in $\delta^{13}\text{C}$ between treatments occurred after lignin removal, EF to HC, whereas the slightest mean offsets occurred after extractive and hemicellulose removal, WW to EF and HC to AC, respectively. Extractive removal resulted in a mean enrichment of 0.26‰ among samples (Figure 2.2). Similarly, Harlow et al. (2006) have shown extractive removal to

account for a mean shift of -0.25‰. They suggested that it may be necessary to remove these mobile contaminants from conifer wood which typically contain high amounts of resin. Moreover, Taylor et al. (2008) have shown that the extractives in heartwood were twice as high as that found in sapwood. Leavitt (1987) and subsequently Taylor et al. (2008) thus recommended extractive removal where both heartwood and sapwood are to be analyzed.

Lignin raises % C since it is comprised of about 67% C (Vertregt and Penning De Vries 1987) and contains around 50% more carbon per unit weight than cellulose (Benner et al. 1987). Removal of lignin was accompanied by a mean decrease of nearly 15% C and enrichment of 1.64‰ after HC was isolated from EF (Figure 2.2). In contrast, Harlow et al. (2006) have reported a relatively consistent $\delta^{13}\text{C}$ offset of about +1.07‰ following lignin removal from EF among their samples. Helle and Schleser (2004), in closer agreement with results from our study, found a +0.50-1.80‰ offset from WW to HC in *Fagus sylvatica* L., which they indicate may have been caused by varying proportions of lignin among tree-rings. For example, compression wood has a higher lignin-to-cellulose content compared to normal wood (Timell 1967). Lignin should therefore also be removed since it is a secondary metabolite and most strongly influences tree-ring $\delta^{13}\text{C}$ values after cellulose.

Increased processing, from HC to AC has been shown to yield enriched mean $\delta^{13}\text{C}$ values ranging from 0.34-1.03‰ in C_3 plants (Borella et al. 1998; Hoper et al. 1998). However, other studies, including ours, have reported contradictory results of

more depleted $\delta^{13}\text{C}$ values in AC in comparison to HC (Cullen and Macfarlane 2005; Boettger et al. 2007). According to Boettger et al. (2007), isotopic differences in sign of change from HC to AC relate to the presence of residual hemicelluloses after treatment with NaOH solution. Since pure AC is referred to that portion of HC insoluble in 17.5% NaOH (Pettersen 1984), differing results could be expected from those studies where less concentrated solutions were used during purification. In our study, % C measured in AC remained consistent throughout our samples ranging from 40.1 to 40.8% with the lowest standard deviation of ± 0.2 (Table 2.1; Figure 2.1b). Percent C measured in AC was very close to that of the expected range (~41-45%) of relative carbon content for cellulose (Brendel et al. 2000) as well as the theoretical carbon composition of pure cellulose, $\text{C}_6\text{H}_{10}\text{O}_5$, (Pettersen 1984) of 44% as per stoichiometry. The greater consistency of % C values in our AC samples over those of other wood components may further indicate slightly better reproducibility regarding $\delta^{13}\text{C}$ values for AC. Laboratories that used 4 – 10% NaOH solutions were found to yield more $\delta^{13}\text{C}$ -enriched cellulose (Boettger et al. 2007). For example, studies where $\leq 5\%$ NaOH solution (Borella et al. 1998; Hoper et al. 1998) was used as the final step in cellulose purification resulted in incomplete removal of $\delta^{13}\text{C}$ -enriched hemicelluloses and therefore the final product could still be considered as HC rather than AC (Boettger et al. 2007). In light of this, it remains uncertain why several studies have reported mixed results (both enriched as well as depleted AC relative to HC) despite having treated their samples with 17% NaOH solution (Sheu and Chiu 1995; Van de Water 2002). One reason may be the inclusion of reaction wood in their analysis. Hemicelluloses are present at unusually high quantities in reaction wood (Pettersen 1984) some of which may still reside during $\delta^{13}\text{C}$ analysis of AC contributing

to elevated values. It should be noted that the presence of wood ash along with samples during analysis should not significantly affect $\delta^{13}\text{C}$ results since ash usually constitutes less than one percent of wood from temperate zones and it was shown to be present in *T. occidentalis* wood at 0.5% (Pettersen 1984). Nonetheless, precise extraction techniques require that all $\delta^{13}\text{C}$ variations be accounted to ensure the robustness of dendroisotopic research.

It is important to underscore the benefit to the dendroisotopic research community of standardizing an extracted cellulose component for isotopic analysis. Just as ring-width chronologies all contain annual ring-width measurements; a standard cellulose unit of comparison would encourage researchers to develop isotope networks more readily, thereby enabling them to answer questions of broader scope. Alternatively, Van de Water (2002) suggested the use of predetermined constants to extrapolate tree-ring $\delta^{13}\text{C}$ results thereby allowing the researcher to conduct inter-study comparisons where different wood components were analyzed. In our study, HC was found to be enriched by a mean of 0.40‰ relative to AC in agreement with the maximum of that found by Boettger et al. (2007) for six *Pinus* and *Quercus* species. Since this isotopic offset is also usually accompanied by comparably similar $\delta^{13}\text{C}$ inter-annual trends (Loader et al. 2002), extraction to HC is recommended and a $\delta^{13}\text{C}$ adjustment of 0.40‰ should be subtracted from HC to estimate AC where absolute values are desired. However, the estimation of $\delta^{13}\text{C}$ values of either WW or EF from those of HC or AC may not be feasible given that extractive and lignin content have been known to vary among rings.

2.5. Conclusion

Thuja occidentalis tree-ring $\delta^{13}\text{C}$ values were found to fall within the range of those observed for scale-leaved evergreen species but were enriched compared to values for tree species with broad- or needle-leaves published in the literature. Higher water-use efficiency of *T. occidentalis* trees relative to other needle-leaved conifers was indicated by enriched $\delta^{13}\text{C}$ values. Furthermore, the $\delta^{13}\text{C}$ values for HC from modern *T. occidentalis* (this study) exhibited a similar range to those for HC from sub-fossil *T. occidentalis* wood 6420-7095 ^{14}C years before present as reported in the literature. Both extractive and lignin removal in our study resulted in enriched $\delta^{13}\text{C}$ values and decreased % carbon while the inverse was found after hemicellulose removal. We attribute the latter to the enriched $\delta^{13}\text{C}$ values and presumably lower % C of hemicelluloses relative to AC. These results confirm those from previous studies regarding the efficacy of following a well-established chemical extraction methodology in dendroisotopic studies. Additional sources of $\delta^{13}\text{C}$ variation resulting from the presence of extractives and lignin may compromise the precision required for these studies. Lignin extraction resulted in the greatest $\delta^{13}\text{C}$ enrichment among individual processing steps and should not be disregarded since its proportions within samples have been shown to vary as reported in the literature. Both extractive and lignin removal are recommended using the procedure described above although hemicellulose extraction may not be feasible where very narrow tree-rings are present as mean AC % yield was shown to be approximately half that of HC. We recommend extracting to HC for $\delta^{13}\text{C}$ analyses although an isotopic offset of 0.40‰ should be subtracted from HC to estimate AC where absolute values are

desired. However, caution is advised as use of a predetermined offset may only be applicable for stable carbon isotope analyses among tree species with comparable leaf morphology and under similar environmental conditions.

2.6. Acknowledgments

We thank F. Conciatori, our dendrochronology technician, D. Ko Heinrichs for his great help in the field and the lab assistants: J. Waito and S. Gietz. Thanks also go to C. Eastoe from the Environmental Isotope Laboratory, University of Arizona. We also acknowledge the two anonymous reviewers and associate editor for their helpful comments on the manuscript. The Mettler Toledo AX26 electrical balance was kindly provided by the Department of Geography, University of Winnipeg. This research was undertaken, in part, thanks to funding from the Canada Research Chairs Program, the National Sciences and Engineering Research Council of Canada (NSERC) and the University of Winnipeg. During this study, the first author also benefited from a scholarship awarded by the University of Manitoba.

2.7. References

Archambault, S., and Bergeron, Y. 1992. An 802-year tree-ring chronology from the Quebec boreal forest. *Can. J. For. Res.* **22**: 674-682.

Benner, R., Marilyn, L., Fogel, E., Sprague, K., and Hodson, R.E. 1987. Depletion of ^{13}C in lignin and its implications for stable isotope studies. *Nature* **329**(22): 708-710.

Boettger, T., Haupt, M., Knoller, K., Weise, S. M., Waterhouse, J. S., Rinne, K. T., Loader, N. J., Sonninen, E., Jungner, H., Masson-Delmotte, V., Stievenard, M., Guillemin, M. T., Pierre, M., Pazdur, A., Leuenberger, M., Filot, M., Saurer, M., Reynolds, C. E., Helle, G., and Schleser, G. H. 2007. Wood cellulose preparation methods and mass spectrometric analyses of delta C-13, delta O-18, and nonexchangeable delta H-2 values in cellulose, sugar, and starch: An interlaboratory comparison. *Anal. Chem.* **79**(12): 4603–4612.

Borella, S., Leuenberger, M., Saurer, M., and Siegwolf, R. 1998. Reducing the uncertainties in $\delta^{13}\text{C}$ analysis of tree rings: pooling, milling, and cellulose extraction. *J. Geophys. Res.* **103**(D16): 19519-19526.

Brendel, O., Iannetta, P.P.M., and Stewart, D. 2000. A rapid and simple method to isolate pure alpha-cellulose. *Phytochem. Analysis* **11**: 7-10.

Brooks, J.R., Flanagan, L.B., and Ehleringer, J.R. 1998. Responses of boreal conifers to climate fluctuations: indications from tree-ring widths and carbon isotope analyses. *Can. J. For. Res.* **28**: 524-533.

Buckley, B.M., Wilson, R.J.S., Kelly, P.E., Larson, D.W., and Cook, E.R. 2004. Inferred summer precipitation for southern Ontario back to AD 610, as reconstructed from ring widths of *Thuja occidentalis*. *Can. J. For. Res.* **34**(12): 2541-2553.

Cullen, L.E., and Grierson, P.F. 2006. Is cellulose extraction necessary for developing stable carbon and oxygen isotopes chronologies from *Callitris glaucophylla*? *Palaeogeogr. Palaeocl.* **236**: 206-216.

Cullen, L.E., and Macfarlane, C. 2005. Comparison of cellulose extraction methods for analysis of stable isotope ratios of carbon and oxygen in plant material. *Tree Physiol.* **25**: 563-569.

Francey, R.J., and Farquhar, G.D. 1982. An explanation of $^{13}\text{C}/^{12}\text{C}$ variations in tree rings. *Nature* **297**: 28-31.

Gaudinski, J.B., Dawson, T.E., Quideau, S., Schuur, E.A.G., Roden, J.S., Trumbore, S.E., Sandquist, D.R., Oh, S-W., and Wasylishen, R.E. 2005. Comparative analysis of cellulose

preparation techniques for use with ^{13}C , ^{14}C , and ^{18}O isotopic measurements. *Anal. Chem.* **77**: 7212-7224.

Harlow, B.A., Marshall, J.D., and Robinson, A.P. 2006. A multi-species comparison of $\delta^{13}\text{C}$ from whole wood, extractive-free wood and holocellulose. *Tree Physiol.* **26**: 767-774.

Helle, G., and Schleser, G.H. 2004. Beyond CO_2 -fixation by Rubisco – an interpretation of $^{13}\text{C}/^{12}\text{C}$ variations in tree rings from novel intra-seasonal studies on broad-leaf trees. *Plant Cell Environ.* **27**: 367-380.

Hoper, S.T. McCormac, F.G., Hogg, A.G., Higham, T.F.G., and Head, M.J. 1998. Evaluation of wood pretreatments on oak and cedar. *Radiocarbon* **40**(1): 45-50.

Hughes, M.K. 2002. Dendrochronology in climatology – the state of the art. *Dendrochronologia* **20**: 95-116.

Hunter, R.D., Panyushkina, I.P., Leavitt, S.W., Wiedenhoeft, A.C., and Zawiskie, J. 2006. A multiproxy environmental investigation of Holocene wood from a submerged conifer forest in Lake Huron, USA. *Quaternary Res.* **66**: 67-77.

Johnsen, T.N. Jr. 1963. Anatomy of scalelike leaves of Arizona junipers. *Bot. Gaz.* **124**: 220-224.

Johnston, W.F. 1990. Northern white-cedar (*Thuja occidentalis* L.). In *Silvics of North America*. Vol. 1. Conifers. *Edited by* R.M. Burns, and B.H. Honkala. U.S. Department of Agriculture Forest Service. Washington, D.C., Agriculture Handbook 654.

Korol, R.L. 2001. Physiological attributes of 11 Northwest conifer species. For. Serv. Gen. Tech. Rep. RMRS-GTR-73. USDA, Washington.

Larson, D.W., and Melville, L. 1996. Stability of wood anatomy of living and Holocene *Thuja occidentalis* L. derived from exposed and submerged portions of the Niagara Escarpment. *Quaternary Res.* **45**: 210-215.

Leavitt, S.W. 1987. Stable-carbon isotopes in tree rings as environmental indicators. In *The practical applications of trace elements and isotopes to environmental biogeochemistry and mineral resources evaluation*. *Edited by* R.W. Hurst, T.E. Davis, and S.S. Augustithis. Theophrastus Publications, S.A., Athens. pp. 61-73.

Leavitt, S.W., and Danzer, S.R. 1993. Method for batch processing small wood samples to holocellulose for stable-carbon isotope analysis. *Anal. Chem.* **65**: 87-89.

Leavitt, S.W., and Long, A. 1982. Evidence for ^{13}C and ^{12}C fractionation between tree leaves and wood. *Nature* **298**: 742-744.

Leavitt, S.W., Panyushkina, I.P., Lange, T., Wiedenhoeft, A., Cheng, L., Hunter, R.D., Hughes, J., Pranschke, F., Schneider, A.F., Moran, J., and Stieglitz, R. 2006. Climate in the Great Lakes region between 14,000 and 4000 years ago from isotopic composition of conifer wood. *Radiocarbon* **48**(2): 205-217.

Livingston, N.L., and Spittlehouse, D.L. 1996. Carbon isotope fractionation in tree rings early and late wood in relation to intra-growing season water balance. *Plant Cell Environ.* **19**: 768-774.

Loader, N.J., Robertson, I., Lücke, A., and Helle, G. 2002. Preparation of holocellulose from standard increment cores for stable carbon isotope analysis. *Swansea Geographer* **37**: 1-9.

Loader, N.J., Robertson, I., and McCarroll, D. 2003. Comparison of stable carbon isotope ratios in the whole wood, cellulose and lignin of oak tree-rings. *Palaeogeogr. Palaeoclimatol.* **196**: 395-407.

Marshall, J.D., and Zhang, J. 1994. Carbon isotope discrimination and water-use efficiency in native plants of the north-central Rockies. *Ecology* **75**(7): 1887-1895.

McCarroll, D., and Loader, N.J. 2006. Isotopes in tree rings. *In* *Developments in paleoenvironmental research vol. 10: isotopes in palaeoenvironmental research. Edited by M.J. Leng.* Springer, The Netherlands. pp. 67-106.

Miller, R.F., and Shultz, L.M. 1987. Water relations and leaf morphology of *Juniperus occidentalis* in the northern Great Basin. *Forest Sci.* **33**: 690-706.

Park, R., and Epstein, S. 1961. Metabolic fractionation of C¹³ & C¹² in plants. *Plant Physiol.* **36**: 133-138.

Pettersen, R.C. 1984. The chemical composition of wood. *In* *The Chemistry of Solid Wood*. Edited by R.M. Rowell. American Chemical Society, Washington, D.C. pp. 57-126.

Rinne, K.T., Boettger, T., Loader, N.J., Robertson, I., Switsur, V.R., and Waterhouse, J.S. 2005. On the purification of α -cellulose from resinous wood for stable isotope (H, C and O) analysis. *Chem. Geol.* **222**: 75-82.

Rosenfeld, J.S., and Roff, J.C. 1992. Examination of the carbon base in southern Ontario streams using stable isotopes. *J. N. Am. Benthol. Soc.* **11**(1): 1-10.

Scoggan, H.J. 1957. *Flora of Manitoba*. National Museum of Canada. Department of Northern Affairs and National Resources, Ottawa.

Sharp, Z. 2007. *Principles of stable isotope geochemistry*. Prentice Hall, New Jersey.

Sheu, D.D., and Chiu, C.H. 1995. Evaluation of cellulose extraction procedures for stable carbon isotope measurement in tree ring research. *Int. J. Environ. An. Ch.* **59**: 59-67.

Switsur, V.R., and Waterhouse, J.S. 1998. Stable isotopes in tree ring cellulose. *In* *Stable Isotopes: integration of biological, ecological and geochemical processes*. Edited by H. Griffiths. BIOS scientific publishers Ltd., Oxford, U.K. pp. 303-316.

SYSTAT. 2004a. SYSTAT 11: statistics I. Systat Software Incorporated, Richmond, California.

SYSTAT. 2004b. SigmaPlot 9.01. Systat Software Incorporated, Richmond, California.

Tardif, J., and Stevenson, D. 2001. Radial growth-climate association of *Thuja occidentalis* L. at the northwestern limit of its distribution, Manitoba, Canada. *Dendrochronologia* **19**(2): 179-187.

Tardif, J., Conciatori, F., and Leavitt, S. 2008. Tree rings, $\delta^{13}\text{C}$ and climate in *Picea glauca* growing near Churchill, subarctic Manitoba, Canada. *Chem. Geol.* **252**: 88-101.

Taylor, A.M., Brooks, J.R., Lachenbruch, B., Morrell, J.J., and Voelker, S. 2008. Correlation of carbon isotope ratios in the cellulose and wood extractives of Douglas-fir. *Dendrochronologia* **26**: 125-131.

Timell, T.E. 1967. Recent progress in the chemistry of wood hemicelluloses. *Wood Sci. Technol.* **1**: 45-70.

Van de Water, P. 2002. The effect of chemical processing on the $\delta^{13}\text{C}$ value of plant tissue. *Geochim. Cosmochim. Ac.* **66**: 1211-1219.

Vertregt, N., and Penning De Vries, F.W.T. 1987. A rapid method for determining the efficiency of biosynthesis of plant biomass. *J. Theor. Biol.* **128**: 109-119.

Wilson, A.T., and Grinsted, M.J. 1977. $^{12}\text{C}/^{13}\text{C}$ in cellulose and lignin as palaeothermometers. *Nature* **265**: 133-135.

Zhang, J.W., and Cregg, B.M. 1996. Variation in stable carbon isotope discrimination among and within exotic conifer species grown in eastern Nebraska, USA. *Forest Ecol. Manag.* **83**: 181-187.

List of Figures

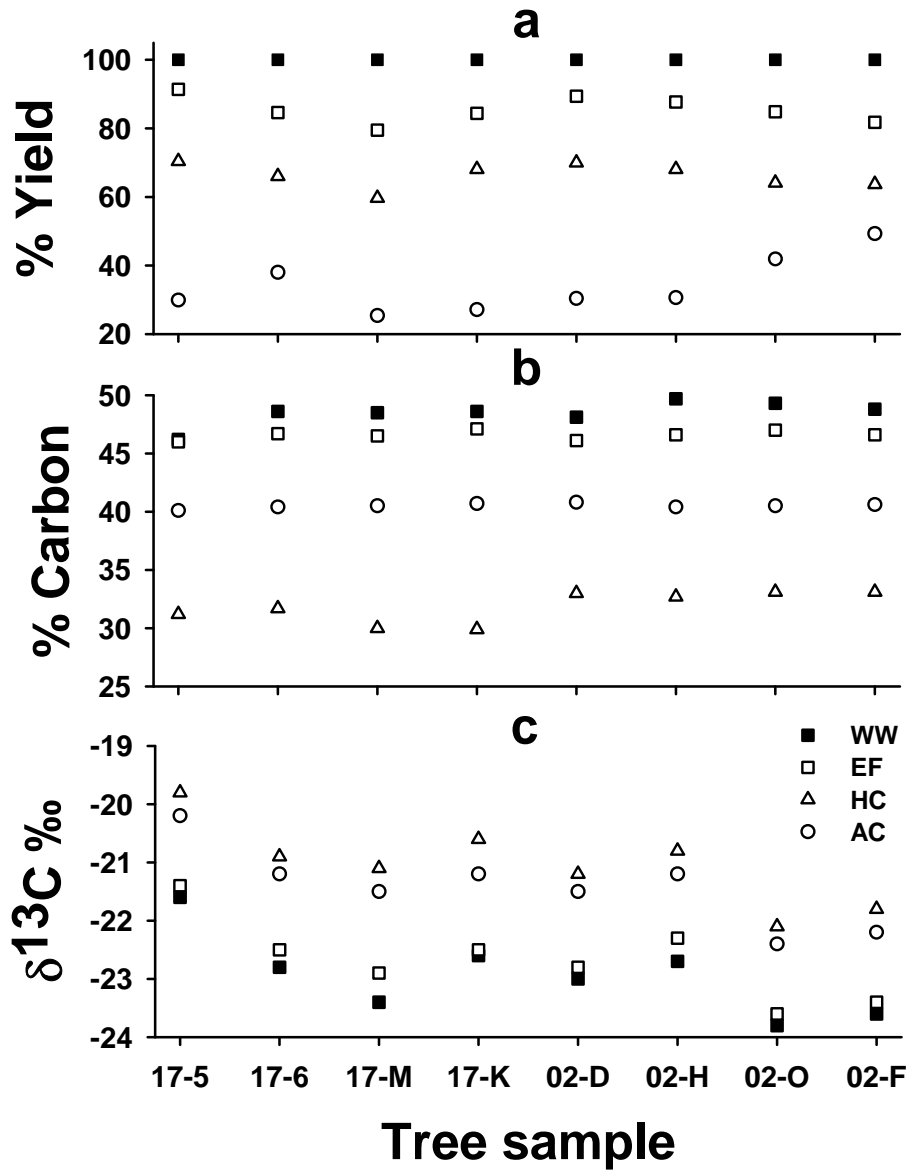


Figure 2.1. *Thuja occidentalis* decadal whole wood (WW), extractive-free wood (EF), holocellulose (HC) and α -cellulose (AC) samples showing a) % yield (EF, n=24; HC, n=16; AC, n=8), b) % carbon (n=8), and c) $\delta^{13}\text{C}$ values (n=8).

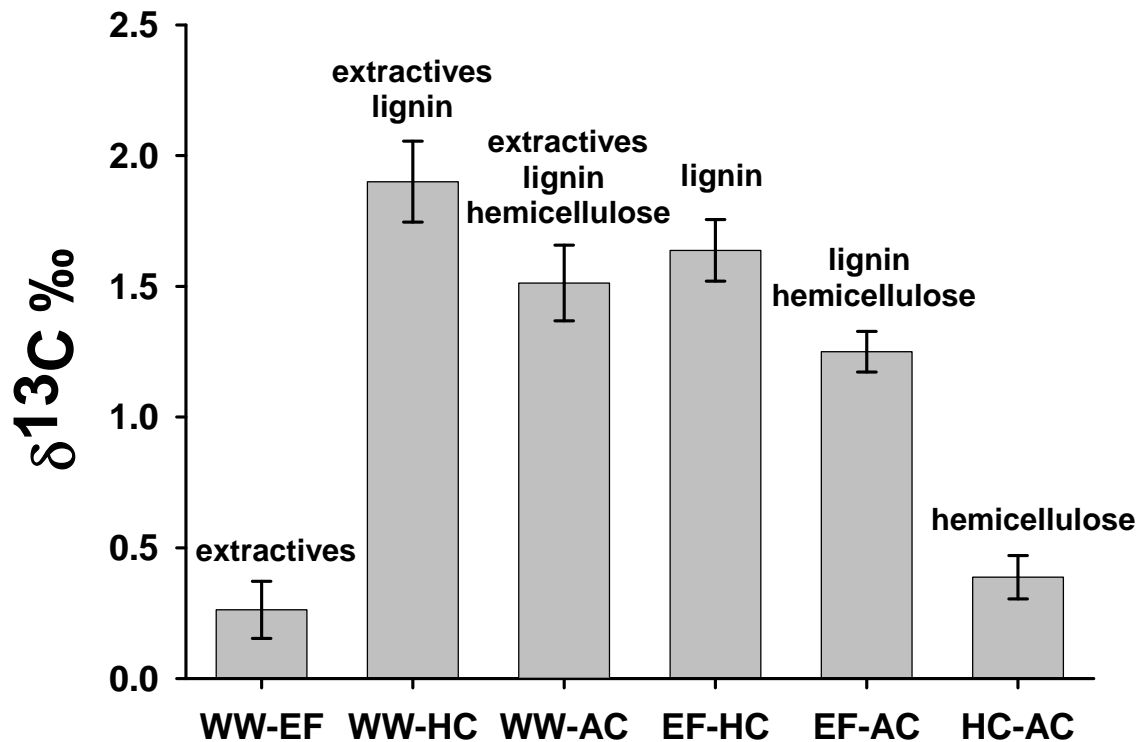


Figure 2.2. Mean absolute difference (offset) of paired wood components as indicated from paired t-tests. The text above each bar lists the wood fraction(s) theoretically removed between the two wood components. All comparisons were found to be statistically significant ($p \leq 0.001$, $n=8$); the 95% confidence intervals are also shown.

List of Tables

Table 2.1. $\delta^{13}\text{C}$ and % C for each decadal tree segment of whole wood (WW), extractive-free wood (EF), holocellulose (HC) and α -cellulose (AC).

Sample	WW		EF		HC		AC	
	$\delta^{13}\text{C}$ ‰	% C	$\delta^{13}\text{C}$ ‰	% C	$\delta^{13}\text{C}$ ‰	% C	$\delta^{13}\text{C}$ ‰	% C
17-5	-21.6	46.2	-21.4	46.0	-19.8	31.2	-20.2	40.1
17-6	-22.8	48.6	-22.5	46.7	-20.9	31.7	-21.2	40.4
17-M	-23.4	48.5	-22.9	46.5	-21.1	30.0	-21.5	40.5
17-K	-22.6	48.6	-22.5	47.1	-20.6	29.9	-21.2	40.7
02-D	-23.0	48.1	-22.8	46.1	-21.2	33.0	-21.5	40.8
02-H	-22.7	49.7	-22.3	46.6	-20.8	32.7	-21.2	40.4
02-O	-23.8	49.3	-23.6	47.0	-22.1	33.1	-22.4	40.5
02-F	-23.6	48.8	-23.4	46.6	-21.8	33.1	-22.2	40.6
Mean	-22.9	48.5	-22.7	46.6	-21.0	31.8	-21.4	40.5
±SD	±0.7	±1.0	±0.7	±0.4	±0.7	±1.4	±0.7	±0.2

3.0 Ring-width and $\delta^{13}\text{C}$ chronologies from *Thuja occidentalis* L. trees as recorders of drought

3.1. Abstract

Stable carbon isotopes ($\delta^{13}\text{C}$) fixed in tree-rings are dependent upon environmental conditions during their assimilation into leaf tissues. Old *Thuja occidentalis* trees were sampled at their northwestern limit of distribution in central Manitoba, Canada. The objectives of the study were 1) to investigate the association between tree-ring $\delta^{13}\text{C}$ values and radial growth in addition to the response of these variables to climate and 2) to provide a multi-century inference of drought events based on tree-ring $\delta^{13}\text{C}$ and ring width analyses. Fifteen *T. occidentalis* trees were selected for $\delta^{13}\text{C}$ analysis and holocellulose was isolated from each tree-ring through standard chemical extraction techniques. The $\delta^{13}\text{C}$ chronology spanned from 1650 to 2006 A.D. and incorporated dead and living *T. occidentalis* trees selected from two sites. Ring-width chronologies were also developed from both dead and living *T. occidentalis* trees from the region. Compared to the $\delta^{13}\text{C}$ values, ring width was more often associated with climate conditions in the year prior to ring formation. During the year of ring-formation, ring width was associated with spring and early summer conditions whereas, $\delta^{13}\text{C}$ was more indicative of overall summer conditions. However, conditions conducive to moisture stress were important for both radial growth and carbon assimilation, particularly during the month of June in the current growing season. During this month, the ring-width index was sensitive to moisture stress (positive and negative association with precipitation and temperature, respectively) whereas the $\delta^{13}\text{C}$ index showed enrichment with increasing

temperature and drought index. Our results also suggest that ring width may be more sensitive to prolonged drought than $\delta^{13}\text{C}$ since periods of decreased radial growth most often coincided with documented drought intervals. Nonetheless, each of ring width and $\delta^{13}\text{C}$ contains individualistic climate information which could be used in tandem for long-term climate reconstruction.

Keywords: dendroclimatology; stable carbon isotope; Northern white-cedar; disjunct population; drought; temporal stability; Manitoba

3.2. Introduction

Tree-ring chronologies developed from old trees whose ring widths are sensitive to climatic variations are essential in dendroclimatology (Fritts 1976; Schweingruber 1996). Conventional tree-ring records i.e. ring-width indices have been used to acquire past climatic information in dendroclimatology (Schweingruber 1996) and they have been utilized for large-scale temperature reconstructions (Jones et al. 1998; Esper et al. 2002; Moberg et al. 2005). Tree growth is, however, influenced by a large number of environmental variables which include but are not limited to stand dynamics, water availability, temperature, solar radiation and available soil nutrients (Fritts 1976; Schweingruber 1996). On the Canadian Prairie region, Ontario and adjacent northern United States (Montana, North Dakota and Minnesota), ring-width chronologies recently showed that drought displayed considerable spatial heterogeneity during the last 500 years (St. George et al. 2009). However, these ring-width chronologies were shown to be relatively poor indicators of drought severity and hydrological conditions. Consequently, St. George et al. (2009) have advocated that more promising results might be obtained by the inclusion of more contemporary tree-ring parameters (earlywood/ latewood width, wood density and tree-ring stable isotopes) along with ring-width chronologies.

European studies have shown that better climate reconstructions may originate with the inclusion of two or more tree-ring parameters in addition to ring width alone i.e. latewood density and tree-ring $\delta^{13}\text{C}$ (McCarroll et al. 2003; Gagen et al. 2006; Kirilyanov et al. 2008). Gessler et al. (2009) have remarked that stable isotopes in

dendrochronology combine the advantage of the precisely dated annual resolution of tree-rings with the sensitivity of stable isotope ratios as governed by ecophysiological processes and ultimately, the environment. Tree-ring $\delta^{13}\text{C}$ indirectly record the available internal leaf CO_2 which is controlled by a balance between stomatal conductance and photosynthetic rate during the growing season (Hemming et al. 2001; McCarroll and Loader 2006). McCarroll and Loader (2006) have suggested that the controls influencing tree-ring $\delta^{13}\text{C}$ are better understood than that potentially controlling ring width. As a result, it is possible that more of the limiting factors responsible for the variation in $\delta^{13}\text{C}$ may be accounted for than compared to those affecting radial growth (Saurer et al. 1995; Gagen et al. 2007).

Despite the demonstrated value of tree-ring $\delta^{13}\text{C}$ analysis, there have been a very limited number of dendroisotopic $\delta^{13}\text{C}$ studies conducted throughout the North American boreal forest (Brooks et al. 1998; Barber et al. 2000; Bukata and Kyser 2007; Simard et al. 2008ab; Buhay et al. 2008; Tardif et al. 2008). Among these studies, enriched tree-ring $\delta^{13}\text{C}$ was a consequence of physiological stress, i.e. reduction of available internal leaf CO_2 . Sensitivity to moisture stress, i.e. the stomatal control of $\delta^{13}\text{C}$, has been documented for several tree-ring $\delta^{13}\text{C}$ studies in the North American boreal forest. In the Alaskan boreal forest, drought stress in white spruce (*Picea glauca* (Moench) Voss) was indicated by negative correlations between tree-ring ^{13}C discrimination and mean temperatures during the current growing season (Barber et al. 2000). Brooks et al. (1998) reported that jack pine (*Pinus banksiana* Lamb.) tree-ring $\delta^{13}\text{C}$ near the northern range limit of their distribution around Thompson, Manitoba, showed a negative relationship

with current year growing season precipitation and positive relationship with previous year winter precipitation. In contrast, moisture stress was not found to be a strong limiting factor for *P. glauca* tree-ring $\delta^{13}\text{C}$ at the northern limit of their distribution in the forest-tundra transition, subarctic Manitoba, Canada (Tardif et al. 2008). Alternatively, the authors speculated that *P. glauca* $\delta^{13}\text{C}$ was controlled by photosynthetic rate since summer temperatures were most strongly associated (positive correlation) with $\delta^{13}\text{C}$.

The great longevity of northern white-cedar (*Thuja occidentalis* L.) trees along with their tolerance to extremely hydric or xeric moisture conditions (Collier and Boyer 1989; Matthes-Sears and Larson 1991) have made this species valuable to dendroclimatologists (i.e. Bergeron and Archambault 1993; Kelly et al. 1994; Tardif and Stevenson 2001; Buckley et al. 2004). *Thuja occidentalis* trees have been reported to exceed 450 years of age in Manitoba (F. Conciatori personal communication 2007), 900 years in the Northwestern Québec boreal forest (Archambault and Bergeron 1992a) and over 1600 years in age on the cliffs of the Niagara Escarpment, Ontario (Larson and Kelly 1991; Larson and Melville 1996), however, only a few studies have examined *T. occidentalis* tree-ring $\delta^{13}\text{C}$. Previous studies have reported $\delta^{13}\text{C}$ values from ancient *T. occidentalis* sub-fossil wood sampled from the Great Lakes region, eastern North America (Hunter et al. 2006; Leavitt et al. 2006). *Thuja occidentalis* trees were found to be the most $\delta^{13}\text{C}$ -enriched among the tree species which grew about 7095 ± 50 ^{14}C yr BP and found submerged in Lake Huron and Lake Michigan (Hunter et al. 2006; Leavitt et al. 2006). In central Manitoba, Canada, Au and Tardif (2009) have obtained similar

enriched values from cross-dated tree-ring decadal segments (formed from 1901 to 1910 A.D.) common among eight *T. occidentalis* trees.

Studies from contrasting areas throughout the *T. occidentalis* range of distribution have, however, reported the species to have complacent tree-rings with low year-to-year variation (Archambault and Bergeron 1992b; Kelly et al. 1994; Tardif and Bergeron 1997; St. George and Nielsen 2001; Tardif and Stevenson 2001; Buckley et al. 2004). Moreover, these research groups have also reported relatively weak correlations between *T. occidentalis* radial growth and climate. Nonetheless, several precipitation reconstructions have been successfully conducted utilizing *T. occidentalis* ring-width chronologies. Buckley et al. (2004) reconstructed June-July precipitation for the past 350 years from *T. occidentalis* growing in the Niagara Escarpment, Southern Ontario. Case (2000) reconstructed September to August precipitation at Dauphin, Manitoba using *T. occidentalis* ring-width chronologies and identified major drought periods throughout the 18th to 20th centuries. *Thuja occidentalis* ring width was also shown to be a good indicator of low-frequency decadal-scale drought at the northwestern limit of their distribution in Manitoba, Canada (Tardif and Stevenson 2001). During the current growing season, *T. occidentalis* radial growth showed a positive association with June precipitation and negative association with June temperature indicating a moisture stress response (Archambault and Bergeron 1992b; Tardif and Stevenson 2001; Buckley et al. 2004). These researchers have, consequently, noted the potential of *T. occidentalis* tree-ring chronologies as recorders of drought.

This is the first study to examine the tree-ring $\delta^{13}\text{C}$ – climate association of *T. occidentalis* trees. An incentive for analyzing tree-ring $\delta^{13}\text{C}$ was therefore to reveal previously undocumented climate information in *T. occidentalis* trees growing at their northwestern limit of distribution. The first objective of this study was to explore the association between *T. occidentalis* ring width and tree-ring $\delta^{13}\text{C}$ and to identify the major climatic factors influencing each ring-width and $\delta^{13}\text{C}$ chronology at the northwestern limit of their distribution in central Manitoba, Canada. Given the available literature regarding the physical and chemical variations within tree-rings, it was hypothesized that *T. occidentalis* tree-ring $\delta^{13}\text{C}$ will respond to climate controls that are independent of those associated with ring width. Another hypothesis was that the tree-ring $\delta^{13}\text{C}$ chronology would show a stronger climate signal than the associated ring-width chronology. It was further expected that moisture stress signals would be observed in *T. occidentalis* $\delta^{13}\text{C}$ as these have been observed in *T. occidentalis* ring-width chronologies developed from the northwestern limit of their distribution. A second objective was to identify past drought events based on ring width and tree-ring $\delta^{13}\text{C}$ analyses.

3.3. Methods

3.3.1. Study area

The study area is located in the Cedar Lake/ northern Interlake region of central Manitoba (Figure 3.1). Throughout this region, small disjunct populations of *T. occidentalis* trees are found about 300 km farther northwest from their continuous distribution limit in southeastern Manitoba and thus correspond to the northwestern range limit of distribution for *T. occidentalis* (Smith et al. 1998; Case 2000; Tardif and

Stevenson 2001). The most northerly disjunct occurrences of *T. occidentalis* are located along The Pas end moraine (Grotte 2007; Ko Heinrichs 2009) which spans from the Long Point area on Lake Winnipeg in the east and then west-northwest to the town of The Pas (Smith et al. 1998). This vast moraine contains calcareous till that was deposited from the Wisconsinian glacial period which ended between 8000 to 13000 years ago (Teller 1975; Smith et al. 1998). The study area is contained within the Pas Moraine ecodistrict which represents a portion of the larger Mid-Boreal Lowlands ecoregion further encompassed by the Boreal Plains ecozone (Smith et al. 1998). The latter represents the transition between the boreal forest in the north and the aspen parkland and prairie in the south.

The extensive bogs and fens within the Pas Moraine ecodistrict are dominated by black spruce (*Picea mariana* (Mill.) BSP.) and eastern larch (*Larix laricina* (Du Roi) K. Koch) (Smith et al. 1998). Tree species which co-occur with *T. occidentalis* in this area include *P. mariana*, paper birch (*Betula papyrifera* Marsh.), *Salix* spp. and *L. laricina* (Weber and Bell 1990) however, quaking trembling aspen (*Populus tremuloides* Michx.), balsam poplar (*Populus balsamifera* L.), *P. banksiana*, *P. glauca* and balsam fir (*Abies balsamea* (L.) Mill.) may also be found in the area (Smith et al. 1998; Grotte 2007; Ko Heinrichs 2009). Although *T. occidentalis* trees grow on a variety of organic soils (lowland) and mineral soils (upland), they are most often associated with cool, moist and nutrient-rich conditions, especially where calcareous soils are present (Johnston 1990).

The Pas Moraine ecodistrict typically experiences short, moderately warm summers and long, cold winters (Smith et al. 1998). This relatively short growing season is shown by the data from the Grand Rapids Hydro meteorological station (53°09'N, 99°17'W, elevation 222.5 m.a.s.l.) which indicated a mean total annual precipitation of 474 mm (of which 76% occurred as rainfall), and a respective mean July and a mean January temperature of 18.6°C and -19.7°C for the reference period 1971-2000 (Environment Canada 2004; Figure 3.2).

Several disturbances have been documented in the vicinity of the study area. The area around Grand Rapids is important for hydroelectric power generation. The completion of a dam by Manitoba Hydro in 1962 along the Saskatchewan River at Grand Rapids flooded about 2200 km² of land and significantly increased the size of Cedar and Moose lakes (Loney 1987). Smith et al. (1998) have noted that the northern most occurrences of *T. occidentalis* trees growing around the Cedar Lake region may have been affected by the flooding. However, Denneler et al. (2008) studied the effects of flooding stress on *T. occidentalis* trees via the double damming of Lake Abitibi, situated in the southeastern Canadian boreal forest, and concluded that radial growth was not affected by damming. Additionally, many trees including those in old-growth *T. occidentalis* stands were felled as a result of a large wildfire which swept through the Long Point area in 1988 (Weber and Bell 1990). Living *T. occidentalis* trees were, however, found to persist in relatively lightly burned areas.

3.3.2. Site selection

Old *T. occidentalis* trees are usually identified by their irregular stunted crowns with sparse foliage and frequent apical mortality (Archambault and Bergeron 1992b). These characteristics of old *T. occidentalis* trees are also well documented throughout Eastern Canada on the Niagara Escarpment, Ontario (Larson and Kelly 1991; Larson 2001) and in the Lake Duparquet region of the Québec boreal forest (Archambault and Bergeron 1992ab). During the summers of 2005 and 2006, twenty-nine accessible old-growth *T. occidentalis* stands were identified and sampled in conjunction with prior studies regarding the disjunct populations of *T. occidentalis* in central Manitoba i.e. the Cedar Lake, Grand Rapids and Long Point areas (Tardif and Stevenson 2001; Grotte 2007; Ko Heinrichs 2009).

Two sites (63B-2, 63B-17) containing old *T. occidentalis* trees, hereafter known as site-A and site-B, respectively, were selected based on an assessment of tree age, longevity and quality of *T. occidentalis* samples collected. Samples were deemed to be of good quality if rot, missing rings, ant tunneling, discoloration, fire scars and/or cracking were absent or minimal. In 2005, fourteen and eight *T. occidentalis* cross-sectional disks, each from a different tree, were cut from dead trees at sites-A and -B, respectively. These two sites were re-visited during the summer of 2006 and six additional cross-sectional disks from dead trees at each site were obtained. To ensure that recent decades were well-represented and to extend the $^{13}\text{C}/^{12}\text{C}$ analysis to 2006, living trees were also cored with a 5 mm diameter increment borer to provide a

continuation of tree-ring samples from each dead cross-section. Subsequently, each dead cross-section sample was overlapped with at least 23 years of a live cored sample.

Considering the adequate sample depth ascertained from previous dendroisotopic studies i.e. Leavitt and Long (1984) and McCarroll and Pawellek (1998), contiguous tree-rings from eight old *T. occidentalis* trees were analyzed for their $^{13}\text{C}/^{12}\text{C}$ ratio. The eight old *T. occidentalis* trees spanned approximately 279-459 years in age although annual carbon isotope analysis began in the late-1600s to early-1700s at site-A and mid-1600 to early-1700s at site-B (Table 3.1; Table 3.2). It should be noted that two of the old *T. occidentalis* trees sampled at site-B were thought to be dead when harvested but small portions of living cambium were later found. These two tree samples were, however, still categorized as dead so as to differentiate them with the younger living trees strictly sampled for the most recent portion of their tree-rings. Additional $^{13}\text{C}/^{12}\text{C}$ analysis was also performed on the most recent portion of tree-rings from four living trees from site-A and three living trees from site-B.

Hydric organic conditions on horizontal topography punctuated by scattered wet depressions prevailed at both sites. Site-A is located on Long Point on Lake Winnipeg, south of Long Point Road (Figure 3.1). The vegetation at this site is indicative of mesic-hydric conditions and is characterized by the presence among others of *Salix spp.*, *Epilobium angustifolium* L., *Aralia nudicaulis* L. and *Rosa acicularis* Lindl. Site-B is located west of Provincial road 327 traveling toward Easterville (Figure 3.1). Many of the *T. occidentalis* trees at this site were observed to be leaning, some at angles of more

than 45°. Eccentric radial growth also characterized many of the trees growing at this site. Compared to site-A, the understory vegetation is indicative of more hydric conditions as suggested by Ringius and Sims (1997) and includes *Rhododendron groenlandicum* (Oeder) Kron & Judd, *Betula pumila* L., *Lonicera villosa* (Michx.) Schult., graminoids and *Equisetum spp.* among others. The dominant tree species at both sites were *P. mariana* with *T. occidentalis* while *L. laricina* was also co-dominant at site-B.

3.3.3. $\delta^{13}C$ chronology development

3.3.3.1. Sample preparation

All collected cross-sections and cores were dried and then sanded with progressively finer sandpaper from 180 to 600 grit to reveal the earlywood and latewood cells of each annual growth increment. Tree-rings were accurately cross-dated by matching patterns of ring widths among several series to identify the correct calendar date of formation for every ring (Swetnam et al. 1985). Cross-dating utilized a technique similar to that of Yamaguchi (1991) to allow the accurate identification of pointer years. Cross-dating was further confirmed by examining pointer years common among the recently sampled *T. occidentalis* and those from the existing *T. occidentalis* chronology developed by Tardif and Stevenson (2001) for the Cedar Lake, Grand Rapids and Long Point areas. Ring-width measurement and cross-dating was also verified using program COFECHA (Holmes 1983).

To prepare the eight cross-dated *T. occidentalis* cross-sections for isotope analysis, two radial segments of 6 mm in both width and thickness spanning from the innermost to the outermost ring were cut from the cross-sectional disc of each tree using a band saw. The radial segments were re-sanded with progressively finer sandpaper on all sides with a palm-sander and the wood dust produced was vacuumed in-between sandings. Two of the cores from each of the seven live trees were also hand-sanded all around so that the boundaries of each annual increment could be clearly identified during cutting. Each decade, half century and century were appropriately marked on both the radial segments and cores using a dissecting pin to avoid contamination from graphite pencils. Each accurately cross-dated annual ring was then carefully excised beginning with the outermost ring and continuing on inward toward earlier calendar rings with a number 15 surgical scalpel and assisted by a binocular microscope.

All wood fiber belonging to each annual growth increment was placed in a labeled vial corresponding to the year of ring formation of the sampled tree. Since *T. occidentalis* trees typically form a very narrow band of latewood (Panshin and de Zeeuw 1970), no attempt was made to separate the earlywood from latewood within each annual growth increment. In addition, wood formed during the same calendar year from both radii was pooled which ensured that potential isotopic differences that may persist among different radial locations of each tree trunk could be averaged out (Leavitt and Long 1984). The pooling of both radii from each tree resulted in 2441 and 315 annual tree-ring samples from the dead and living trees, respectively.

To ensure homogeneity, each annual tree-ring sample (containing the wood fiber from both radii) was ground with a Wiley Intermediate Mill (Thomas Scientific, Swedesboro, NJ) to pass through a 20 mesh screen. Prior to chemical extraction, the wood from each vial was transferred into a separate labeled compartment within an F57 filter pouch (ANKOM Technology, Macedon, NY) and heat sealed. Each filter pouch contained eight compartments. The material of these pouches is designed to allow solvents to pass through so that unwanted wood components may be dissolved while that which is insoluble is unable to migrate from the pouch compartment.

3.3.3.2. *Chemical extraction*

Gaudinski et al. (2005) have reported that the Jayme-Wise method of cellulose extraction was the most reliable compared to the other methods they had studied. In this study, each sample sealed within the compartment of a filter pouch was extracted to holocellulose (HC) following the Jayme-Wise method as modified by Leavitt and Danzer (1993). Processing to HC was deemed preferable since narrow rings were commonly observed in numerous trees and chemical processing of *T. occidentalis* tree-rings beyond HC would likely have resulted in an insufficient amount of material for isotopic analysis (Au and Tardif 2009). Processing to α -cellulose would also have substantially increased the time spent on cutting tree-rings to obtain more cellulose and on chemical extraction.

Chemical processing of tree-ring whole-wood samples underwent a five-day procedure to result in HC. On day 1, the pouches containing the samples were placed in a Soxhlet apparatus with its reservoir flask filled with a 2:1 toluene:ethanol and run for

24 hours in order to remove extractives such as oils and resins from the samples. Three Soxhlet apparatuses, each containing 64 samples, were operated so that multiple batches of samples could be processed simultaneously. On day 2, the pouches were then removed from the Soxhlet apparatuses and then air dried for several hours upon being returned to the Soxhlets. The mixture within each reservoir flask was replaced with 100% ethanol and run for an additional 24 hours. On day 3, the pouches were again air dried for several hours. The pouches were then boiled in distilled and deionized water for six hours. To separate the lignin wood component from the HC, the samples, still wet, were placed in a glacial acetic acid (CH_3COOH) and sodium chlorite (NaClO_2) solution at 70°C for 12 hours. On day 4, three more additions of glacial acetic acid and sodium chlorite were added at 2-hour intervals and allowed to run for 18-hours. On day 5, the pouches were rinsed by decanting the solution with distilled and deionized water until conductivity reached $< 5\mu\text{mho/cm}$ upon which the pouches were oven-dried at 70°C for 12 hours. From the extracted HC obtained for each sample, approximately 0.5mg of HC was weighed and encased in a tin foil capsule. All holocellulose samples were measured for $^{13}\text{C}/^{12}\text{C}$ composition using a continuous flow stable isotope mass-spectrometer at the Environmental Isotope Laboratory, Department of Geosciences, University of Arizona. The $\delta^{13}\text{C}$ values are expressed in ‰ relative to the Vienna PeeDee belemnite (VPDB) standard. The analytical precision for all $^{13}\text{C}/^{12}\text{C}$ measurements was 0.12‰ or better ($n = 472$ Acetanilide standards).

3.3.3.3. $\delta^{13}\text{C}$ standard & residual chronologies

Each of the eight $\delta^{13}\text{C}$ series from dead trees and seven $\delta^{13}\text{C}$ series from live trees (Table 3.1; Table 3.2) was standardized using a cubic spline function with a 50% frequency response of 60 years (Cook and Kairiukstis 1990; Tardif and Stevenson 2001; Tardif et al. 2008). An example of the cubic spline function used in $\delta^{13}\text{C}$ series standardization is given in Figure 3.3. The purpose of standardization is to remove the variation representative of stand dynamics as well as the age related growth trend which may be unique for each series (Cook and Kairiukstis 1990). This is accomplished by dividing the observed value by the expected value denoted by the spline function. The raw values are then transformed into dimensionless indices which retain high-frequency variation but remove medium- and low-frequency variation presumably related to stand dynamics (Cook and Kairiukstis 1990). The standardization procedure serves a similar utility with regard to $\delta^{13}\text{C}$ chronologies in that the “juvenile effect” in these series is removed. Such an effect presents itself in terms of a temporary depletion in $\delta^{13}\text{C}$ values which could last up to 50 years beginning from the initial year of growth (Freyer and Belacy 1983). The “juvenile effect” has been attributed to a reduction in carbon isotope discrimination (stomatal conductance) associated with an increase in stem height, thereby lessening hydraulic conductivity, as young trees age (McDowell et al. 2002). Another contributor to the “juvenile effect” may be the recycling of $\delta^{13}\text{C}$ -depleted respired air by younger trees whose canopies remain closer to the ground (Schleser and Jayasekera 1985).

As a standard procedure in dendrochronology, residual series were produced by removing temporal autocorrelation from each standardized series using autoregressive modeling. The presence of autocorrelation diminishes the number of independent observations in a data set and therefore effectively reduces the robustness of any statistical test performed (Legendre and Legendre 1998). Residual series were then averaged using a bi-weight robust mean to enhance the common signal and eliminate any anomalously high or low ring-width values which were not contemporaneous among series (Cook 1985). These procedures optimized the common signal in the chronology and eliminated the persistence. The tree-ring measurements were transformed into residual indices using the ARSTAN for Windows (version 40c) program (Cook and Holmes 1986). Three *T. occidentalis* $\delta^{13}\text{C}$ residual chronologies were created and included series from, i) only site-A (A- $\delta^{13}\text{C}$), ii) only site-B (B- $\delta^{13}\text{C}$) and iii) both sites-A and -B (AB- $\delta^{13}\text{C}$).

3.3.3.4. $\delta^{13}\text{C}$ discrimination

Another phenomenon readily observable within many $\delta^{13}\text{C}$ chronologies is termed the Suess effect or the large-scale release of atmospheric CO_2 coinciding with the onset of industrialization (Freyer and Belacy 1983). Freyer (1986) estimated that there was a decrease in atmospheric $\delta^{13}\text{C}$ of 1.5‰ corresponding to the increased combustion of fossil fuels since industrialization (1850 AD) and subsequent release of isotopically light carbon. However, statistical detrending may remove associated climate phenomena which parallel the rise of the non-climatic rise in atmospheric CO_2 levels. Aside from statistical detrending, amelioration in the climatic signal may be obtained by expressing

$\delta^{13}\text{C}$ values in terms of discrimination of the heavier isotope (McCarroll and Loader 2006). Expressing $\delta^{13}\text{C}$ values in terms of discrimination may also be useful to analyze the low-frequency physiological or environmental trends which may have occurred within the same time scale as the decline of atmospheric $\delta^{13}\text{C}$ since about 1850 AD (McCarroll and Loader 2006). These adjustments based on the Antarctic ice core record obtained by Francey et al. (1999) account for recent changes in the atmospheric $\delta^{13}\text{C}$ values relative to the pre-industrial standard (-6.4 ‰). Subsequently, the long-term discrimination values of individual series were calculated using equations 2 and 3 (see also chapter 1 where the equations were introduced). Farquhar et al. (1982) expressed the isotopic composition of C3 plants (‰) using the equation:

$$\delta^{13}\text{C}_p = \delta^{13}\text{C}_a - a - (b - a)(c_i / c_a), \quad [2]$$

where $\delta^{13}\text{C}_a$ and $\delta^{13}\text{C}_p$ are the isotopic values of atmospheric CO_2 and plant, respectively, a is discrimination against ^{13}C during diffusion ($\sim -4.4\text{‰}$), b is discrimination against ^{13}C during carboxylation ($\sim -27\text{‰}$) and c_i and c_a are the intercellular leaf and ambient air CO_2 concentrations, respectively. Accordingly, discrimination (Δ) against ^{13}C (‰) during photosynthesis is obtained through the following equation:

$$\Delta = \frac{(\delta^{13}\text{C}_a - \delta^{13}\text{C}_p)}{(1 + \delta^{13}\text{C}_p/1000)}, \quad [3]$$

After discrimination values were calculated for each *T. occidentalis* $\delta^{13}\text{C}$ series, a standardized discrimination (Δ) chronology was constructed using series from both sites. Each $\delta^{13}\text{C}$ series was standardized using a horizontal line through its mean in order to

retain all low-frequency variation. Therefore, the standardized and not the residual chronology was used in subsequent analysis in order to keep low-frequency variation.

3.3.4. Ring-width chronology development

The ring widths from all the *T. occidentalis* cross-sections and cores sampled were measured with a precision of 0.001 mm using a Velmex slide stage micrometer interfaced with a computer. Ring-width chronologies were developed following the same procedures as those previously described for $\delta^{13}\text{C}$ in section 3.3.3.3 above. Similar to $\delta^{13}\text{C}$ chronology development, standardization removes growth-related age trends in individual ring-width series to result in dimensionless indices (Cook and Kairiukstis 1990). For the purposes of this study, four *T. occidentalis* ring-width chronologies were developed. The individual indexed ring-width series obtained from the same trees on which carbon isotope analysis was performed were used to construct site chronologies for sites-A and -B. This resulted in the construction of three site-specific residual chronologies that included *T. occidentalis* ring-width series from i) only site-A (A-RWL), ii) only site-B (B-RWL) and iii) both sites-A and -B (AB-RWL; Table 3.2). The regional ring-width residual chronology (REG-RWL) contains the same *T. occidentalis* series sampled by Tardif and Stevenson (2001) from the Cedar Lake, Grand Rapids and Long Point areas. However, in contrast to the original Tardif and Stevenson (2001) *T. occidentalis* chronology, only *T. occidentalis* series sampled from hydric sites were included for this study and the REG-RWL was extended and updated to 1519-2006 (231 series) by F. Conciatori, an experienced dendrochronology technician.

3.3.5. Temporal stability of the *Thuja occidentalis* ring width and $\delta^{13}\text{C}$ relationship

In order to first assess the association between *T. occidentalis* ring-width series and $\delta^{13}\text{C}$ series, Pearson correlation analysis was performed between both the corresponding dead and living tree ring-width and $\delta^{13}\text{C}$ series. Second, to investigate whether any temporal change in association existed between the ring width and $\delta^{13}\text{C}$ time-series, simple running Pearson correlation coefficients were calculated between the REG-RWL and AB- $\delta^{13}\text{C}$ standard chronologies for overlapping 11-year periods with an advance of 1-year beginning from 1650 to 2006.

Third, a regime shift detection procedure (see Rodionov 2006) was also employed in order to assess whether periodic changes in observations above or below the mean value of each of the REG-RWL, $\delta^{13}\text{C}$ discrimination (Δ) and AB- $\delta^{13}\text{C}$ standard chronologies were artifacts of red noise processes. Red noise processes (serial correlation or autocorrelation) may influence time-series by generating values that consistently remain above or below the average value for long periods of time and could then be mistaken as climate regimes (Rodionov 2006). To remove this red noise component, Rodionov (2006) proposed the pre-whitening procedure thereby factoring out serial correlation and allowing the implementation of regime shift detection to determine whether the regimes present in the time-series are more than a realization of a red noise process. This procedure was shown to handle the detection of multi-decadal shifts in relatively long time-series better than in shorter time-series. The computer program used to calculate the regime shift detection with correction for serial correlation is written in Visual Basic for Application in Excel and can be downloaded at

www.beringclimate.noaa.gov. Any regime shifts in the mean above the selected 8-year cut-off length threshold were thus identified. The other selected program settings were as follows: probability $\sigma = 0.10$, serial correlation (AR(1)) was estimated using the IP4 method, Huber's weight parameter = 1 and sub-sample size = 4.

Fourth, to further assess the common variance among the four *T. occidentalis* ring-width (REG-RWL, AB-RWL, A-RWL, B-RWL) and three *T. occidentalis* $\delta^{13}\text{C}$ (AB- $\delta^{13}\text{C}$, A- $\delta^{13}\text{C}$, B- $\delta^{13}\text{C}$) residual chronologies, principal components analysis (PCA) performed on a correlation matrix was conducted over 1681-2005 (longest period of data common among chronologies). Principal components analysis is an ordination technique involving the eigenanalysis of either a correlation matrix or a covariance matrix of the descriptors (Legendre and Legendre 1998). The selection of a correlation matrix was important since the chronologies showed different variance being derived from the ring-width and $\delta^{13}\text{C}$ measurements. The descriptors in a correlation matrix are standardized so that they are independent of variance and contribute equally to the distribution of objects in reduced space (Legendre and Legendre 1998).

Moreover, subtle temporal changes in the relationship of tree-ring chronologies may be examined on the basis of overlapping periods common among the chronologies. Additional PCAs (see procedure in previous paragraph) included five 100-year intervals, consecutively shifted 50 years beginning from 1700 to 1999 and held in common by all chronologies. A sixth (1900-1959) interval and a seventh (1960-2005) interval were also included to assess the stability in relationship among all seven residual chronologies since

the latter period roughly corresponded to the completion of the Grand Rapids Hydro Dam in 1962 (coverage of meteorological records: 1966-2006) as well as the incorporation of the living *T. occidentalis* trees into the $\delta^{13}\text{C}$ chronologies. In addition, to assess the signal strength of the dead and living $\delta^{13}\text{C}$ series altogether, modified site chronologies consisting of the optimum overlap period between the dead and living *T. occidentalis* series were constructed. Correspondingly, the A- $\delta^{13}\text{C}^*$ and B- $\delta^{13}\text{C}^*$ chronologies were constructed spanning 1965-1987 and 1970-1993, respectively.

3.3.6. Dendroclimatic analysis

The meteorological data used to assess the climate-growth associations were interpolated using program BioSIM (Régnière and Bolstad 1994; Régnière 1996). Program BioSIM adjusts daily weather data from selected stations for differences in latitude, longitude, elevation, slope and aspect among the source stations and a specified location (Régnière and Bolstad 1994). Climate data were interpolated based on data from three of the nearest meteorological stations. For each year from 1900-2005, climate data originating from nearer meteorological stations received greater weight during the interpolation of climate data at the mid-point of our two study sites (52°98'N, 99°27'W; Figure 3.1). A notable change in mean station distance was, however, observed when records at the Grand Rapids Hydro Station became available from 1966 onwards (mean station distance < 100 km) for both temperature and precipitation data (Figure A1.1). The climate variables used in dendroclimatic analysis included mean monthly minimum and maximum temperature (°C), total monthly precipitation (mm), mean monthly relative humidity (%), mean monthly dew point temperature (°C), total monthly frost days (days)

and total monthly radiation (MJ/m^2). The approximation of frost days was based on the criterion of whether temperature reached below $0\text{ }^\circ\text{C}$ (Régnière 1996). The number of monthly frost days was determined by summing the total number of days during the month where the minimum temperature dropped below zero. It should be noted that relative humidity and dew point temperature data were unavailable prior to 1953.

The MT-CLIM model (Glassy and Running 1994) estimated radiation based on the observation that the daily diurnal amplitude in near-surface air temperature (fluctuation in minimum and maximum temperature) is a close approximation to daily total solar radiation (Thornton and Running 1999). A potential radiation model adjusted for slope and aspect and accounted for the east and west horizon of the site. The model was then used to calculate direct and diffuse solar radiation incident on a horizontal surface which both may affect total transmittance (Bristow and Campbell 1984). The final estimate of incident solar radiation ($\text{kilojoules per m}^2$) considered that above atmosphere radiation was reduced by this atmospheric transmittance (Glassy and Running 1994).

Additionally, Grand Rapids Hydro was the nearest meteorological station from 1966 to present and is located 19 km from the mid-point of our two study sites (Figure 3.1). Tardif and Stevenson (2001) found high correlations with the Grand Rapids Hydro station and surrounding meteorological stations for the period 1966 to 1998 suggesting that the regional climate data could be used in combination and as a surrogate for data from the Grand Rapids Hydro station. To examine the validity of the climate data

interpolated by BioSIM, monthly cross-correlations were conducted between the former and all available climate data from Grand Rapids Hydro which spanned from 1966-2006. All monthly cross-correlations were significant at $p < 0.001$ (lowest correlation for July minimum temperature = 0.92; lowest correlation for January maximum temperature = 0.88; and lowest correlation for December total precipitation = 0.94).

The Canadian Drought Code (CDC), a component of the Canadian Fire Weather Index system, is used as an indicator of daily drought in boreal conifer stands and accounts for precipitation, evaporation and soil moisture capacity (Van Wagner 1987; Girardin et al. 2004). More specifically, the daily CDC value is a numerical rating used to assess the average moisture content of deep organic layers (Turner 1972). Daily CDC values were calculated using daily maximum temperature and daily precipitation data interpolated from BioSIM and followed the procedure of Van Wagner (1987). Mean monthly average CDC values were then calculated and included in climate analysis. The minimum CDC value of zero indicates the maximum soil water holding capacity, while that of 300 and above indicates extreme drought severity.

Pearson correlation analysis was conducted between each of the seven *T. occidentalis* residual chronologies and mean monthly minimum and maximum temperature, total monthly precipitation, mean monthly average CDC values, mean monthly relative humidity, mean monthly dew point temperature, total monthly frost days and total monthly radiation over a 17-month period from May prior to the year of ring formation ($t-1$) to September of the year of ring formation (t). The period of analysis was

1900-2005 for all climate variables except for relative humidity and dew point temperature (1953-2005). The variables for the summer months (June, July, August and September) of the year of ring formation were also seasonalized and used in the analyses. Additional correlation analysis was performed in the same manner as described above between the loadings of the first and second principal components and climate variables for the periods: 1900-2005, 1900-1959 and 1960-2005. The latter two periods were assessed in order to test the stability of the climate associations for the first and second principal components. Correlation analyses were conducted using Systat (v. 11) for Windows (SYSTAT 2004).

3.3.7. *Thuja occidentalis* cross-species comparisons

In the two previous dendroisotopic studies from Manitoba (Brooks et al. 1998; Tardif et al. 2008), the *P. banksiana* and *P. glauca* trees were sampled at the northern range of their distribution and at the northern limit of their distribution, respectively. In this study, *T. occidentalis* trees were similarly sampled at the northwestern limit of their distribution. The resulting *T. occidentalis* $\delta^{13}\text{C}$ chronology was compared against both the *P. glauca* $\delta^{13}\text{C}$ chronology from subarctic Manitoba (Tardif et al. 2008) and the *P. banksiana* $\delta^{13}\text{C}$ chronology from Thompson, Manitoba (Brooks et al. 1998) to test if any similarity existed at a larger scale. The *P. banksiana* $\delta^{13}\text{C}$ time series were retrieved online (<http://www.daac.ornl.gov>) from the Oak Ridge National Laboratory Distributed Active Archive Center, Oak Ridge, Tennessee.

First-differencing has been shown by Schleser et al. (1999) to minimize the effects of long-term trends i.e. the rising atmospheric CO₂ on $\delta^{13}\text{C}$ values without relying on CO₂ measurements derived from other proxies. Consequently, first-differencing was applied to the untransformed $\delta^{13}\text{C}$ series. Gleichläufigkeit (GLK) tests and cross-correlation comparisons were then conducted among the first-differenced *T. occidentalis* $\delta^{13}\text{C}$ (ab- $\delta^{13}\text{C}$), *P. glauca* $\delta^{13}\text{C}$ (pgl- $\delta^{13}\text{C}$) and *P. banksiana* $\delta^{13}\text{C}$ (pba- $\delta^{13}\text{C}$) chronologies. The GLK is a statistical measure of the number of similar departures of corresponding intervals between two curves (Schweingruber 1988). Synchronicity in change of sign between the two curves is accepted if the number of similarities, expressed as a percentage, is much greater than the dissimilarities. Additional GLK tests were calculated between the ab- $\delta^{13}\text{C}$ and first-differenced *T. occidentalis* ring-width (ab-rwl) chronologies.

3.4. Results

3.4.1. Thuja occidentalis ring-width and $\delta^{13}\text{C}$ site statistics

General statistics showed that the mean annual radial growth among *T. occidentalis* trees differed between the sites (Table 3.1). The mean ring width of *T. occidentalis* trees growing at site-A (0.61mm) was much greater than compared to that at site-B (0.39mm). In contrast, the mean tree-ring $\delta^{13}\text{C}$ values analyzed from the same *T. occidentalis* trees were similar regardless of site (site-A, -22.1‰; site-B, -21.2‰; Table 3.2). Mean ring-width and $\delta^{13}\text{C}$ sensitivity were low for *T. occidentalis* growing in the Cedar Lake/ northern Interlake region. There were, however, no major site-specific differences in ring-width or tree-ring $\delta^{13}\text{C}$ mean sensitivity (Table 3.1; Table 3.2).

3.4.2. Cross-correlations between *Thuja occidentalis* ring-width and $\delta^{13}\text{C}$ series

Overall, cross-correlations between standardized *T. occidentalis* $\delta^{13}\text{C}$ series from live and dead trees showed high positive associations (Table 3.3; Table A1.1; A1.2). In contrast, weak associations were found between corresponding ring-width and $\delta^{13}\text{C}$ standardized series from dead trees (Table 3.4). In fact, the highest correlations for some isotope series ($A\delta^{13}\text{C-F}$, $A\delta^{13}\text{C-H}$, $B\delta^{13}\text{C-5}$ and $B\delta^{13}\text{C-M}$) were found with ring-width series sampled from other trees. Associations were generally positive, although negative associations were observed for $B\delta^{13}\text{C-M}$ and $B\delta^{13}\text{C-K}$ which emphasizes the importance of site/ tree-specific limitations. Correlation coefficients between corresponding standardized ring-width and $\delta^{13}\text{C}$ series from dead trees at site-A were shown to be stronger than those at site-B emphasizing inter-site differences (Table 3.4). Fewer significant correlation coefficients were, however, shown among standardized ring-width and $\delta^{13}\text{C}$ series from live trees (Table 3.5). Cross-correlations among these ring-width and $\delta^{13}\text{C}$ series were rarely significant and did not show any overall dominant pattern of association over albeit, a relatively shorter time span compared to the series obtained from the longer-lived dead trees. Moreover, the highest significant Pearson correlation coefficients between the standardized ring-width and $\delta^{13}\text{C}$ series from live trees generally did not belong to corresponding tree samples (Table 3.5).

3.4.3. Low frequency trends in $\delta^{13}\text{C}$ series

The raw $\delta^{13}\text{C}$ measurements of all series spanning from 1650 to 2006 illustrated the low-frequency trend of decreasing $\delta^{13}\text{C}$ values associated with the simultaneous

increase in fossil fuel emissions from 1850 AD onward (Figure 3.4). Prior to 1850 AD (from 1650 to 1849), the minimum and maximum $\delta^{13}\text{C}$ values were -22.8‰ and -18.8‰, respectively, while those thereafter (from 1850 to 2006) were -24.3‰ and -19.3‰, respectively and shown to be more depleted. A steeper gradient of $\delta^{13}\text{C}$ depletion was also observed among the $\delta^{13}\text{C}$ series roughly starting in the 1960s (Figure 3.4). For tree B-5, severe growth suppression and missing rings were frequently observed following 1958 AD. Correspondingly, $\delta^{13}\text{C}$ analysis of B $\delta^{13}\text{C}$ -5 did not proceed after this date and the response to the rise of atmospheric CO_2 was not as pronounced as those shown in other series. The latter series also displayed much greater $\delta^{13}\text{C}$ enrichment (maximum $\delta^{13}\text{C}$ value of -18.8‰) (Table 3.2) as well as higher mean ring-width sensitivity (Table 3.1) compared to that of the other series. Furthermore, the innermost years of growth of many of the *T. occidentalis* cross-sections from dead trees were not analyzed as a result of rot although some $\delta^{13}\text{C}$ series did contain samples within decades or closer to the initial year of growth i.e. series A $\delta^{13}\text{C}$ -D (Table 3.2). In addition, only a portion of the outermost rings were analyzed for $^{13}\text{C}/^{12}\text{C}$ from the live trees. Subsequently, the “juvenile effect” or observation that $\delta^{13}\text{C}$ series may show a short period of depletion at the beginning of tree growth was relatively minor among the live and dead trees in this study. Instead, the “juvenile effect” was only observed for series A $\delta^{13}\text{C}$ -H, where $\delta^{13}\text{C}$ analysis began one year after the initial year of growth (Table 3.2), and lasted for approximately 50 years (Figure 3.4).

3.4.4. Signal strength in *Thuja occidentalis* ring-width and $\delta^{13}\text{C}$ residual chronologies

The common signal, inferred from the EPS statistic, for all the regional chronologies (AB- $\delta^{13}\text{C}$, AB-RWL, REG-RWL and AB- Δ) covering a common period of 1736-1958 AD achieved the conservative threshold ($\text{EPS} \geq 0.85$) used to define a chronology with acceptable signal strength (Table 3.6; Figure 3.5). General statistics computed for the combined-site ring-width and $\delta^{13}\text{C}$ chronologies (AB-RWL, AB- $\delta^{13}\text{C}$) illustrated a similar strength in common signal between the chronologies (Table 3.6; Figure 3.5). The AB- $\delta^{13}\text{C}$ chronology exhibited a higher inter-series correlation and common variance than compared to those of the AB-RWL chronology (Table 3.6). Although the AB-RWL chronology contained double the number of series (2 radii per tree) of the AB- $\delta^{13}\text{C}$ chronology, the signal strength of the former, however, could still be improved with the inclusion of ring-width series from additional sites. Therefore, since the REG-RWL chronology contained the strongest common signal ($\text{EPS} = 0.96$), much higher replication ($n = 231$) and exhibited a high correlation with the AB-RWL chronology over the period 1681-2005 (Table 3.7), subsequent *T. occidentalis* regional ring width – climate analysis was displayed only with the residual REG-RWL chronology.

In contrast to the regional chronologies, the common signals in the ring-width and $\delta^{13}\text{C}$ site chronologies were comparatively lower, except in A-RWL (Table 3.6). The common signal was slightly enhanced when both sites (A and B) were combined in the AB- $\delta^{13}\text{C}$ chronology but the same was not observed for the AB-RWL chronology which may suggest a greater dependence on site conditions for ring width. Instead, the common

signal for AB-RWL was slightly lowered, in part, due to the incorporation of B-RWL (retaining a lower EPS). In fact, the common signals for both the ring-width and $\delta^{13}\text{C}$ chronologies at site-A were higher than compared to those at site-B. In agreement, the $\delta^{13}\text{C}$ site chronologies, whose duration coincided with the period of overlap between the $\delta^{13}\text{C}$ series from living and dead trees at each site (site-A: 1965-1987; site-B: 1970-1993), showed a stronger common signal at site-A (A- $\delta^{13}\text{C}$ * EPS value: 0.92) than compared to site-B (B- $\delta^{13}\text{C}$ * EPS value: 0.62).

3.4.5. Low-frequency trends in regional chronologies

Generally, more extended periods of change were detected in the discrimination and ring-width indices than in $\delta^{13}\text{C}$ indices (Figure 3.6). However, the difference in the number of changes detected between the discrimination and $\delta^{13}\text{C}$ indices was a consequence of different standardization approaches having been applied. Periods of prolonged enriched $\delta^{13}\text{C}$ values approximately included: 1675-1685, 1795-1820, 1840-1855, 1925-1935, 1965-1980 and 1990-1995. Ring width most often recorded the most extended change observed as periods of decreased radial growth which approximately included: 1700-1705, 1715-1725, 1785-1800, 1835-1850, 1885-1900, 1930-1935 and 1960-1975. Corresponding in-phase periods were identified with the regime shift program among the ring-width, discrimination and $\delta^{13}\text{C}$ standard chronologies (Figure 3.6). Periods of low radial growth, decreased discrimination and enriched $\delta^{13}\text{C}$ values were generally observed during the 1790s, 1840s, 1890s, 1930s and 1965-75 (Figure 3.6). Interestingly, a period of high radial growth and discrimination and low $\delta^{13}\text{C}$ also occurred during 1685-95.

Subsequent 11-year moving interval correlations between the regional ring-width and $\delta^{13}\text{C}$ standard chronologies showed more periods of extended significant positive associations (1725-1730, 1818-1822 and 1911-1918) than those of significant negative association (~1670-1680). However, negative correlations generally coincided with the periods of low radial growth and enriched $\delta^{13}\text{C}$ values described above (Figure A1.2). Negative correlations, each as the median year of an 11-year period, were correspondingly observed during 1803, 1894-1907, 1934 and 1961.

3.4.6. Temporal stability of *Thuja occidentalis* ring-width and $\delta^{13}\text{C}$ residual chronologies

During 1681-2005, all correlations between the ring-width and $\delta^{13}\text{C}$ chronologies were non-significant with the exception of the weak positive correlation between these chronologies at site-A (Table 3.7). A low inter-annual synchronicity was also shown between the ab-rwl and ab- $\delta^{13}\text{C}$ chronologies (GLK value: 55%; 1651-2005 AD). Similarly, the PCA illustrated an approximate 90° angle between the ring-width and $\delta^{13}\text{C}$ vectors (Figure 3.7a). The correlation structure among the *T. occidentalis* ring-width and $\delta^{13}\text{C}$ residual chronologies also remained relatively stationary among the five 100-year overlapping sub-periods covering 1700 to 1999 (Figure 3.7b-f). Moreover, positive loadings for ring-width and $\delta^{13}\text{C}$ were shown on PC1 and PC2, respectively, with the percentage of variance explained by the PCA for PC1 and PC2 remaining relatively constant among all periods. The variance explained by PC1 ranged from 44.9% to 59.2% while that for PC2 ranged from 29.5% to 38.4% throughout all eight periods analyzed (Figure 3.7). The ring-width chronologies were shown to be highly correlated to PC1

with loadings exceeding 0.7 for A-RWL and B-RWL while loadings generally exceeded 0.9 for AB-RWL and REG-RWL. Similarly, the loadings for the $\delta^{13}\text{C}$ chronologies generally exceeded 0.8 and were highly correlated to PC2. These results showed the distinct signal contained in each ring width and $\delta^{13}\text{C}$.

Aside from the PCAs conducted over the 100-year sub-periods, an apparent change in relative positioning between the ring-width and $\delta^{13}\text{C}$ chronologies was observed when the first and second portions of the 20th century were separately examined (Figure 3.7gh). Greater similarity between the chronologies was illustrated during the first period compared to the second one. Both ring-width and $\delta^{13}\text{C}$ chronologies shared greater common variance during 1900-1959 as indicated by the acute general angle formed between the ring-width and $\delta^{13}\text{C}$ vectors (Figure 3.7g). This was also shown by the high loadings of all chronologies on PC1, while the loadings on PC2 for A- $\delta^{13}\text{C}$, B- $\delta^{13}\text{C}$ and AB- $\delta^{13}\text{C}$ all dropped below 0.8 during this period (Figure 3.7g). However, when PCAs conducted over 50-year sub-periods were examined (Figure A1.3), similar changes in association between the ring-width and $\delta^{13}\text{C}$ chronologies were also shown to occur prior to the 20th century as approximated by subtle changes between their respective vectors throughout these sub-periods (Figure A1.3.a-f). Greater similarity between the ring-width and $\delta^{13}\text{C}$ chronologies was shown during 1700-1749, 1800-1849 and 1900-1949 (Figure A1.3.ace).

3.4.7. *Thuja occidentalis* ring-width association with climate

Monthly correlations between climate variables and PC1 were very similar to correlations observed with REG-RWL (Figure 3.8ab) while the correlations between climate variables and PC2 were likewise similar to those observed with AB- $\delta^{13}\text{C}$ (Figure 3.8cd). The residual ring-width and $\delta^{13}\text{C}$ regional chronologies, however, shared little commonality in their association with climate variables except for the inverse associations with current July summer CDC and summer precipitation (Figure 3.8bd). Overall, ring width showed more association with climate variables during the year prior to ring formation (Figure 3.8b) whereas $\delta^{13}\text{C}$ was more often associated with conditions prevailing during the current year growing season (Figure 3.8d).

During the year prior to ring formation, the ring-width index was negatively correlated with June ($t-1$) and September ($t-1$) CDC indices as well as with August ($t-1$) maximum temperature and positively correlated with May ($t-1$) precipitation (Figure 3.8b). The impact of moisture stress was more clearly illustrated by the negative correlations between PC1 and the June ($t-1$), August ($t-1$), September ($t-1$) and October ($t-1$) CDC indices (Figure 3.8a). Climate conditions during the fall and winter prior to ring formation, especially in November ($t-1$) and December ($t-1$), were also associated with radial growth of the following year (Figure 3.8b). Strong positive correlations were observed between ring width and the previous November ($t-1$) and December ($t-1$) minimum and maximum temperatures. Additionally, radial growth was negatively associated with November ($t-1$) precipitation and November ($t-1$) to February (t) total radiation.

Climate conditions during the year of ring formation were also important for radial growth (Figure 3.8b). During the current growing season, ring width was positively associated with May (t) minimum and maximum temperatures (Figure 3.8b). Ring width was also negatively associated with June (t) maximum temperature and inversely with June (t) and July (t) precipitation stressing the importance of water availability for radial growth during the early growing season. The importance of moisture stress over the current summer was further corroborated by the negative association between ring width and the summer CDC indices, particularly during July (t) and August (t).

3.4.8. *Thuja occidentalis* $\delta^{13}C$ association with climate

In contrast to ring width, climate conditions during the year prior to ring formation were considerably less important for tree-ring $\delta^{13}C$ (Figure 3.8bd). The dominant controls for tree-ring $\delta^{13}C$ were mainly temperature and the CDC over the course of the current growing season. Tree-ring $\delta^{13}C$ was positively correlated with maximum temperature during May (t), June (t), August (t) and the current summer season (Figure 3.8d). In addition, the CDC index was positively associated with $\delta^{13}C$ during June (t), July (t) and September (t) as well as the current summer season (Figure 3.8d). These results suggest that moisture stress i.e. warm and dry conditions during the current summer contributed to enriched $\delta^{13}C$ values. Precipitation and relative humidity, in contrast to temperature/drought code, had relatively minor effect on $\delta^{13}C$. Precipitation was, however, found to be negatively associated to $\delta^{13}C$ over the current summer season.

Likewise, the importance of relative humidity was also lacking as the only significant correlation coefficient between relative humidity and AB- $\delta^{13}\text{C}$, although high, was reached in September (t_{-1}) (Figure 3.8d).

The response to climate at the regional scale also corresponded to that observed at the site level for both ring width and $\delta^{13}\text{C}$ (Figure 3.8; Figure A3.1). It should be noted that although frequent cambial dieback was observed in trees at site-B as opposed to those at site-A, Pearson correlation coefficients were very similar between ring-width/ $\delta^{13}\text{C}$ residual chronologies and climate variables between sites-A and -B (Tables A2.1; A2.2; A2.4; A2.5; Figure A3.1). Stronger positive and negative correlations with the CDC and precipitation, respectively, were shown for the $\delta^{13}\text{C}$ chronology at site-A compared to that at site-B whilst the $\delta^{13}\text{C}$ chronology at the latter site showed stronger positive correlations with temperature during the current growing season. Correlations between the ring-width chronology at site-A and climate variables were also shown to be generally stronger than those at site-B. Both the ring-width and $\delta^{13}\text{C}$ chronologies at the site level, however, continued to share little commonality in their responses to climate.

3.4.9. Temporal stability of ring width and $\delta^{13}\text{C}$ – climate associations

Principal component loadings observed between the sub-periods (1900-1959; 1960-2005) for the ring-width and $\delta^{13}\text{C}$ chronologies showed that these parameters exhibited greater similarity during the first portion of the 20th century (1900-1959) compared to the later part (1960-2005) (Figure 3.7gh). Correspondingly, climate associations for both these sub-periods were thus examined (A3.2; Figure 3.9). In the

period 1900-1959, the ring-width and $\delta^{13}\text{C}$ chronologies were both associated with similar conditions during the year prior to growth. Specifically, both chronologies were positively associated with November ($t-1$) and December ($t-1$) temperatures (Figure 3.9ac).

Conversely, the PCA results also showed less common variation shared between ring-width and $\delta^{13}\text{C}$ vectors during the period 1960-2005 compared to the period 1900-1959 (Figure 3.7gh). In the period 1960-2005, the CDC indices in the current summer were negatively and positively correlated with ring width and $\delta^{13}\text{C}$, respectively (Figure 3.9bd). Correlations conducted with ring width revealed a change in importance of previous year drought during the first period to that of current year drought during the second period (Figure 3.9ab). The same change from previous year drought during 1900-1959 to current year drought during 1960-2005 was observed with PC1 (Figure A3.2). This change was, however, not apparent for climate analysis conducted over the entire period (1900-2005) of available meteorological data (Figure 3.8). Warmer winter (December ($t-1$) through March (t)) and spring (April (t) and May (t)) temperatures were also more important for radial growth during 1960-2005 than compared to 1900-1959.

For $\delta^{13}\text{C}$, the period 1960-2005 showed fewer significant associations during the year prior to ring formation than compared to the period 1900-1959. Moreover, the greater importance of the CDC indices for $\delta^{13}\text{C}$ over the current summer was also observed during the period 1960-2005 than compared to the period 1900-1959 (Figure 3.9cd). However, the correlation coefficients observed during the period 1900-1959 between temperature and $\delta^{13}\text{C}$ in both the previous and current year spring and summer

(A2.10; Figure 3.9c) were weaker during the 1960-2005 (A2.11; Figure 3.9d).

Nonetheless, generally similar correlation coefficients differing mainly in strength were observed between $\delta^{13}\text{C}$ and climate during the current growing season over both sub-periods (Figure 3.9cd).

3.4.10. Comparing *Thuja occidentalis* $\delta^{13}\text{C}$ with previous $\delta^{13}\text{C}$ chronologies from Manitoba

The first-differenced *T. occidentalis* $\delta^{13}\text{C}$ chronology portrayed the lowest $\delta^{13}\text{C}$ sensitivity among the chronologies while the highest was shown for *P. banksiana* (Figure 3.10). Pearson correlations yielded non-significant associations between first-differenced *T. occidentalis* ($\text{ab-}\delta^{13}\text{C}$) and both *P. glauca* ($\text{pgl-}\delta^{13}\text{C}$) ($r=0.31$, $p=0.09$, $n=30$; GLK value: 57%; 1962-1991 AD; Figure 3.10) and *P. banksiana* ($\text{pba-}\delta^{13}\text{C}$) ($r=0.09$, $p=0.65$, $n=30$; GLK value: 60%; 1962-1991 AD; Figure 3.10). Nonetheless, synchronous years of high and low $\delta^{13}\text{C}$ values among all chronologies were observed during their period of overlap from 1962 to 1992. Enriched years were observed among all three $\delta^{13}\text{C}$ chronologies during: 1967, 1973, 1979, 1981, 1983 and 1992 while depleted years common among the chronologies included: 1965, 1972, 1974, 1978, 1982 and 1985. Interestingly, $\text{pgl-}\delta^{13}\text{C}$ and $\text{pba-}\delta^{13}\text{C}$ were found to be significantly associated and exhibited a high similarity in the year-to-year change of the chronologies ($r=0.42$, $p<0.05$, $n=30$; GLK value: 77%; 1962-1991 AD; Figure 3.10). A weak association was also shown between $\text{ab-}\delta^{13}\text{C}$ and $\text{pgl-}\delta^{13}\text{C}$ when the full extent of the first-differenced chronologies was considered ($r=0.16$, $p<0.05$, $n=249$; GLK value: 58%; 1751-1999 AD).

3.5. Discussion

3.5.1. Ring width and $\delta^{13}\text{C}$ association/ common signal

In this study, correlations between *T. occidentalis* ring width and $\delta^{13}\text{C}$ generally displayed a weak to absent association as well as low synchronicity in year-to-year change of sign. These findings are consistent with those of the other studies in Manitoba (Brooks et al. 1998; Tardif et al. 2008) and suggest that the physiological processes governing each tree-ring parameter are generally distinct. No significant association ($p=0.82$) was found between the same tree-ring parameters in *P. banksiana* trees near Thompson, Manitoba (Brooks et al. 1998). Similarly, Tardif et al. (2008) also showed an absence of any consistent relationship between ring width and $\delta^{13}\text{C}$ among *P. glauca* trees. Interestingly, McCarroll et al. (2003) have reported positive correlations between Scots pine (*Pinus sylvestris* L.) $\delta^{13}\text{C}$ and ring width ($p<0.05$), latewood density ($p<0.01$) and maximum density ($p<0.01$). In contrast, Andreu et al. (2008) reported negative associations ($p<0.05$) between ring width and $\delta^{13}\text{C}$ of *Pinus* species. A negative association is intuitive to the current theory that $\delta^{13}\text{C}$ -enrichment should result from tree stress, i.e. moisture deficit and hence reduced radial growth (McCarroll and Loader 2006). In our study, the generally absent association between ring width and $\delta^{13}\text{C}$ could indicate the independence of the principal climatic factors influencing each parameter. Kirilyanov et al. (2008) and Tardif et al. (2008) have also suggested that the time periods over which radial growth and carbon fixation occur may not take place simultaneously.

Aside from containing climatic information independent of ring width, tree-ring $\delta^{13}\text{C}$ generally requires fewer series to construct a representative regional chronology compared to ring width (see review of McCarroll and Loader 2006). Accordingly, less replication was required to achieve suitable signal strength for $\delta^{13}\text{C}$ compared to ring width in this study. The signal strength was also enhanced for $\delta^{13}\text{C}$ when both sites-A and -B were combined, but decreased slightly when the same was done with ring width. Similarly, Andreu et al. (2008) have found stronger inter-site correlations among $\delta^{13}\text{C}$ chronologies compared to ring-width chronologies of *Pinus* species growing on the Iberian Peninsula, Spain. The researchers consequently suggested that $\delta^{13}\text{C}$, rather than ring-width chronologies, could be a better recorder of large spatial-scale climate signals. Gagen and McCarroll (2004) have also found the strongest climate signal in latewood $\delta^{13}\text{C}$ of *Pinus* species from two sites in the driest areas of the French Alps compared to tree-growth chronologies (latewood width and density) which showed largely inconsistent climate correlations between sites.

It was expected that *T. occidentalis* $\delta^{13}\text{C}$ would contain a stronger common signal relative to ring width, however, this was not observed. The *T. occidentalis* ring-width and $\delta^{13}\text{C}$ combined-site chronologies contained common signals of similar strength (EPS ~ 0.85). In this study, the threshold for statistically robust signal strength, $\text{EPS} \geq 0.85$, was passed with the inclusion of eight $\delta^{13}\text{C}$ series for *T. occidentalis* trees. Similar results were found at the tree-line of subarctic Manitoba, where an assessment of signal strength in of *P. glauca* $\delta^{13}\text{C}$ suggested that the sampling of eight to ten trees was sufficient to reach this baseline EPS (Tardif et al. 2008). Since high variation was shown

among the *P. glauca* $\delta^{13}\text{C}$ series, Tardif et al. (2008) further suggested that there was no single dominant environmental influence for *P. glauca* trees growing at the tree-line near Churchill, Manitoba. In contrast, the baseline EPS was reached with only three trees per site in southwest Finland (Robertson et al. 1997a) and four to five trees per site in east England using English oak (*Quercus robur* L.) $\delta^{13}\text{C}$ series (Robertson et al. 1997b). In our study, the requirement of more series to attain a suitable common signal than in the *Q. robur* studies could be related to the effect of local stand dependant factors, i.e. fire, gap dynamics and disease, on both *T. occidentalis* ring width and $\delta^{13}\text{C}$. The evidence of low-intensity surface fires have been observed in living *T. occidentalis* trees growing in the northern Interlake region, Manitoba (Ko Heinrichs 2009). Hence, surface fires within this area could have altered stand conditions enough to affect tree-ring $\delta^{13}\text{C}$. McDowell et al. (2003) have found that stand density reductions resulted in higher stomatal conductance and greater $\delta^{13}\text{C}$ discrimination in Ponderosa pine (*Pinus ponderosa* Douglas ex C. Lawson) as a result of increased soil moisture which could last up to 15 years. In contrast, increased stand thinning was also shown to lower $\delta^{13}\text{C}$ discrimination of Monterey pine (*Pinus radiata* D. Don) and Maritime pine (*Pinus pinaster* Aiton) via increased photosynthesis by greater interception of radiation post-thinning (Warren et al. 2001).

3.5.2. Site differences in soil moisture influence the climatic information contained in *Thuja occidentalis* $\delta^{13}\text{C}$

Both well-replicated *T. occidentalis* $\delta^{13}\text{C}$ site chronologies constructed in this study show remarkably similar correlations with climate. However, differences were

observed in the strength of climate association between the two $\delta^{13}\text{C}$ site chronologies which could be related to subtle differences in soil drainage. The latter may be inferred by comparison of the dominant understory vegetation observed at either site. The dominant understory vegetation, i.e. *Epilobium angustifolium*, *Aralia nudicaulis*, noted at site-A is indicative of more mesic conditions compared to those at site-B which contained more hydrophilic plants, i.e. *Rhododendron groenlandicum*, *Betula pumila*, *Equisetum spp* (Ringius and Sims 1997). Additionally, the moisture-saturated conditions at site-B, i.e. numerous scattered wet depressions, could have contributed to the much lower mean *T. occidentalis* radial growth observed at this site than compared to site-A. Correspondingly, significant associations to drought conditions and precipitation were observed for *T. occidentalis* $\delta^{13}\text{C}$ at site-A (more mesic) while these associations at site-B (more hydric) were somewhat weaker and non-significant. Instead, $\delta^{13}\text{C}$ at site-B was more strongly correlated to temperature throughout the current growing season compared to $\delta^{13}\text{C}$ at site-A.

Soil moisture status, therefore, also has an appreciable influence on the stomatal conductance of *T. occidentalis* trees at the northwestern limit of their distribution. These findings are consistent with those of Saurer et al. (1995) who have compared the climate associations of common beech (*Fagus sylvatica* L.) $\delta^{13}\text{C}$ growing at dry and humid sites in the Swiss Central Plateau. Stronger negative correlations with precipitation were found for tree-ring $\delta^{13}\text{C}$ at dry sites compared to the humid site. Similarly, the whole-leaf and cellulose $\delta^{13}\text{C}$ of various shrub and tree species sampled on hummocks were shown to be enriched compared to those sampled from depressions suggesting that the drier

hummock conditions were more conducive to moisture stress in northern Scandinavia (Loader and Rundgren 2006).

Saurer et al. (1995) also reported that weaker tree-ring $\delta^{13}\text{C}$ associations to both precipitation and temperature resulted from *F. sylvatica* trees growing in humid conditions compared to those growing in dry conditions in the Swiss Central Plateau. *Thuja occidentalis* $\delta^{13}\text{C}$, in contrast, showed a stronger association with temperature, but weaker association with precipitation during the current summer season at the more hydric site-B compared to site-A. These results could be related to the broad tolerance of *T. occidentalis* trees to a wide range of hydrological conditions (Collier and Boyer 1989; Matthes-Sears and Larson 1991). The importance of excessive soil moisture conditions on tree-ring $\delta^{13}\text{C}$ was stressed by Buhay et al. (2008) who have suggested that the root function of *P. glauca* trees growing on a site prone to flooding could be limited by anaerobic soil conditions. Contrasting results were, however, reached with *Q. robur* latewood $\delta^{13}\text{C}$ at two sites with differing moisture availability on the Island of Ruissalo, Turku, Finland (Robertson et al. 1997a). Similar cross-correlations between climate and $\delta^{13}\text{C}$ were observed regardless of the site-specific moisture conditions, i.e. dry or wet site, which the authors suggested could be attributable to the ability of *Q. robur* to tap underground water reservoirs. Hence, the ability of tree-ring $\delta^{13}\text{C}$ to track moisture conditions will also depend on phenotypic characteristics of the particular tree species.

3.5.3. Ring-width and $\delta^{13}\text{C}$ sensitivity to drought periods on the Boreal Plains

In this study, the susceptibility of *T. occidentalis* radial growth to moisture stress was observed by negative correlations between ring width and the CDC during June ($t-1$) and September ($t-1$). Water deficits during the year prior to ring formation could inhibit leaf, bud and root system development and could reduce the total photosynthetic area and fine-root branches thereby lowering the ability to take advantage of more favorable climatic conditions the following year (Fritts 1976). *Thuja occidentalis* radial growth was also negatively correlated with the CDC during the current growing season and was especially prone to moisture stress during June (t) as evidenced by the positive and negative responses to precipitation and temperature, respectively. Corresponding moisture stress responses to June (t) temperature and precipitation were also observed from *T. occidentalis* trees growing in the boreal forest of western Québec (Archambault and Bergeron 1992b; Tardif and Bergeron 1997) and in the Cedar Lake/ northern Interlake region, central Manitoba (Tardif and Stevenson 2001).

It was consequently expected that *T. occidentalis* $\delta^{13}\text{C}$ would be influenced by moisture stress since *T. occidentalis* radial growth was shown to be dependant on water availability. Our results confirmed this hypothesis. Monthly climate correlations with $\delta^{13}\text{C}$ yielded results consistent with the current theory involving the dominance of the stomatal control to carbon assimilation i.e. enriched $\delta^{13}\text{C}$ showed positive correlations with temperature and negative correlations with precipitation (Schleser et al. 1999). Enriched tree-ring $\delta^{13}\text{C}$ was therefore a consequence of a limited supply of intercellular leaf CO_2 reduced by low stomatal conductance as synthesized by McCarroll and

Pawellek (2001). The current theory involving the stomatal control of intercellular CO₂ concentration indicates that precipitation and relative humidity should strongly limit tree-ring $\delta^{13}\text{C}$ variation (McCarroll and Pawellek 2001; McCarroll and Loader 2006). In this study, $\delta^{13}\text{C}$ was only shown to be correlated with precipitation for the summer season during the year of growth which could be related to the importance of preexisting moisture availability, rather than individual monthly precipitation, over the growing season (McCarroll and Pawellek 2001). Moisture stress was, however, demonstrated by the positive association of the CDC indices with $\delta^{13}\text{C}$ during June (t), July (t) and September (t) and the current summer season. To corroborate our findings, Edwards and Dixon (1995a) studied the physiological responses to drought stress in *T. occidentalis* trees and concluded that stomatal resistance (closure) was the principal mechanism for water conservation. In fact, reduced transpiration was evident even in mildly water stressed *T. occidentalis* trees suggesting that the mechanisms limiting stomatal aperture were responsive to slight changes in moisture availability.

Sensitivity to moisture stress throughout the *T. occidentalis* chronologies were observed as periods of low radial growth, decreased discrimination and enriched $\delta^{13}\text{C}$ values during the 1790s, 1840s, 1890s, 1930s and 1965-75. Case (2000) also reconstructed the annual precipitation of Dauphin, Manitoba over 1528-1997 AD using the *T. occidentalis* growing near Easterville, the northern Interlake region of Manitoba. Major decadal drought periods identified throughout this record included: the 1700's, 1790's, 1840's, 1890's and 1930's. These periods, as well as those identified in our

study, also coincide with three major drought intervals: 1838-1848, 1885-1896 and 1929-1937 in western Canada emphasized from historical climate data (Hope 1938).

Our findings also show that the 1790s, 1840s, 1890s, 1930s and 1965-75 moisture stress periods corresponded to periods of decreased growth in other tree species and large fires documented elsewhere in Manitoba. Pronounced growth depressions during the 1750's, early 1800's, 1840's, mid-1880's, 1930's and early-1960's were observed in *P. banksiana* and *P. mariana* ring-width chronologies from the Duck Mountain Provincial Forest (DMPF) situated in the boreal plains of western Manitoba (Tardif 2004). Tardif (2004) also reported fire scar years during the early 1750s, mid 1840s, 1875 and late 1880s coincident with the periods of reduced growth. Correspondingly, the July Canadian Drought Code reconstruction of the Boreal Plains region of Manitoba also showed persistent dry summers during: 1735-1743, 1838-1843, 1887-1892, 1936-1940 and 1958-1963 (Girardin et al. 2006). These findings show synchronous growth responses with other conifers in the same ecozone and provide strong evidence that the *T. occidentalis* ring-width and $\delta^{13}\text{C}$ chronologies are also representative of climate over a larger area. However, moisture stress responses similar to the growth reductions of conifers observed during the 1750's and early 1800's in DMPF were not shown in *T. occidentalis* trees.

The dry periods shown to correspond to periods of low radial growth and enriched $\delta^{13}\text{C}$ values (lower discrimination against the heavier stable carbon isotope; ^{13}C) during the 1790s, 1890s, and 1965-75 were, however, better characterized by the *T. occidentalis*

ring-width chronology than compared to $\delta^{13}\text{C}$. During these periods, the reduction of *T. occidentalis* radial growth was visibly more pronounced than the enrichment of *T. occidentalis* $\delta^{13}\text{C}$ which was more variable. The 1790 and 1890 droughts are common characteristics in tree-ring precipitation reconstructions from the Canadian Prairies (Sauchyn and Beaudoin 1998). Extremely destructive forest fires were also documented in DMPF during 1885-1895 (Gill et al. 1930) and also constituted a very destructive period with estimated 83% of DMPF burning in this decade (Tardif 2004). In this study, 1961 coincided with the second highest CDC value (457) of our records which was only surpassed in 1929. Although these drought periods are well documented from independent sources, they are more pronounced in ring width than $\delta^{13}\text{C}$ suggesting that ring width could be more sensitive to prolonged drought periods in the northern Interlake region.

The *T. occidentalis* ring-width and $\delta^{13}\text{C}$ chronologies may also each record a different major wet interval throughout the 19th century. The *T. occidentalis* $\delta^{13}\text{C}$ chronology was shown to be depleted during the 1820s-1830s but did not show an extended period of depletion during the 1850s. Instead, enhanced radial growth was observed for the *T. occidentalis* ring-width chronology during this latter period. St. George and Nielsen (2002) reconstructed August ($t-1$) to July (t) precipitation for southern Manitoba using bur oak (*Quercus macrocarpa* Michx.) and reported that hydro-climate variability was relatively stable over the past 200 years. These researchers found, however, that wet periods occurred during the late 1820s and 1850s. Rannie (2006) also reported similar wet summers for the eastern Prairies inferred from historical records

spanning the periods: 1824-1834 and 1849-1861, during which archival accounts indicated that almost every summer was wetter than normal. These findings suggest that both *T. occidentalis* ring width and $\delta^{13}\text{C}$ could provide complementary information during wet intervals. More studies are, however, required to support this finding.

3.5.4. *Thuja occidentalis* ring width and $\delta^{13}\text{C}$ display individualistic climatic windows

Environmental conditions during the year prior to *T. occidentalis* ring-formation were shown to influence radial growth to a much greater extent than compared to carbon assimilation in the northern Interlake region, central Manitoba. Minimum and maximum temperature during November (t_{-1}) and December (t_{-1}) were found to be positively associated with *T. occidentalis* radial growth. The positive association between late-fall temperature of the year prior to growth and radial growth was also commonly observed in dendroclimatic studies conducted from northern to southern Manitoba and in various conifer species (Jacoby and Ulan 1982; Case 2000; Tardif and Stevenson 2001; Girardin et al. 2005; Au and Tardif 2007; Tardif et al. 2008; Hoffer and Tardif 2009). In the northern Interlake region, Tardif and Stevenson (2001) hypothesized that warm late-fall temperatures could reduce the structural damage of *T. occidentalis* leaves and/or reduce the depth at which the soil becomes frozen, since they observed similar associations with temperature during November (t_{-1}) and December (t_{-1}). Case (2000) reported that the positive association between *T. occidentalis* radial growth and November (t_{-1}) maximum temperature could be related to the ability to develop greater food reserves during this period. Surprisingly, *T. occidentalis* ring width was also negatively correlated to radiation (kilojoules per m^2) from November (t_{-1}) through to February (t). Desiccation

damage of *T. occidentalis* leaves and twigs have been documented under natural conditions (Curry and Church 1952; Sakai 1970) which have been suggested to result from a combination of exposure to sunshine and freezing (Sakai 1970). These findings could indicate that the longer duration of sunshine received from late-fall through winter prior to growth could promote desiccation injury whereby leaves lose water through transpiration.

In this study, few correlations were found to be significant for $\delta^{13}\text{C}$ in the year prior to ring-formation. Monserud and Marshall (2001) suggested that correlations between tree-ring $\delta^{13}\text{C}$ and climate conditions in the year prior to ring formation could result if photosynthates produced from a previous year are used to produce cellulose during the current year of growth. Our results suggest that photosynthates produced in the year prior to ring-formation were not utilized during wood formation. In support of this hypothesis, Glerum and Balatinecz (1980) demonstrated that food reserves played a supporting role but were not directly used in xylem formation of *P. banksiana* seedlings during the resumption of growth in the spring. Instead, a pronounced decrease in ^{14}C throughout *P. banksiana* seedlings indicated that reserves were largely utilized to maintain plant respiration in the spring to prepare the tree for active photosynthesis whereas, photosynthates produced over the current growing season were important for new growth i.e. wood formation. Alternatively, Kagawa et al. (2006) have found that the earlywood of *Larix gmelinii* (Rupr.) Rupr. trees relied on reserves accumulated from both the current growing season as well as those from previous growing seasons whereas, latewood mainly contained photosynthates produced over the current year. Other studies

have shown that stored food reserves are rapidly consumed during respiration by expanding buds and shoot growth early in the growing season (Kozlowski and Gentile 1958; Kozlowski and Winget 1964). Therefore, photosynthates produced at the leaf-level are directly incorporated into cellulose for *T. occidentalis* in central Manitoba. Balatinecz et al. (1966) investigated the movement of ^{14}C in eight-month-old *P. banksiana* seedlings via photosynthesis in C^{14}O_2 . The researchers found that although some ^{14}C remained mobile throughout the plant after several days, all radioactive carbon was deposited into wood tissue and remained non-mobile after the relatively short time span of six days.

Thuja occidentalis ring width could thus be a better recorder of persistent multi-year droughts than compared to $\delta^{13}\text{C}$ since the former was more strongly influenced by conditions during the year prior to growth. Further evidence exists suggesting that stomatal conductance may be adjusted by the plant following exposure to drought conditions. Edwards and Dixon (1995b) exposed six-year-old *Thuja occidentalis* trees to successive cycles of mild or moderate moisture stress to determine whether trees exposed to drought conditions would develop a tolerance to subsequent water deficit. After exposing *T. occidentalis* trees to a nine-day severe drought, they found lower transpiration rates (as much as 38% less) for trees previously exposed to cycles of moderate moisture stress than compared to those previously exposed to mild moisture stress or those previously well-watered. A drought tolerance was indicated for moderately water stressed trees since these trees exhibited less stress compared to trees in the other categories. In this study, the conditioning of *T. occidentalis* stomatal

functioning to drought conditions could also explain the absence of consistent year-to-year enriched $\delta^{13}\text{C}$ values during extended dry periods. Stomatal functioning preconditioned to the prior year's water deficit could therefore adapt to a subsequent drought of similar magnitude thereby translating into less enriched $\delta^{13}\text{C}$ being assimilated into the tree-ring during a given year.

During the year of ring-formation, both *T. occidentalis* ring width and $\delta^{13}\text{C}$ associations with climate corroborated with previous reports of the initiation and cessation of the *T. occidentalis* growing season in the boreal forest (Forster et al. 2000; Ko Heinrichs et al. 2007). Ko Heinrichs et al. (2007) studied xylem production by repeatedly taking microcore samples from the stems of six tree species growing in the same region. The onset of xylem cell production of *T. occidentalis* trees were found to have begun during the second half of May in the boreal forest region of western Québec, Canada (Ko Heinrichs et al. 2007). Correspondingly, May (t) maximum temperature was significantly associated with both radial growth and carbon assimilation.

Furthermore, Ko Heinrichs et al. (2007) found that about 50% of annual *T. occidentalis* radial growth was formed by the end of June and the date of the greatest xylem cell production (June 21) also occurred within this month in the boreal forest region of western Québec, Canada. These findings suggest that the month of June is crucial for *T. occidentalis* trees and is consistent with the importance of June (t) maximum temperature for both radial growth and carbon assimilation. Alternatively, August (t) maximum temperature was only restrictive for $\delta^{13}\text{C}$ and coincided with the

onset of *T. occidentalis* latewood tracheid production reported by Ko Heinrichs et al. (2007) which began near the start of August and ended (date of 90% of cell production) shortly after in early-August. In fact, latewood tracheids have much thicker cell walls, 7.0–8.0 μm , than those of earlywood tracheids, 1.5–3.0 μm (Vaganov et al. 2006). Bannan (1955) found that although the division of xylem cells had ceased by the end of September, continued secondary wall thickening was, however, still evident in *T. occidentalis* trees. These findings indicate that photosynthates continued to be deposited during secondary xylem wall thickening well after the majority of radial growth had been completed.

In this study, the climatic window for *T. occidentalis* radial growth included the previous year and current spring and summer conditions whereas that for carbon assimilation was more representative of current summer conditions. These findings are consistent with those of other studies which have shown that the climatic windows for ring width and $\delta^{13}\text{C}$ are not distributed over the same seasonal interval. Tardif et al. (2008) showed that the climatic window for radial growth was set early in the growing season (June and July) while that for $\delta^{13}\text{C}$ mainly predominated later in the growing season (July and August) for *P. glauca* trees growing near the tree-line in subarctic Manitoba, Canada. Correspondingly, Gagen et al. (2006) have also found different climatic windows of response among latewood width, density and $\delta^{13}\text{C}$ chronologies of *P. sylvestris* and mountain pine (*Pinus uncinata* Mill. ex Mirb.) growing at the sub-alpine tree-line, southern French Alps. Latewood width was correlated with May precipitation, latewood $\delta^{13}\text{C}$ with July and August precipitation and latewood density with August and

September maximum temperature. Therefore, the ability to infer different climate information from $\delta^{13}\text{C}$ distinguishes the latter from ring width as a unique proxy of climate.

3.5.5. Temporal stability of ring width and $\delta^{13}\text{C}$ – climate associations

In dendroclimatology, the analysis of the stability in climate association is an important consideration for studies which attempt to reconstruct climate using tree-ring parameters. It was expected that the *T. occidentalis* $\delta^{13}\text{C}$ / ring width – climate association would be temporally stable throughout the 20th century. However, we found an apparent change in the importance from previous year drought since the beginning of the 20th century up until 1960 whereby current year drought became important henceforth for *T. occidentalis* ring width. During the period 1960-2005, a stronger association to drought was also recorded in $\delta^{13}\text{C}$ in the summer season during the year of ring-formation. The effect of higher quality climate data on the climate correlations during the more recent period cannot be completely discounted since a substantially closer mean meteorological station distance was observed at approximately the onset of the period 1960-2005. Moreover, ring width and $\delta^{13}\text{C}$ were shown to share slightly less common variation during the period 1960-2005 than compared to during the period 1900-1959. It could thus be argued that the introduction of $\delta^{13}\text{C}$ series from younger trees during 1964-70 could have influenced the climate correlations observed with $\delta^{13}\text{C}$. This scenario is unlikely, however, since high correlations were observed between standardized $\delta^{13}\text{C}$ series from live (generally young) and dead *Thuja occidentalis* trees. Analysis of 50-year periods (PCA analyses) suggested that such slight changes in association between ring

width and $\delta^{13}\text{C}$ have also occurred throughout the duration of our records, i.e. throughout the 18th and 19th centuries, and not only during the 20th century. We therefore, propose that the apparent change in importance from previous year to current year drought conditions for ring width was likely the result of the natural variability in climate. Further analysis of 100-year sub-periods covering 1700 to 1999 showed that the correlation structure among the *T. occidentalis* ring-width and $\delta^{13}\text{C}$ residual chronologies remained stationary. These results are important for the dendroclimatic potential of *T. occidentalis* trees at the northwestern limit of their distribution, especially for reconstructions using both ring width and $\delta^{13}\text{C}$.

We also observed a decreased importance of maximum summer temperature for $\delta^{13}\text{C}$ during the period 1960-2005. Similarly, Saurer et al. (2008) have found a reduction in $\delta^{13}\text{C}$ sensitivity to July-August temperature after about 1960 in *F. sylvatica*, sessile oak (*Quercus petraea* (Mattuschka) Liebl.), silver fir (*Abies alba* Mill.), Norway spruce (*Picea abies* (L.) H. Karst.) and *P. sylvestris* growing in Switzerland. They hypothesized that the sensitivity was related to a physiological response coinciding with the accelerated rise in atmospheric CO_2 concentration. Fluctuations in CO_2 concentrations could affect plant physiological function since atmospheric CO_2 is the substrate of photosynthesis (Marshall and Monserud 1996). Elevated CO_2 concentrations have resulted in increased water-use efficiency through decreased transpiration in some seasonally dry regions (Eamus and Jarvis 1989; Mooney et al. 1991; Pitelka 1994). Conversely, Marshall and Monserud (1996) have found relatively constant water-use efficiency over the past century in three coniferous species in western United States. It may be that a constant or

varying intercellular leaf CO₂ adjustment to elevated ambient CO₂ concentrations could be dependant on the species (Ehleringer and Cerling 1995; Waterhouse et al. 2004) and/or differences in micro-environmental variables.

3.5.6. Tree-ring $\delta^{13}\text{C}$ chronologies in Manitoba show different limitations to carbon assimilation

Drought stress (stomatal control of photosynthesis) was shown to be the most likely limitation to $\delta^{13}\text{C}$ in seasonally dry climates (Warren et al. 2001).

Correspondingly, the *T. occidentalis* trees sampled from the northern Interlake region, Manitoba, Boreal Plains ecozone, and the *P. banksiana* trees sampled from Thompson, Manitoba, Boreal Shield ecozone were both found to be sensitive to moisture stress.

Winter and growing season precipitation were found to be dominant factors controlling *P. banksiana* $\delta^{13}\text{C}$ (Brooks et al. 1998) while *T. occidentalis* $\delta^{13}\text{C}$ was strongly associated with current growing season drought indices. In contrast to either *T. occidentalis* or *P. banksiana* $\delta^{13}\text{C}$, Tardif et al. (2008) demonstrated that tree-ring $\delta^{13}\text{C}$ from *P. glauca* trees growing near the tree-line at Churchill, Manitoba, Hudson Plains ecozone was dominated by a temperature signal (photosynthetic rate of control). Since the study area was adjacent to Hudson Bay and characterized by poorly drained wetlands, Tardif et al. (2008) suggested that the cold and moist maritime air from Hudson Bay could have reduced evapotranspiration along with the importance of the stomatal control of photosynthesis.

Interestingly, the *P. glauca* and *P. banksiana* $\delta^{13}\text{C}$ chronologies were found to be significantly associated while only a weak association was observed between the former and *T. occidentalis*. Moreover, the lack of association observed between *T. occidentalis* and *P. banksiana* $\delta^{13}\text{C}$ could have resulted from differences in the soil moisture regimes and therefore, relative humidity at each respective study area. Site conditions consisted of organic wetlands for the *T. occidentalis* trees while the *P. banksiana* trees grew on a well-drained, sandy soil. Alternatively, differences among the $\delta^{13}\text{C}$ chronologies could also be a consequence of varying species-specific/ physiological traits controlling the intercellular leaf to ambient air CO_2 concentrations (Zhang and Cregg 1996; Andreu et al. 2008). *Thuja occidentalis* scale-leaf architecture, in comparison to the needle-leaf architecture of *P. glauca* and *P. banksiana*, could have resulted in differences in water-use efficiency (Zhang and Cregg 1996; Au and Tardif 2009). Munro (1989) showed that the stomatal conductance of *T. occidentalis* was much lower and less variable over the course of the day than either the broad-leaved *Fraxinus nigra* Marsh. and *Alnus rugosa* (Du Roi.) Spreng trees. In fact, stomatal conductance of *F. nigra* was almost an order of magnitude greater than that of *T. occidentalis*, while still greater overall conductance was exhibited by *A. rugosa*. We speculate that the distinction in leaf architecture may well have contributed to the lower $\delta^{13}\text{C}$ sensitivity observed in *T. occidentalis* compared to those of *P. glauca* and *P. banksiana*. No other studies have, however, reported the analysis of continuous tree-ring $\delta^{13}\text{C}$ time series of scale-leaf conifers.

Individualistic responses in tree-ring $\delta^{13}\text{C}$ could further be related to differences in large-scale climatic influences as well as the distinction in overall growing season

length since *P. glauca* $\delta^{13}\text{C}$ responded to temperature later in the summer than compared to *T. occidentalis* $\delta^{13}\text{C}$. The first month of the year where minimum temperature rises well above 0°C was June for *T. occidentalis* at central Manitoba while this was July for *P. glauca* at Churchill, Manitoba. Correspondingly, temperature was most strongly associated (positively) with *T. occidentalis* $\delta^{13}\text{C}$ during June (t) and with *P. glauca* $\delta^{13}\text{C}$ during July (t). These findings underscore the effect of growing season length on the carbon assimilation of trees separated by long latitudinal differences in central Canada.

3.6. Conclusion

The results from this study have shown that both the *T. occidentalis* ring-width and $\delta^{13}\text{C}$ parameters are sensitive to moisture stress at their northwestern limit of distribution in central Manitoba, Canada. As synthesized in the literature, higher vapor pressure deficit during times of drought causes a reduction in stomatal aperture which results in greater utilization of pre-existing intercellular leaf CO_2 by the photosynthetic enzyme. Drought, therefore, contributed to physiological stress which was recorded in the chronologies as periods of reduced radial growth along with $\delta^{13}\text{C}$ enrichment (limited by stomatal conductance). However, these tree-ring parameters showed a near absence of association, suggesting that each parameter contained individualistic climate information. Climate variables during the year prior to *T. occidentalis* ring-formation were shown to influence radial growth to a much greater extent than compared to carbon assimilation. Ring width was negatively associated with summer drought and positively associated with November and December temperatures during the year prior to ring-formation. During the current summer, ring width and $\delta^{13}\text{C}$ were negatively and positively

associated with the CDC, respectively. Nonetheless, the ring-width chronology showed a greater correspondence than that of $\delta^{13}\text{C}$ to prolonged drought documented from tree-ring records and historical accounts. It is suggested that the greater importance of climate conditions during the year prior to ring-formation could have resulted in radial growth as a better recorder of extended drought periods.

Interestingly, principal components analysis showed that the ring-width and $\delta^{13}\text{C}$ chronologies shared slightly less common variability during 1960-2005 than compared to 1900-1959. This slight change in chronology association was accompanied by an apparently greater importance of drought for both ring width and $\delta^{13}\text{C}$ during 1960-2005. However, frequent re-current changes in association between these parameters were also found to have occurred in the past suggesting that the introduction of younger trees over the later portion of the 20th century was not responsible for this change in association. Instead, we speculate that changes in association between the chronologies could be related to natural climatic variability.

The climatic window during the year of ring formation for *T. occidentalis* radial growth included the current spring and early summer (May and June maximum temperature as well as June and July precipitation) whereas, that for $\delta^{13}\text{C}$ was more integrative of summer temperatures (May, June and August maximum temperature). This indicated that photosynthates continued to be deposited after a majority of radial growth had been completed in line with other studies. The robust ring-width and $\delta^{13}\text{C}$ chronologies presented in this study indicate that independent climatic information is

contained in each tree-ring parameter which could be used in the reconstruction of climate. Future studies could examine tree-ring $\delta^{18}\text{O}$ of *T. occidentalis* trees which may reveal additional information on summer precipitation, since this parameter is also dependent on relative humidity.

3.7. Acknowledgements

We would like to thank France Conciatori (dendrochronology technician) and Derrick Ko Heinrichs (field assistant). Thanks go to Dr. Martin Girardin for calculating the Canadian Drought Code and for useful discussions regarding time-series analysis. Thanks are also due to the laboratory assistants, Justin Waito, Stephen Gietz and Anton Zavialov. Dr. Chris Eastoe of the Environmental Isotope Laboratory, University of Arizona, overlooked operation of the stable isotope mass spectrometer. Financial assistance was provided by the Canada Research Chairs Program, the Faculty of Science Graduate Studentship from the University of Manitoba, the National Sciences and Engineering Research Council of Canada (NSERC) and the University of Winnipeg.

3.8. References

Archambault, S. and Bergeron, Y. 1992a. Discovery of a living 900 year-old northern white cedar, *Thuja occidentalis*, in northwestern Québec. Canadian Field-Naturalist **106**(2): 192-195.

Archambault, S. and Bergeron, Y. 1992b. An 802-year tree-ring chronology from the Québec boreal forest. Canadian Journal of Forest Research **22**: 674-682.

Andreu, L., Planells, O., Gutiérrez, E., Helle, G. and Schleser, G.H. 2008. Climatic significance of tree-ring width and $\delta^{13}\text{C}$ in a Spanish pine forest network. Tellus **60B**: 771-781.

Au, R. and Tardif, J.C. 2007. Allometric relationships and dendroecology of the dwarf shrub *Dryas integrifolia* near Churchill, subarctic Manitoba. Canadian Journal of Botany **85**: 585-597.

Au, R. and Tardif, J.C. 2009. Chemical pretreatment of *Thuja occidentalis* tree-rings: implications for dendroisotopic studies. Canadian Journal of Forest Research **39**: 1777-1784.

- Balatinecz, J.J., Forward, D.F. and Bidwell, R.G.S. 1966. Distribution of photoassimilated $C^{14}O_2$ in young jack pine seedlings. *Canadian Journal of Botany* **44**: 362-364.
- Bannan, M.W. 1955. The vascular cambium and radial growth in *Thuja occidentalis* L. *Canadian Journal of Botany* **33**: 113-138.
- Barber, V., Juday, G. and Finney, R. 2000. Reduced growth of Alaska white spruce in the twentieth century from temperature-induced drought stress. *Nature* **405**: 668-672.
- Bergeron, Y. and Archambault, S. 1993. Decreasing frequency of forest fires in the southern boreal zone of the Québec and its relation to global warming since the end of the 'Little Ice Age'. *The Holocene* **3**: 255-259.
- Bristow, K.L. and Campbell, G.S. 1984. On the relationship between incoming solar radiation and daily maximum and minimum temperature. *Agricultural and Forest Meteorology* **31**: 159-166.
- Brooks, J.R., Flanagan, L.B. and Ehleringer, J.R. 1998. Responses of boreal conifers to climate fluctuations: indications from tree-ring widths and carbon isotope analyses. *Canadian Journal of Forest Research* **28**: 524-533.

Buckley, B.M., Wilson, R.J.S., Kelly, P.E., Larson, D.W. and Cook, E.R. 2004. Inferred summer precipitation for southern Ontario back to AD 610, as reconstructed from ring widths of *Thuja occidentalis*. *Canadian Journal of Forest Research* **34**(12): 2541-2553.

Buhay, W.M., Timsic, S., Blair, D., Reynolds, J., Jarvis, S., Petrash, D., Rempel, M. and Bailey, D. 2008. Riparian influences on carbon isotopic composition of tree rings in the Slave River Delta, Northwest Territories, Canada. *Chemical Geology* **252**: 9-20.

Bukata, A.R. and Kyser, T.K. 2007. Carbon and nitrogen isotope variations in tree-rings as records of perturbations in regional carbon and nitrogen cycles. *Environmental Science and Technology* **41**(4): 1331-1338.

Case, R.A. 2000. Dendrochronological investigations of precipitation and streamflow for the Canadian Prairies. Ph.D. Thesis, Department of Geography, University of California, Los Angeles.

Collier, D.E. and Boyer, M.G. 1989. The water relations of *Thuja occidentalis* L. from two sites of contrasting moisture availability. *Botanical Gazette* **150**: 445-448.

Cook, E.R. 1985. A time series analysis approach to tree-ring standardization. Ph.D. dissertation, University of Arizona, Tucson.

Cook, E.R. and Holmes, R., 1986. Guide for computer program ARSTAN. Laboratory of Tree-Ring Research. University of Arizona, Tucson, Arizona.

Cook, E.R. and Kairiukstis, L.A., eds. 1990. Methods of dendrochronology: applications in the environmental science. International Institute for Applied Systems Analysis. Kluwer Academic Publishers, Dordrecht, The Netherlands.

Curry, J. R. and Church, T.W. 1952. Observations on winter drying of conifers in the Adirondacks. *Journal of Forestry* **50**: 114-116.

Denneler, B., Bergeron, Y., Bégin, Y. and Asselin, H. 2008. Growth responses of riparian *Thuja occidentalis* to the damming of a large boreal lake. *Botany* **86**: 53-62.

Eamus, D. and Jarvis, P.G. 1989. The direct effects of increase in the global atmospheric CO₂ concentration on natural and commercial temperate trees and forests. *Advances in Ecological Research* **19**: 1-55.

Edwards, D.R. and Dixon, M.A. 1995a. Mechanisms of drought response in *Thuja occidentalis* L. I. water stress conditioning and osmotic adjustment. *Tree Physiology* **15**: 121-127.

Edwards, D.R. and Dixon, M.A. 1995b. Mechanisms of drought response in *Thuja occidentalis* L. II. post-conditioning water stress and stress relief. *Tree Physiology* **15**: 129-133.

Ehleringer, J.R. and Cerling, T.E. 1995. Atmospheric CO₂ and the ratio of intercellular to ambient CO₂ concentrations in plants. *Tree Physiology* **15**: 105-111.

Environment Canada. 2004. Climate normals 1971-2000. Canadian climate program. Environment Canada. Atmospheric Environment Service, Downsview, Ontario.

Esper, J., Cook, E.R. and Schweingruber, F.H. 2002. Low-frequency signals in long tree-ring chronologies for reconstructing past temperature variability. *Science* **295**: 2250-2253.

Farquhar, G.D., O'Leary, M.H. and Berry, H.A. 1982. On the relationship between carbon isotope discrimination and intercellular carbon dioxide concentration in leaves. *Australian Journal of Plant Physiology* **9**: 121-137.

Forster, T., Schweingruber, F.H. and Denneler, B. 2000. Increment puncher: a tool for extracting small cores of wood and bark from living trees. *IAWA Journal* **21**: 169-180.

- Francey, R.J., Allison, C.E., Etheridge, D.M., Trudinger, C.M., Enting, I.G., Leuenberger, M., Langengelds, R.L., Michel, E. and Steele, L.P. 1999. A 1000-year high precision record of $\delta^{13}\text{C}$ in atmospheric CO_2 . *Tellus* **51B**: 170-193.
- Freyer, H.D. 1986. Interpretation of the northern hemispheric record of $^{13}\text{C}/^{12}\text{C}$ trends of atmospheric CO_2 in tree rings. *In Changing carbon cycle, a global analysis. Edited by J.R. Trabalka and D.E. Reichle. Springer-Verlag, New York, New York. pp.125-150.*
- Freyer, H.D. and Belacy, N. 1983. $^{13}\text{C}/^{12}\text{C}$ records in northern hemispheric trees during the past 500 years-anthropogenic impact and climatic superpositions. *Journal of Geophysical Research* **88**: 6844-6852.
- Fritts, H.C. 1976. *Tree rings and climate. Academic Press, New York, New York.*
- Gagen, M. and McCarroll, D. 2004. Latewood width, maximum density, and stable carbon isotope ratios of pine as climate indicators in a dry subalpine environment, French Alps. *Arctic, Antarctic and Alpine Research* **36**: 166-171.
- Gagen, M., McCarroll, D. and Edouard, J-L. 2006. Combining ring width, density, and stable carbon isotope proxies to enhance the climate signal in tree-rings: an example from the southern French Alps. *Climate Change* **78**: 363-379.

Gagen, M., McCarroll, D., Loader, N.J., Robertson, I., Jalkanen, R. and Anchukaitis, K.J. 2007. Exorcising the 'segment length curse': summer temperature reconstruction since AD 1640 using non-detrended stable carbon isotope ratios from pine trees in northern Finland. *The Holocene* **17**(4): 435-446.

Gaudinski, J.B., Dawson, T.E., Quideau, S., Schuur, E.A.G., Roden, J.S., Trumbore, S.E., Sandquist, D.R., Oh, S-W., and Wasylishen, R.E. 2005. Comparative analysis of cellulose preparation techniques for use with ^{13}C , ^{14}C , and ^{18}O isotopic measurements. *Analytical Chemistry* **77**: 7212-7224.

Gessler, A., Brandes, E., Buchmann, N., Helle, G., Rennenberg, H. and Barnard, R.L. 2009. Tracing carbon and oxygen isotope signals from newly assimilated sugars in the leaves to the tree-ring archive. *Plant, Cell and Environment* **32**: 780-795.

Gill, C.B. 1930. Cyclic forest phenomena. *Forestry Chronicle* **6**: 42-56.

Girardin, M-P., Tardif, J., Flannigan, M.D., Wotton, B.M. and Bergeron, Y. 2004. Trends and periodicities in the Canadian drought code and their relationships with atmospheric circulation for the southern Canadian boreal forest. *Canadian Journal of Forest Research* **34**: 103-119.

Girardin, M-P., Berglund, E., Tardif, J. and Monson, K. 2005. Radial growth of tamarack (*Larix laricina*) in the Churchill area (Manitoba) in relation to climate and larch sawfly (*Pristiphora erichsonii*) herbivory. *Arctic, Antarctic and Alpine Research* **37**: 206-217.

Girardin, M-P., Tardif, J.C., Flannigan, M.D. and Bergeron, Y. 2006. Synoptic-scale atmospheric circulation and Boreal Canada summer drought variability of the past three centuries. *Journal of Climate* **19**: 1922-1947.

Glassy, J.M. and Running, S.W. 1994. Validating diurnal climatology of the MT-CLIM model across a climatic gradient in Oregon. *Ecological Applications* **4**: 248-257.

Glerum, C. and Balatinecz, J.J. 1980. Formation and distribution of food reserves during autumn and their subsequent utilization in jack pine. *Canadian Journal of Forest Research* **58**: 40-54.

Grotte, K. 2007. Old-growth northern white-cedar (*Thuja occidentalis* L.) stands in the mid-boreal lowlands of Manitoba. B.Sc. thesis, Department of Biology, University of Winnipeg, Winnipeg, Manitoba.

Hemming, D., Fritts, H., Leavitt, S.W., Wright, W., Long, A. and Shashkin, A. 2001. Modelling tree-ring $\delta^{13}\text{C}$. *Dendrochronologia* **19**(1): 23-38.

Hoffer, M. and Tardif, J.C. 2009. False rings in jack pine and black spruce trees from eastern Manitoba as indicators of dry summers. *Canadian Journal of Forest Research* **39**: 1722-1736.

Holmes, R.L. 1983. Computer assisted quality control in tree-ring dating and measurement. *Tree-Ring Bulletin* **43**: 69-78.

Hope, E.C. 1938. Weather and crop history in western Canada. *Canadian Society of Technical Agriculturalists Review* **16**: 347-358.

Hunter, R.D., Panyushkina, I.P., Leavitt, S.W., Wiedenhoeft, A.C., and Zawiskie, J. 2006. A multiproxy environmental investigation of Holocene wood from a submerged conifer forest in Lake Huron, USA. *Quaternary Research* **66**: 67-77.

Jacoby, G.C. and Ulan, L.D. 1982. Reconstruction of past ice conditions in a Hudson Bay estuary using tree-rings. *Nature* **298**: 637-639.

Johnston, W.F. 1990. Northern white-cedar (*Thuja occidentalis* L.). *In* *Silvics of North America*. Vol. 1. Conifers. Agriculture Handbook 654. *Edited by* R.M. Burns and B.H. Honkala. U.S. Department of Agriculture Forest Service. Washington, D.C.

Jones, P.D., Briffa, K.R., Barnett, T.P. and Tett, S.F.B. 1998. High-resolution paleoclimatic records for the last millennium: interpretation, integration and comparison with General Circulation Model control-run temperatures. *The Holocene* **8**: 455-471.

Kagawa, A., Sugimoto, A. and Maximov, T.C. 2006. ^{13}C pulse-labeling of photoassimilates reveals carbon allocation within and between tree rings. *Plant, Cell and Environment* **29**: 1571-1584.

Kelly, P.E., Cook, E.R. and Larson D.W. 1994. A 1397-year tree-ring chronology of *Thuja occidentalis* from cliff faces of the Niagara Escarpment, southern Ontario, Canada. *Canadian Journal of Forest Research* **24**: 1049-1057.

Kirilyanov, A.V., Treydte, K.S., Nikolaev, A., Helle, G. and Schleser, G.H. 2008. Climate signals in tree-ring width, density and $\delta^{13}\text{C}$ from larches in Eastern Siberia (Russia). *Chemical Geology* **252**: 31-41.

Ko Heinrichs, D. 2009. Ecology of northern white-cedar (*Thuja occidentalis* L.) stands at their northwestern limit of distribution in Manitoba, Canada. M.Sc. thesis, Department of Biological Sciences, University of Manitoba, Winnipeg, Manitoba.

Ko Heinrichs, D., Tardif, J.C. and Bergeron, Y. 2007. Xylem production in six tree species growing on an island in the boreal forest region of western Quebec, Canada. *Canadian Journal of Botany* **85**: 518-525.

Kozlowski, T.T. and Gentile, A.C. 1958. Respiration of white pine buds in relation to oxygen availability and moisture content. *Forest Science* **4**: 147-152.

Kozlowski, T.T. and Winget, C.H. 1964. The role of reserves in leaves, branches, stems, and roots on shoot growth of red pine. *American Journal of Botany* **51**: 522-529.

Larson, D.W. 2001. The paradox of great longevity in a short-lived tree species. *Experimental Gerontology* **36**: 651-673.

Larson, D.W. and Kelly, P.E. 1991. The extent of old-growth *Thuja occidentalis* on cliffs of the Niagara Escarpment. *Canadian Journal of Botany* **69**: 1628-1636.

Larson, D.W. and Melville, L. 1996. Stability of wood anatomy of living and Holocene *Thuja occidentalis* L. derived from exposed and submerged portions of the Niagara Escarpment. *Quaternary Research* **45**: 210-215.

Leavitt, S.W. and Danzer, S.R. 1993. Method for batch processing small wood samples to holocellulose for stable-carbon isotope analysis. *Analytical Chemistry* **65**: 87-89.

Leavitt, S.W. and Long, A. 1984. Sampling strategy for stable carbon isotope analysis of tree rings in pine. *Nature* **311**(13): 145-147.

Leavitt, S.W., Panyushkina, I.P., Lange, T., Wiedenhoeft, A., Cheng, L., Hunter, R.D., Hughes, J., Pranschke, F., Schneider, A.F., Moran, J., and Stieglitz, R. 2006. Climate in the Great Lakes region between 14,000 and 4000 years ago from isotopic composition of conifer wood. *Radiocarbon* **48**(2): 205-217.

Legendre, P. and Legendre, L. 1998. *Numerical Ecology*. Elsevier Scientific Publishing Co., New York.

Loader, N.J. and Rundgren, M. 2006. The role of inter-specific, micro-habitat and climatic factors of the carbon isotope ($\delta^{13}\text{C}$) variability of a modern leaf assemblage from northern Scandinavia: implications for climate reconstruction. *Boreas* **35**: 188-201.

Loney, M. 1987. The construction of dependency: the case of the Grand Rapids hydro project. *Canadian Journal of Native Studies* **7**: 57-78.

Marshall, J.D. and Monserud, R.A. 1996. Homeostatic gas-exchange parameters inferred from $^{13}\text{C}/^{12}\text{C}$ in tree rings of conifers. *Oecologia* **105**: 13-21.

Matthes-Sears, U. and Larson, D.W. 1991. Growth and physiology of *Thuja occidentalis* L. from cliffs and swamps: Is variation habitat or site specific? *Botanical Gazette* **152**: 500-508.

McCarroll, D. and Loader, N.J. 2006. Isotopes in tree rings. *In* Developments in paleoenvironmental research vol. 10: isotopes in palaeoenvironmental research. *Edited by* M.J. Leng. Springer, The Netherlands. pp. 67-106.

McCarroll, D. and Pawellek, F. 1998. Stable carbon isotope ratios of latewood cellulose in *Pinus sylvestris* from northern Finland: variability and signal strength. *The Holocene* **8**: 675-684.

McCarroll, D. and Pawellek, F. 2001. Stable carbon isotope ratios of *Pinus sylvestris* from northern Finland and the potential for extracting a climate signal from long Fennoscandian chronologies. *The Holocene* **11**(5): 517-526.

McCarroll, D., Jalkanen, R., Hicks, S., Tuovinen, M., Gagen, M., Pawellek, F., Eckstein, D., Schmitt, U., Autio, J. and Heikkinen, O. 2003. Multiproxy dendroclimatology: a pilot study in northern Finland. *The Holocene*: **13**(6): 829-838.

McDowell, N.G., Phillips, N., Lurch, C., Bond, B.J. and Ryan, M.G. 2002. An investigation of hydraulic limitation and compensation in large, old Douglas-fir trees. *Tree Physiology* **22**: 763-774.

Moberg, A., Sonechki, D.M., Holmgren, K., Datsenko, N.M. and Karlén, W. 2005. Highly variable Northern Hemisphere temperatures reconstructed from low-and high-resolution proxy data. *Nature* **433**: 613-617.

Monserud, R.A. and Marshall, J.D. 2001. Time-series analysis of $\delta^{13}\text{C}$ from tree rings. I. Time trends and autocorrelation. *Tree Physiology* **21**: 1087-1102.

Mooney, H.A., Drake, B.G., Luxmoore, R.J., Oechel, W.C. and Pitelka, L.F. 1991. Predicting Ecosystem Responses to Elevated CO_2 Concentrations. *BioScience* **41**(2): 96-104.

Munro, D.S. 1989. Stomatal conductances and surface conductance modeling in a mixed wetland forest. *Agricultural and Forest Meteorology* **48**: 235-249.

Panshin, A.J. and de Zeeuw, C. 1970. Textbook of wood technology vol. 1 Structure, identification, uses and properties of the commercial woods of the United States and Canada. 3rd ed. McGraw-Hill, New York.

Pitelka, L.F. 1994. Ecosystem response to elevated CO_2 . *Trends in Ecology and Evolution* **9**(6): 204-207.

Rannie, W.F. 2006. Evidence for unusually wet 19th century summers in the eastern Prairies and northwestern Ontario. *Prairie Perspectives* **9**: 85-104.

Régnière, J. 1996. Generalized approach to landscape-wide seasonal forecasting with temperature-driven simulation models. *Environmental Entomology* **25**: 869-881.

Régnière, J. and Bolstad, P. 1994. Statistical simulation of daily air temperature patterns in Eastern North America to forecast seasonal events in insect pest management.

Environmental Entomology **23**: 1368-1380.

Ringius, G.S. and Sims, R.A. 1997. Indicator plant species in Canadian Forests, Canadian Forest Service, Natural Resource Canada, Ottawa, ON.

Robertson, I., Rolfe, J., Switsur, V.R., Carter, A.H.C., Hall, M.A., Barker, A.C. and Waterhouse, J.S. 1997a. Signal strength and climate relationships in $^{13}\text{C}/^{12}\text{C}$ ratios of tree ring cellulose from oak in southwest Finland. *Geophysical Research Letters* **24**(12):

1487-1490.

Robertson, I., Switsur, V.R., Carter, A.H.C., Barker, A.C., Waterhouse, J.S., Briffa, K.R. and Jones, P.D. 1997b. Signal strength and climate relationships in $^{13}\text{C}/^{12}\text{C}$ ratios of tree ring cellulose from oak in east England. *Journal of Geophysical Research* **102**(D16):

19507-19516.

Rodionov, S.N. 2006. Use of prewhitening in climate regime shift detection. *Geophysical Research Letters* **33**: L12707.

Sakai, A. 1970. Mechanism of desiccation damage of conifers wintering in soil-frozen areas. *Ecology* **51**: 657-664.

- Sauchyn, D.J. and Beaudoin, A.B. 1998. Recent environmental change in the southwestern Canadian Plains. *The Canadian Geographer* **42**: 337-353.
- Saurer, M., Siegenthaler, U. and Schweingruber, F. 1995. The climate-carbon isotope relationship in tree rings and the significance of site conditions. *Tellus* **47B**: 320-330.
- Saurer, M., Cherubini, P., Reynolds-Henne, C.E., Treydte, K.S., Anderson, W.T. and Siegwolf, R.T.W. 2008. An investigation of the common signal in tree ring stable isotope chronologies at temperate sites. *Journal of Geophysical Research* **113**: G04035.
- Schleser, G.H. and Jayasekera, R. 1985. $\delta^{13}\text{C}$ variations in leaves of a forest as an indication of reassimilated CO_2 from the soil. *Oecologia* **65**: 536-542.
- Schleser, G.H., Helle, G., Lücke, A. and Vos, H. 1999. Isotope signals as climate proxies: the role of transfer functions in the study of terrestrial archives. *Quaternary Science Reviews* **18**: 927-943.
- Schweingruber, F.H. 1988. *Tree Rings: Basics and Applications of Dendrochronology*. Kluwer Academic Publishers, Dordrecht, Holland.
- Schweingruber, F.H. 1996. *Tree rings and environment dendroecology*. Paul Haupt Publishers, Bern, Switzerland.

Simard, S., Morin, H. and Krause, C. 2008a. Natural and artificial defoliation impact on tree ring stable isotopes. TRACE conference April 27-30, Zakopane, Poland, volume 7: 108-114.

Simard, S., Elhani, S., Morin, H., Krause, C. and Cherubini, P. 2008b. Carbon and oxygen stable isotopes from tree-rings to identify spruce budworm outbreaks in the boreal forest of Québec. *Chemical Geology* **252**: 80-87.

Smith, R.E., Veldhuis, H., Mills, G.F., Eilers, R.G., Fraser, W.R. and Lelyk, G.W. 1998. Terrestrial ecozones, ecoregions, and ecodistricts of Manitoba: An ecological stratification of Manitoba's natural landscapes. Technical Bulletin 1998-9E. Land Resource Unit, Brandon Research Centre, Research Branch, Agriculture and Agri-Food Canada, Winnipeg, MB.

St. George, S. and Nielsen, E. 2001. Paleoclimatic potential of ring width and densitometric records from *Thuja occidentalis*, *Pinus strobus*, and *Pinus resinosa* in southeast Manitoba and northwest Ontario. *In* Climate extremes in southern Manitoba during the past millennium. *Edited by* S. St. George, T.W. Anderson, D. Forbes, C.F.M. Lewis, E. Nielsen, and L.H. Thorleifson. Final Report. Climate Change Action Fund, Environment Canada.

St. George, S. and Nielsen, E. 2002. Hydroclimatic change in southern Manitoba since A.D. 1409 inferred from tree rings. *Quaternary Research* **58**: 103-111.

St. George, S., Meko, D.M., Girardin, M-P., MacDonald, G.M., Nielsen, E., Pederson, G.T., Sauchyn, D.J., Tardif, J.C. and Watson, E. 2009. The tree-ring record of drought on the Canadian Prairies. *Journal of Climate* **22**: 689-710.

Swetnam, T.W., Thompson, M.A. and Sutherlan, E.K. 1985. Using dendrochronology to measure radial growth of defoliated trees. U.S. Department of Agriculture, Agriculture Handbook **639**: 1-39.

Tardif, J. 2004. Fire history in the Duck Mountain Provincial Forest, western Manitoba. Sustainable Forest Management Network. Project Report 2003/2004 Series. University of Alberta, Edmonton, Alta.

Tardif, J. and Bergeron, Y. 1997. Comparative dendroclimatological analysis of two black ash and two white cedar populations from contrasting sites in the Lake Duparquet region, northwestern Québec. *Canadian Journal of Forest Research* **27**: 108-116.

Tardif, J. and Stevenson, D. 2001. Radial growth-climate association of *Thuja occidentalis* L. at the northwestern limit of its distribution, Manitoba, Canada. *Dendrochronologia* **19**(2): 179-187.

Tardif, J., Conciatori, F. and Leavitt, S. 2008. Tree rings, $\delta^{13}\text{C}$ and climate in *Picea glauca* growing near Churchill, subarctic Manitoba, Canada. *Chemical Geology* **252**: 88-101.

Teller, J.T. 1975. The ice age in Manitoba. *Manitoba Nature*, Autumn: 4-26.

Thornton, P.E. and Running, S.W. 1999. An improved algorithm for estimating incident daily solar radiation from measurements of temperature, humidity, and precipitation. *Agricultural and Forest Meteorology* **93**: 211-228.

Turner, J.A. 1972. The drought code component of the Canadian Forest Fire Behavior System. Canadian Forest Service Publication 1316.

Vaganov, E.A., Hughes, M.K. and Shashkin, A.V. 2006. Growth dynamics of conifer tree rings. Images of past and future environments. *Ecological Studies*, Vol. 183. Springer Verlag, Berlin, Heidelberg, New York.

Van Wagner, C.E. 1987. Development and structure of the Canadian Forest Fire Weather Index System. Canadian Forest Service, Forestry Technical Report 35.

Warren, C.R., McGraft, J.F. and Adams, M.A. 2001. Water availability and carbon isotope discrimination in conifers. *Oecologia* **127**: 476-486.

Waterhouse, J.S., Switsur, V.R., Barker, A.C., Carter, A.H.C., Hemming, D.L., Loader, N.J. and Robertson, I. 2004. Northern European trees show a progressively diminishing response to increasing atmospheric carbon dioxide concentrations. *Quaternary Science Reviews* **23**: 803-810.

Weber, M.G. and Bell, J.W. 1990. Report on activities in and around Long Point Ecological Reserve in 1990. Forestry Canada. Petawawa National Forestry Institute, Chalk River, Ontario.

Yamaguchi, D.K. 1991. A simple method for cross-dating increment cores from living trees. *Canadian Journal of Forest Research* **21**: 414-416.

Zhang, J.W. and Cregg, B.M. 1996. Variation in stable carbon isotope discrimination among and within exotic conifer species grown in eastern Nebraska, USA. *Forest Ecology and Management* **83**: 181-187.

List of Figures

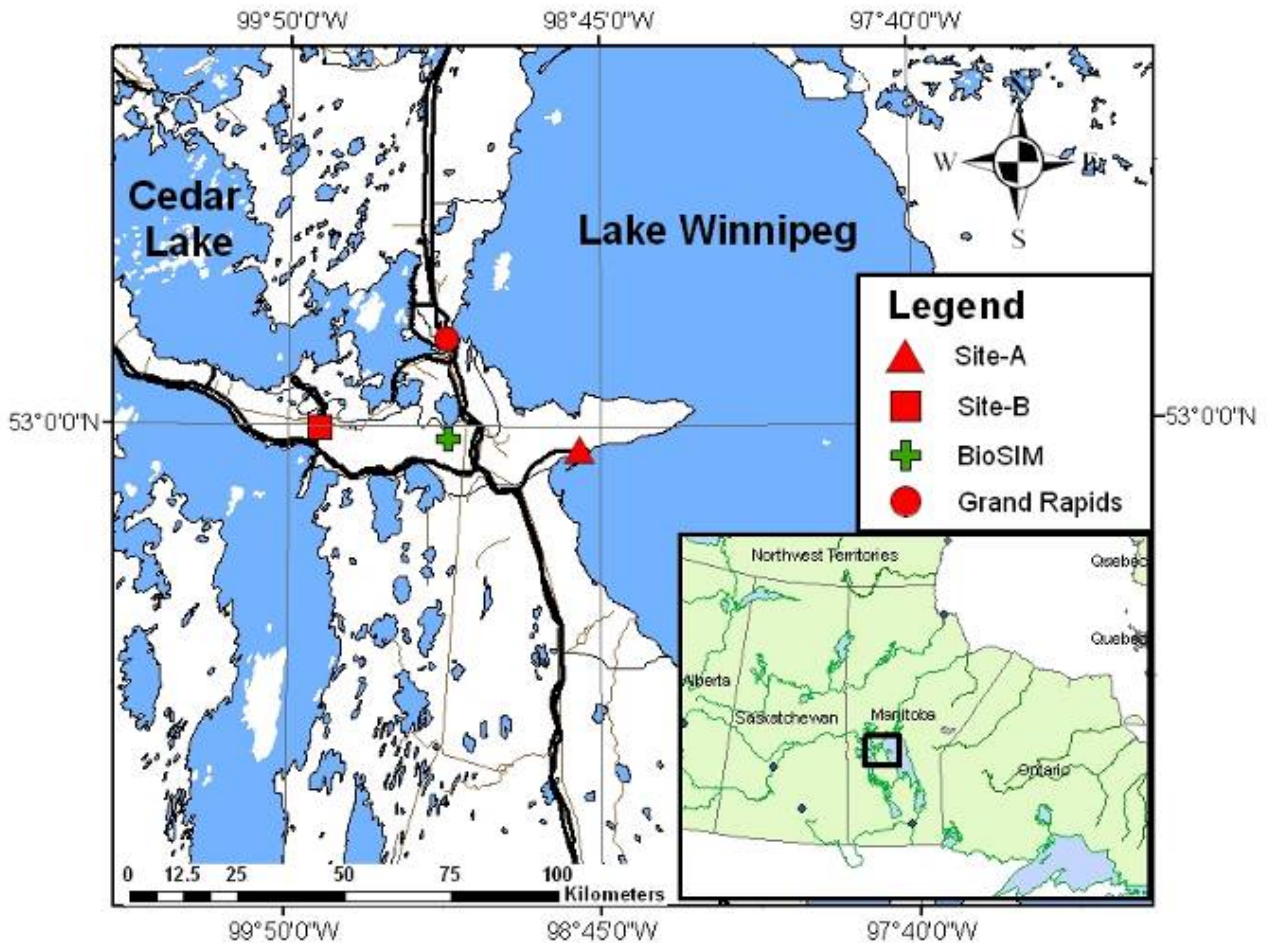


Figure 3.1. Map of the study area showing the location of sampling sites -A (red triangle) and -B (red square). The red circle indicates the location of the town of Grand Rapids, Manitoba. The green cross indicates the location where climate data were interpolated to using the BioSIM computer program. BioSIM adjusted daily weather data among three of the nearest meteorological stations for differences in latitude, longitude, elevation, slope and aspect for the selected location. The inset map shows the general location of the study area within the province of Manitoba, Canada.

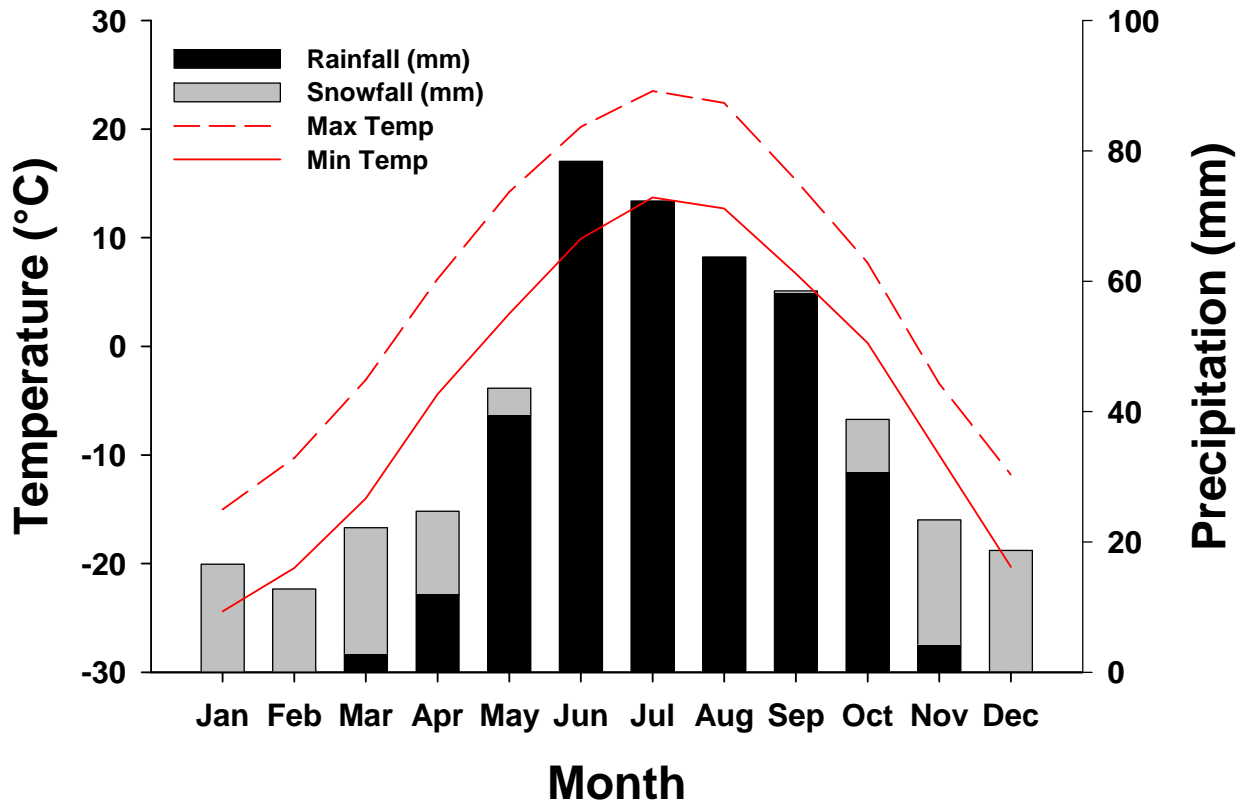


Figure 3.2. Monthly average temperature and total precipitation for Grand Rapids Hydro from January to December and during the reference period of 1971-2000.

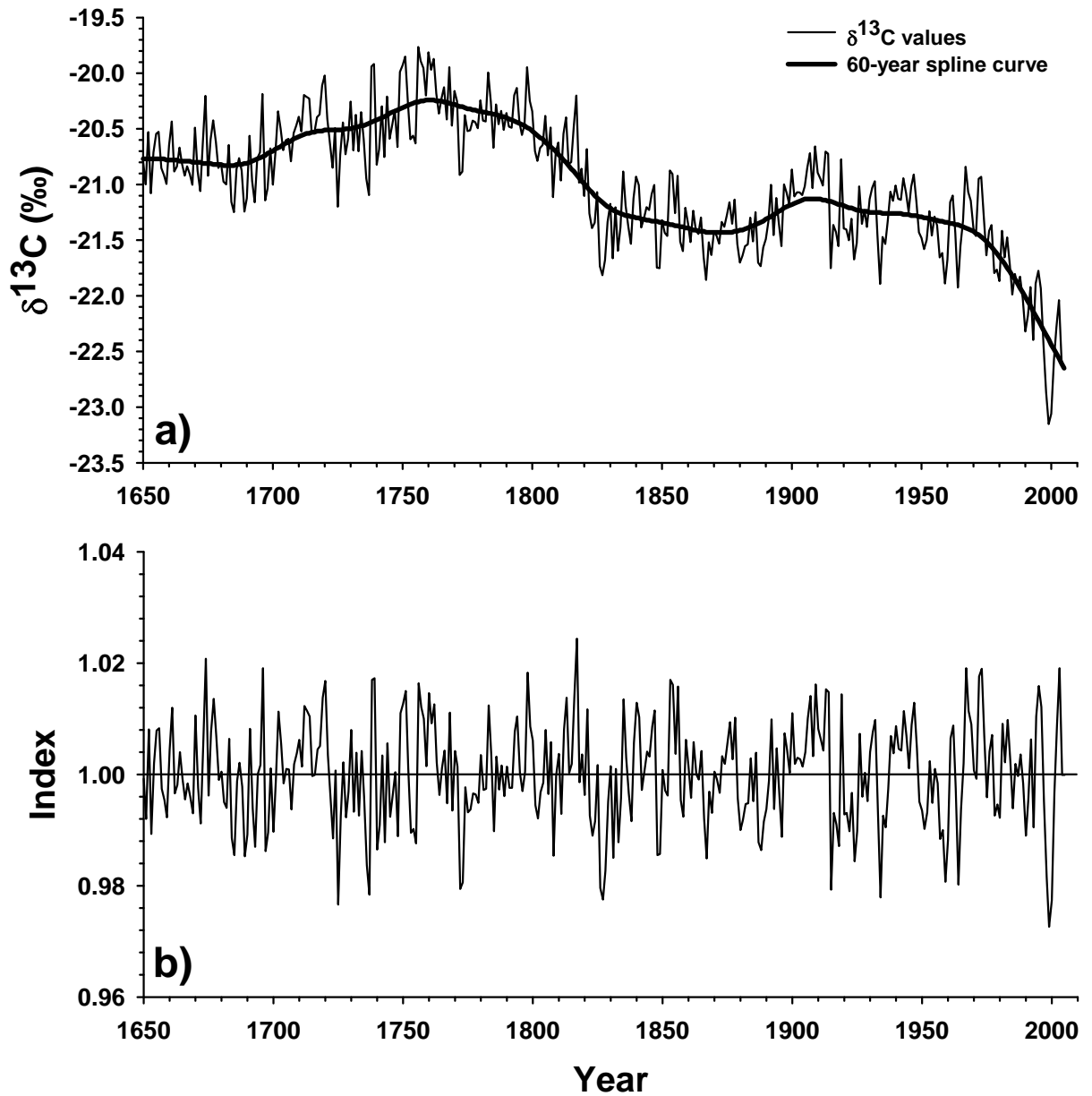


Figure 3.3. Example of the standardization procedure for *Thuja occidentalis* tree number B-6. a) the carbon isotope series ($\delta^{13}\text{C}$ values) is represented by a thin line and the 60-year cubic spline curve is indicated by the thick line. b) the resultant dimensionless indices after each $\delta^{13}\text{C}$ value was divided by its corresponding value estimated by the spline curve.

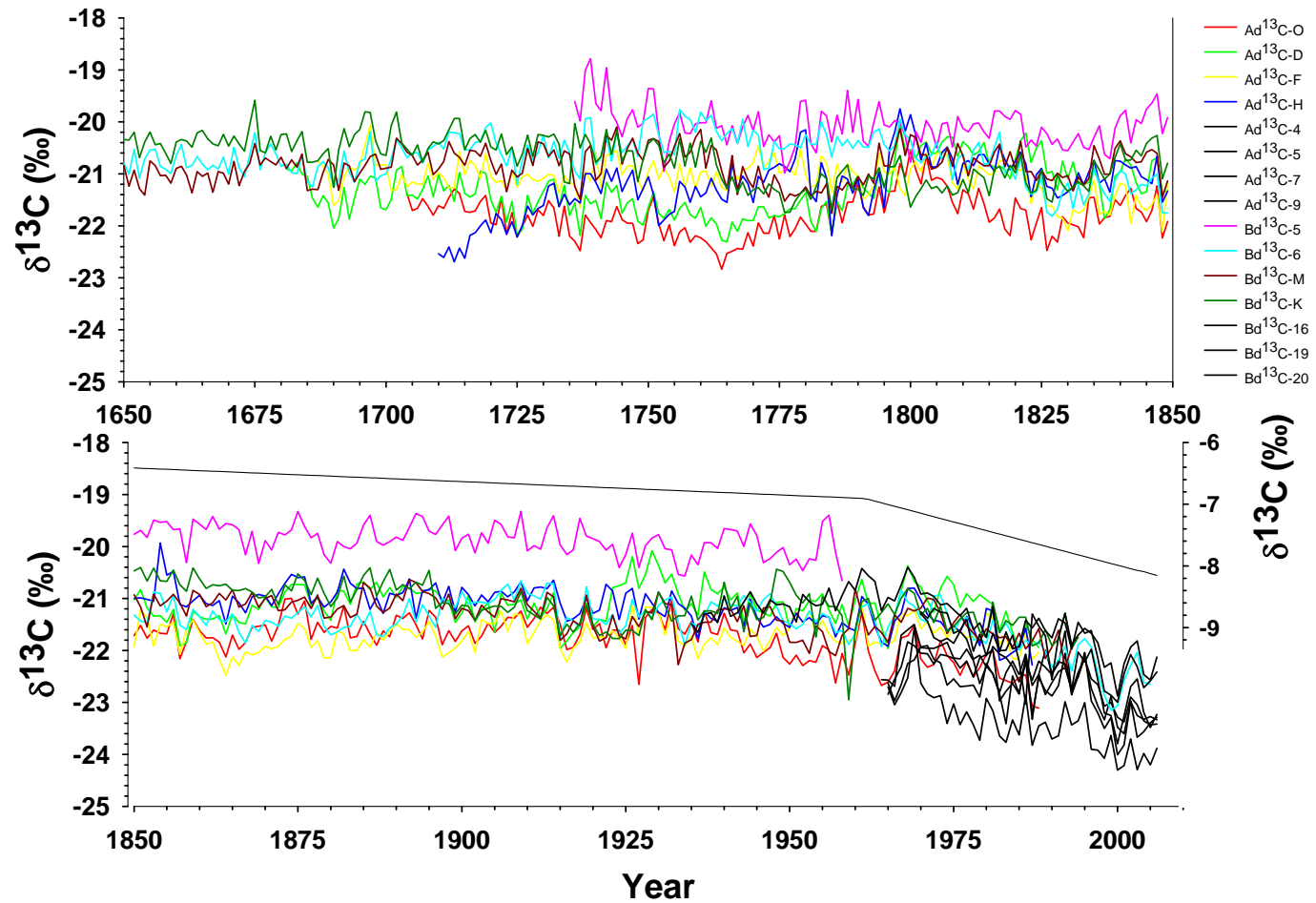


Figure 3.4. Carbon isotope series ($\delta^{13}\text{C}$ values) for the period 1650 to 2006. The live (black lines) and dead (colored lines) *Thuja occidentalis* trees are shown. The decline in atmospheric $\delta^{13}\text{C}$ (scale on right y-axis) since 1850 AD is also superimposed over the lower sub-figure as reported by McCarroll and Loader (2006).

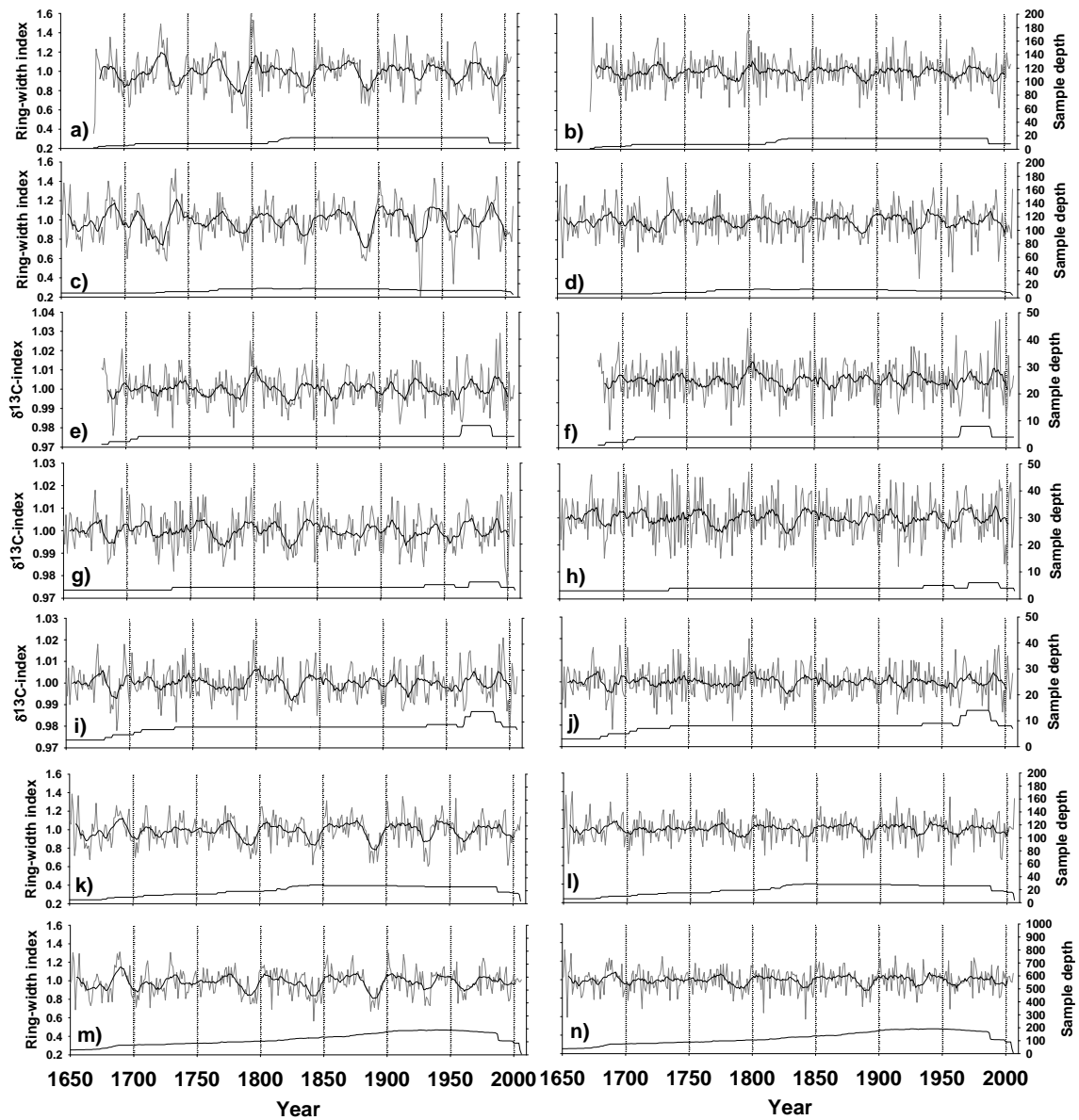


Figure 3.5. The standard (*left panel*) and residual (*right panel*) *Thuja occidentalis* chronologies for both $\delta^{13}\text{C}$ and ring width: ab) A-RWL, cd) B-RWL, ef) A- $\delta^{13}\text{C}$, gh) B- $\delta^{13}\text{C}$, ij) AB- $\delta^{13}\text{C}$, kl) AB-RWL and mn) REG-RWL. All chronologies were also smoothed with an 11-year un-weighted moving average (black line) to highlight the low-frequency trends.

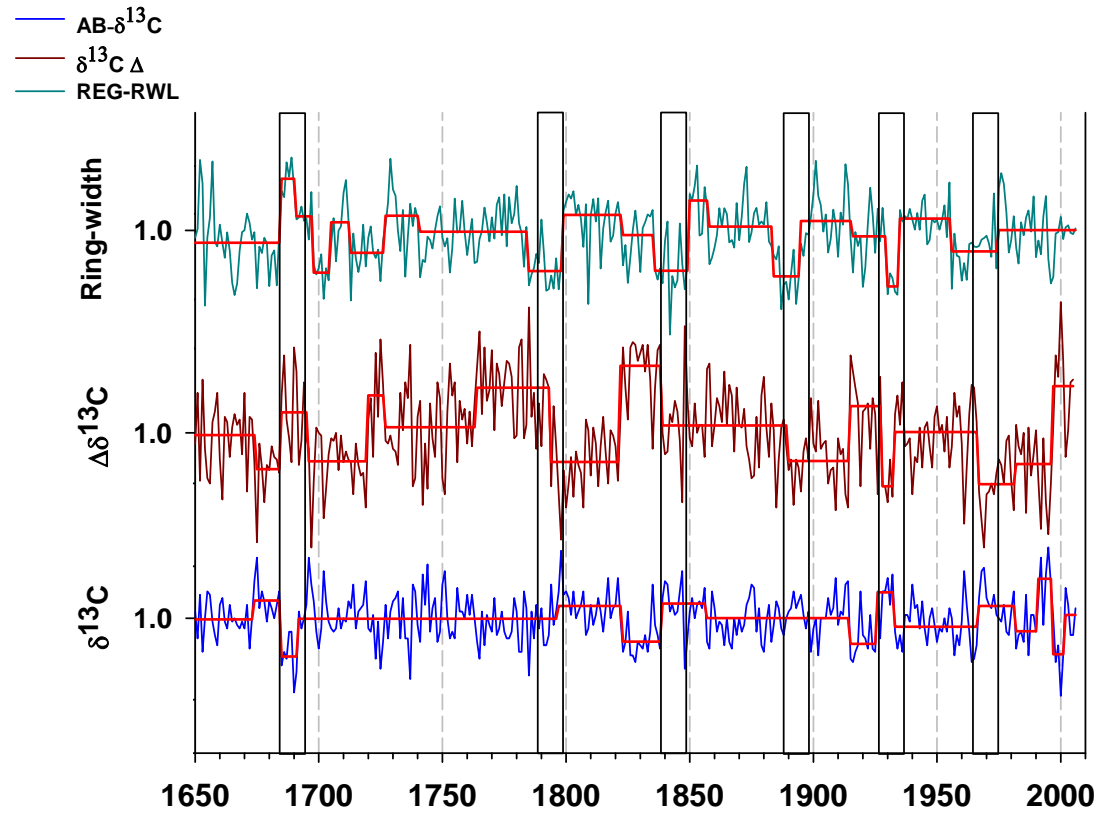


Figure 3.6. *Thuja occidentalis* REG-RWL, $\delta^{13}\text{C}$ discrimination (Δ) and AB- $\delta^{13}\text{C}$ standard chronologies. The regime shift detection (solid red line) for each chronology verified that changes in the mean from one period to another did not emerge from a red noise process (probability $\sigma = 0.10$, cut-off length = 8 years). The black boxes marked synchronicity in regime shifts among two or all the chronologies and were visually determined.

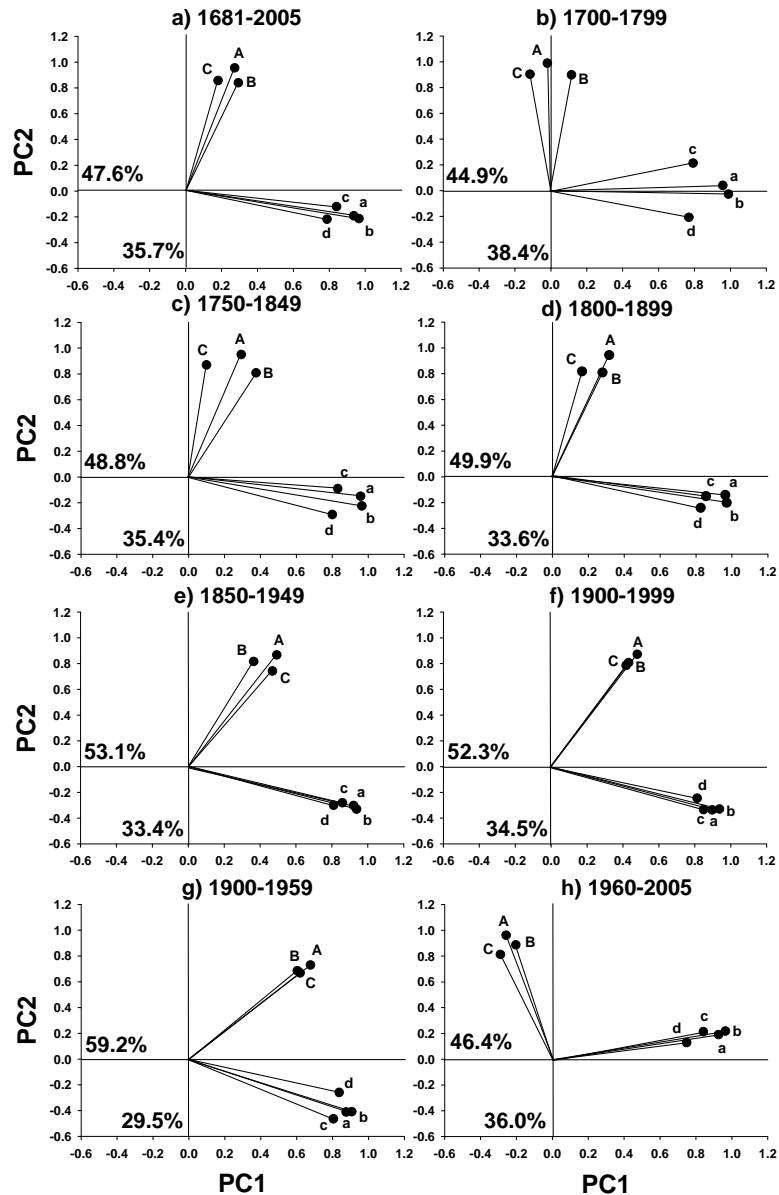


Figure 3.7. Principal components analyses (PCA) performed on correlation matrices conducted for the period 1681-2005 (a), five overlapping 100-year periods beginning in 1700 and ending in 1999 (b-f) and for the periods: 1900-1959 (g) and 1960-2005 (h) illustrating the relationships among the three *T. occidentalis* $\delta^{13}\text{C}$ residual chronologies (A; AB- $\delta^{13}\text{C}$, B; A- $\delta^{13}\text{C}$ and C; B- $\delta^{13}\text{C}$) and the four *T. occidentalis* ring-width residual chronologies (a; REG-RWL, b; AB-RWL, c; A-RWL and d; B-RWL). Percentages of variation explained by PC1 and PC2 are displayed for each PCA.

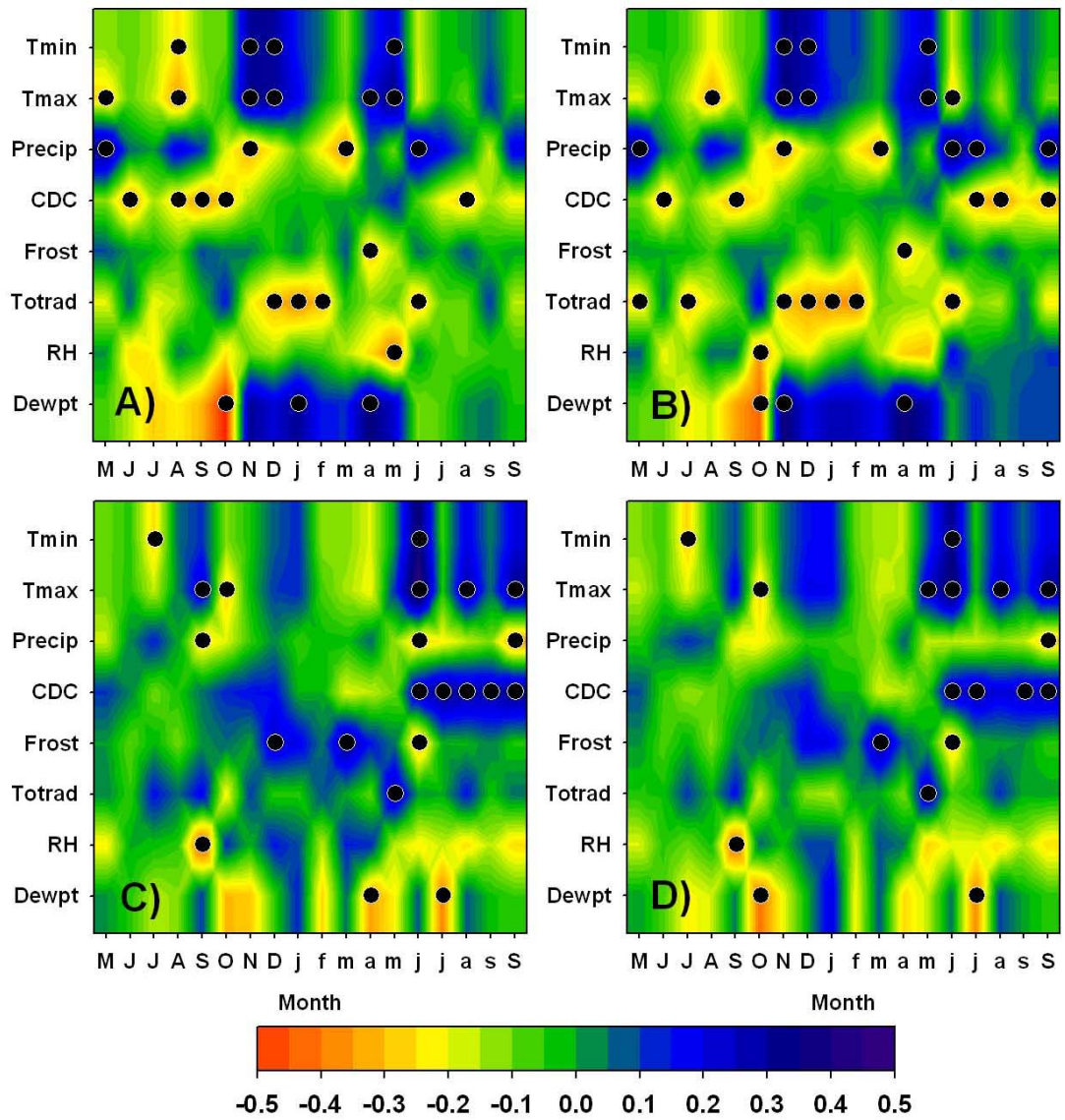


Figure 3.8.

Figure 3.8. Pearson correlation coefficients between A) PC1, B) REG-RWL, C) PC2 and D) AB- $\delta^{13}\text{C}$ and monthly climate variables from May of the year prior to ring formation (large caps) to September of the year of ring formation (small caps). The seasonalized summer variable (S) included the current June, July, August and September months. From top to bottom, the climate variables included: mean monthly minimum temperature (Tmin), mean monthly maximum temperature (Tmax), total monthly precipitation (Precip), mean monthly average Canadian Drought Code values (CDC), total monthly frost days (Frost), total monthly radiation (Totrad), mean monthly relative humidity (RH) and mean monthly dew point temperature (Dewpt). All correlation coefficients that were significant at $p < 0.05$ are indicated by black dots. The period of analysis was 1953-2005 for RH and Dewpt and 1900-2005 for all other climate variables.

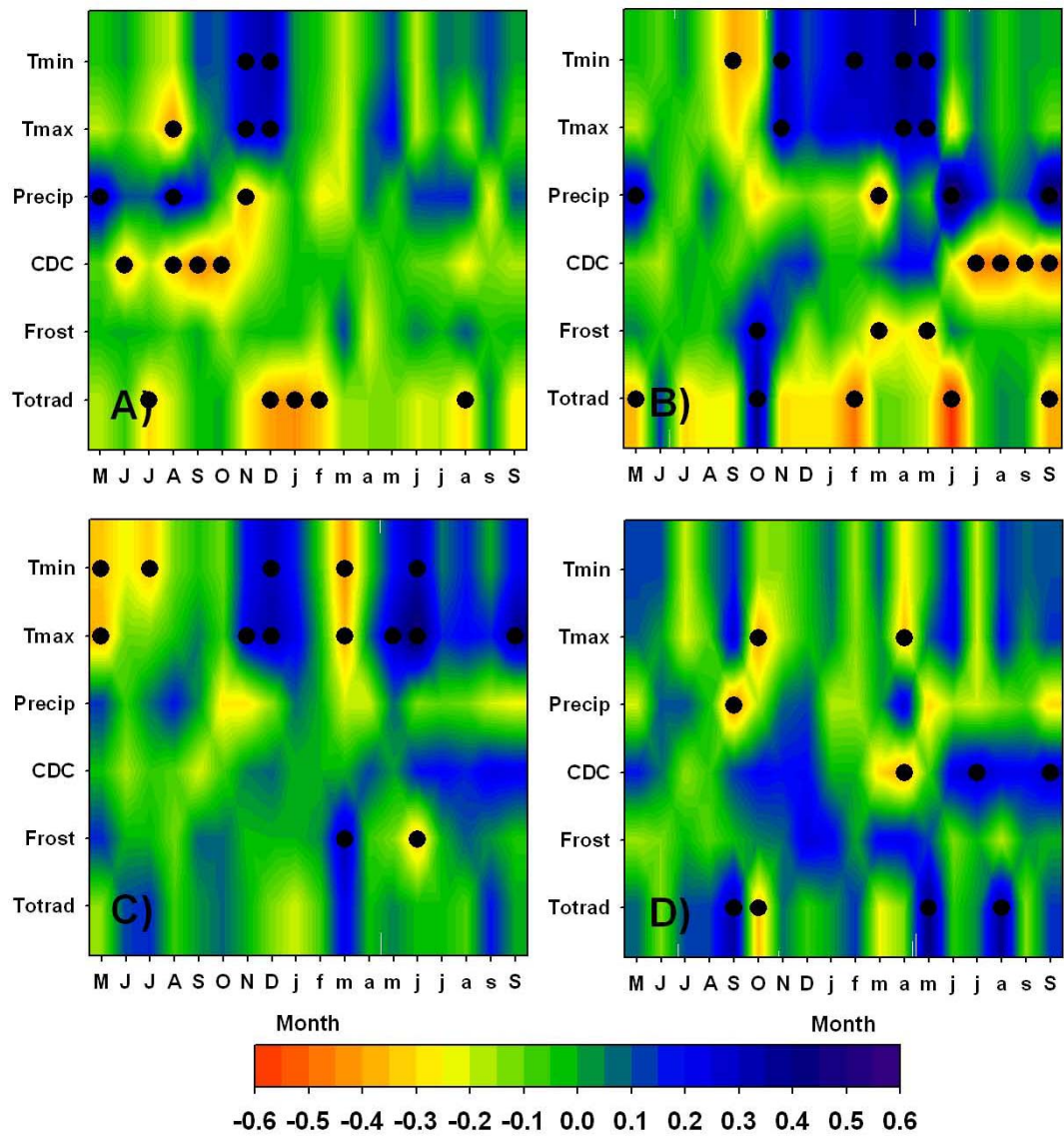
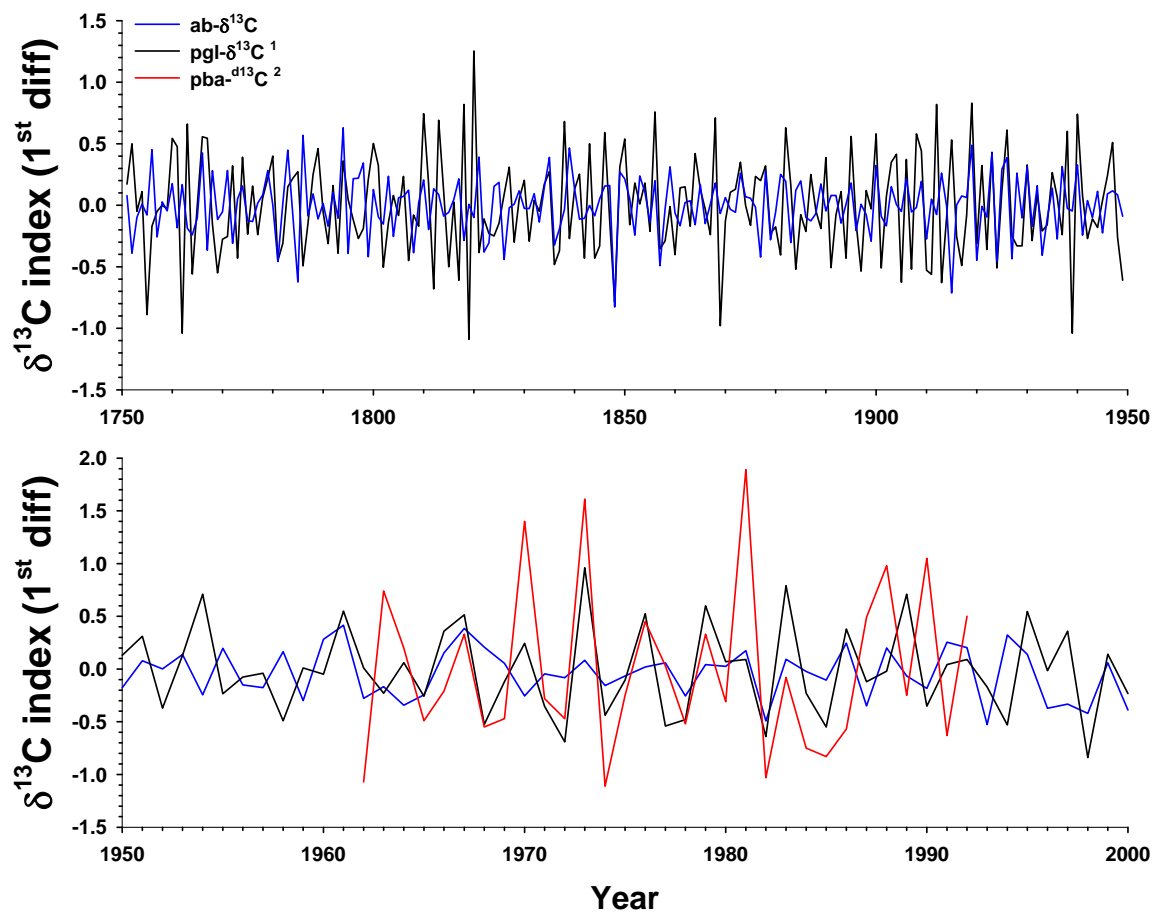


Figure 3.9.

Figure 3.9. Pearson correlation coefficients between REG-RWL (*top panel*) A) during 1900-1959 and B) during 1960-2005 and AB- $\delta^{13}\text{C}$ (*bottom panel*) C) during 1900-1959 and D) 1960-2005 and monthly climate variables from May of the year prior to ring formation (large caps) to September of the year of ring formation (small caps). The seasonalized summer variable (S) included the current June, July, August and September months. From top to bottom, the climate variables included: mean monthly minimum temperature (Tmin), mean monthly maximum temperature (Tmax), total monthly precipitation (Precip), mean monthly average Canadian Drought Code values (CDC), total monthly frost days (Frost) and total monthly radiation (Totrad). All correlation coefficients that were significant at $p < 0.05$ are indicated by black dots.



¹ Tardif et al. 2008

² Ehleringer, J., J. R. Brooks, and L. Flanagan. 1998. BOREAS TE-05 Tree Ring and Carbon Isotope Ratio Data. Data set. Available on-line [<http://www.daac.ornl.gov>] from Oak Ridge National Laboratory Distributed Active Archive Center, Oak Ridge, Tennessee, U.S.A.

Figure 3.10. First-differenced $\delta^{13}\text{C}$ chronologies of *Thuja occidentalis* ($\text{ab-}\delta^{13}\text{C}$), *Picea glauca* ($\text{pgl-}\delta^{13}\text{C}$) and *Pinus banksiana* ($\text{pba-}\delta^{13}\text{C}$).

List of Tables

Table 3.1. Descriptive statistics for dead and living *Thuja occidentalis* ring-width (RWL) measurement series.

Site-Sample	Innermost Complete ring	Outermost Complete ring	Series Length	Mean RWL (mm)	Min. RWL (mm)	Max. RWL (mm)	Mean Sensitivity	Standard Deviation
ARWL-OA	1686	1987	302	0.491	0.158	2.737	0.200	0.277
ARWL-OB	1704	1987	284	0.506	0.203	1.308	0.175	0.196
ARWL-DA	1676	1987	312	0.730	0.099	2.133	0.184	0.413
ARWL-DB	1822	1987	166	0.859	0.197	1.578	0.180	0.240
ARWL-FA	1680	1987	308	0.471	0.114	1.950	0.185	0.334
ARWL-FB	1680	1987	308	0.532	0.179	2.123	0.180	0.325
ARWL-HA	1709	1987	279	0.804	0.129	1.846	0.162	0.358
ARWL-HB	1709	1987	279	0.767	0.083	2.185	0.167	0.452
ARWL-4C	1814	2005	192	0.532	0.199	1.612	0.239	0.247
ARWL-4E	1824	2005	182	0.432	0.113	1.161	0.230	0.199
ARWL-5A	1823	2005	183	0.658	0.154	1.984	0.214	0.385
ARWL-5B	1822	2005	184	0.765	0.188	1.929	0.180	0.413
ARWL-7B	1831	2005	175	0.644	0.261	2.017	0.165	0.292
ARWL-7D	1826	2005	180	0.716	0.206	1.695	0.175	0.318
ARWL-9D	1814	2005	192	0.399	0.095	1.240	0.240	0.164
ARWL-9E	1814	2005	192	0.401	0.157	0.719	0.239	0.126
BRWL-5A ¹	1725	2004	280	0.555	0.000	1.617	0.243	0.247
BRWL-5B ¹	1732	1816	85	0.490	0.058	1.533	0.306	0.348
BRWL-6A ¹	1613	2004	392	0.429	0.026	1.320	0.178	0.225
BRWL-6B ¹	1613	1850	238	0.423	0.122	0.905	0.180	0.154
BRWL-MA	1542	1908	367	0.409	0.031	1.616	0.189	0.283
BRWL-MB	1542	2000	459	0.394	0.034	1.634	0.197	0.246
BRWL-KA	1611	1997	387	0.448	0.046	1.437	0.203	0.173
BRWL-KB	1611	1930	320	0.368	0.060	1.202	0.235	0.186
BRWL-16C	1804	2005	202	0.404	0.072	1.004	0.183	0.137
BRWL-16D	1840	2005	166	0.432	0.000	0.779	0.195	0.133
BRWL-19A	1774	2006	233	0.302	0.047	0.833	0.267	0.147
BRWL-19B	1774	2006	233	0.271	0.020	0.632	0.366	0.134
BRWL-20A	1767	2006	240	0.314	0.031	0.765	0.226	0.143
BRWL-20B	1767	2006	240	0.243	0.022	0.960	0.255	0.125

¹ a cross-section of this tree was sampled in the field since there appeared to be no living canopy; however, laboratory analysis revealed that the tree was living

Table 3.2. Descriptive statistics for dead and living *Thuja occidentalis* $\delta^{13}\text{C}$ series.

Site-Sample	Tree Status	Pith Present	Innermost Year	Outermost Year	Period of $\delta^{13}\text{C}$ analysis	Series Length	Mean $\delta^{13}\text{C}$ (‰)	Min. $\delta^{13}\text{C}$ (‰)	Max. $\delta^{13}\text{C}$ (‰)	Mean Sensitivity	Standard deviation(‰)
A $\delta^{13}\text{C}$ -O	Dead	N	1685	1988	1704-1988	285	-21.8	-23.1	-20.5	0.010	0.042
A $\delta^{13}\text{C}$ -D	Dead	Y	1676	1988	1681-1988	308	-21.2	-22.3	-20.1	0.009	0.045
A $\delta^{13}\text{C}$ -F	Dead	N	1679	1988	1687-1988	302	-21.4	-22.5	-20.1	0.009	0.044
A $\delta^{13}\text{C}$ -H	Dead	Y	1709	1988	1710-1987	278	-21.2	-22.7	-19.7	0.009	0.047
A $\delta^{13}\text{C}$ -4	Living	N	1813	2006	1965-2006	42	-23.4	-24.3	-21.6	0.014	0.056
A $\delta^{13}\text{C}$ -5	Living	N	1821	2006	1964-2006	43	-22.4	-23.4	-21.5	0.010	0.052
A $\delta^{13}\text{C}$ -7	Living	N	1825	2006	1965-2006	42	-22.6	-24.0	-21.8	0.012	0.056
A $\delta^{13}\text{C}$ -9	Living	Y	1814	2006	1965-2006	42	-22.7	-23.7	-21.9	0.013	0.048
B $\delta^{13}\text{C}$ -5	Living ¹	N	1724	2005	1736-1958	223	-20.0	-21.0	-18.8	0.010	0.036
B $\delta^{13}\text{C}$ -6	Living ¹	Y	1613	2005	1650-2005	356	-21.0	-23.1	-19.8	0.008	0.058
B $\delta^{13}\text{C}$ -M	Dead	Y	1542	2000	1650-1993	344	-21.1	-22.3	-20.1	0.009	0.042
B $\delta^{13}\text{C}$ -K	Dead	Y	1611	1997	1650-1994	345	-20.9	-22.9	-19.6	0.009	0.048
B $\delta^{13}\text{C}$ -16	Living	N	1803	2006	1970-2006	37	-21.9	-23.0	-21.2	0.014	0.046
B $\delta^{13}\text{C}$ -19	Living	Y	1774	2006	1970-2006	37	-22.4	-23.8	-21.3	0.011	0.059
B $\delta^{13}\text{C}$ -20	Living	Y	1767	2006	1935-2006	72	-21.4	-23.0	-20.4	0.009	0.059

¹ a cross-section of this tree was sampled in the field since there appeared to be no living canopy; however, laboratory analysis revealed that the tree was living

Table 3.3. Pearson correlation matrix* between standardized *Thuja occidentalis* $\delta^{13}\text{C}$ series from live and dead trees at sites-A and -B

	A$\delta^{13}\text{C}$-4	A$\delta^{13}\text{C}$-5	A$\delta^{13}\text{C}$-7	A$\delta^{13}\text{C}$-9	B$\delta^{13}\text{C}$-16	B$\delta^{13}\text{C}$-19	B$\delta^{13}\text{C}$-20
A$\delta^{13}\text{C}$-O	0.549 24	0.655 25	0.641 24	0.342 24	-0.258 19	-0.055 19	0.355 54
A$\delta^{13}\text{C}$-D	0.241 24	0.628 25	0.684 24	0.210 24	0.035 19	0.209 19	0.359 54
A$\delta^{13}\text{C}$-F	0.570 24	0.528 25	0.662 24	0.422 24	-0.341 19	0.287 19	0.318 54
A$\delta^{13}\text{C}$-H	0.728 23	0.676 24	0.755 23	0.655 23	-0.167 18	0.305 18	0.587 53
B$\delta^{13}\text{C}$-5	. 0	. 0	. 0	. 0	. 0	. 0	0.406 24
B$\delta^{13}\text{C}$-6	0.211 41	0.485 42	0.461 41	0.150 41	0.523 36	0.673 36	0.575 71
B$\delta^{13}\text{C}$-M	0.049 29	0.042 30	0.048 29	0.239 29	0.128 24	0.108 24	0.226 59
B$\delta^{13}\text{C}$-K	0.463 30	0.443 31	0.312 30	0.178 30	-0.044 25	0.250 25	0.067 60

Note: each series was standardized with a 60-year spline function with a 50% frequency response

Bolded correlation coefficients are significant at $p < 0.05$

* Sampling size is indicated under each correlation coefficient

Table 3.4. Pearson correlation matrix* between standardized *Thuja occidentalis* ring-width and $\delta^{13}\text{C}$ series from dead trees at sites-A and -B

	$\text{A}\delta^{13}\text{C-O}$	$\text{A}\delta^{13}\text{C-D}$	$\text{A}\delta^{13}\text{C-F}$	$\text{A}\delta^{13}\text{C-H}$	$\text{B}\delta^{13}\text{C-5}$	$\text{B}\delta^{13}\text{C-6}$	$\text{B}\delta^{13}\text{C-M}$	$\text{B}\delta^{13}\text{C-K}$
ARWL-OA	0.272 284	0.198 302	0.002 301	0.386 278	-0.059 223	0.077 302	0.192 302	-0.078 302
ARWL-OB	0.259 284	0.226 284	0.116 284	0.137 278	0.017 223	0.100 284	0.091 284	-0.009 284
ARWL-DA	0.218 284	0.236 307	0.120 301	0.307 278	0.032 223	0.059 312	0.101 312	-0.028 312
ARWL-DB	-0.050 166	0.191 166	0.180 166	0.120 166	0.078 137	0.089 166	-0.044 166	0.074 166
ARWL-FA	0.141 284	0.146 307	0.118 301	0.247 278	0.098 223	0.093 308	0.012 308	-0.001 308
ARWL-FB	0.129 284	0.108 307	0.164 301	0.176 278	0.074 223	0.061 308	-0.036 308	-0.007 308
ARWL-HA	0.118 279	0.198 279	0.118 279	0.303 278	-0.049 223	0.081 279	0.101 279	-0.032 279
ARWL-HB	-0.100 279	-0.095 279	0.068 279	0.043 278	0.042 223	0.082 279	-0.024 279	-0.045 279
BRWL-5A	-0.084 264	-0.146 264	-0.039 264	-0.004 263	0.166 223	0.028 280	-0.116 269	0.080 270
BRWL-5B	-0.213 85	-0.048 85	0.113 85	0.147 85	0.017 81	-0.167 85	-0.403 85	-0.192 85
BRWL-6A	0.043 285	-0.023 308	0.104 302	0.070 278	0.174 223	0.262 355	0.015 344	0.093 345
BRWL-6B	-0.083 147	0.005 170	0.080 164	0.175 141	0.089 115	0.003 201	-0.146 201	-0.100 201
BRWL-MA	-0.050 205	-0.053 228	-0.015 222	0.081 199	0.079 173	0.037 259	-0.094 259	-0.101 259
BRWL-MB	-0.012 285	-0.062 308	0.070 302	0.016 278	0.184 223	0.102 351	-0.003 344	0.064 345
BRWL-KA	-0.097 285	-0.027 308	0.058 302	0.075 278	0.043 223	-0.023 348	-0.170 344	-0.035 345
BRWL-KB	0.012 227	-0.113 250	0.123 244	0.127 221	0.013 195	-0.011 281	-0.217 281	-0.127 281

Note: each series was standardized with a 60-year spline function with a 50% frequency response

Bolded correlation coefficients are significant at $p < 0.05$

* Sampling size is indicated under each correlation coefficient

Table 3.5. Pearson correlation matrix* between standardized *Thuja occidentalis* ring-width and $\delta^{13}\text{C}$ series from live trees at sites-A and -B

	A $\delta^{13}\text{C}$ -4	A $\delta^{13}\text{C}$ -5	A $\delta^{13}\text{C}$ -7	A $\delta^{13}\text{C}$ -9	B $\delta^{13}\text{C}$ -16	B $\delta^{13}\text{C}$ -19	B $\delta^{13}\text{C}$ -20
ARWL-4C	0.180 41	-0.118 42	0.050 41	-0.027 41	-0.026 36	0.062 36	-0.099 71
ARWL-4E	0.052 41	-0.183 42	-0.094 41	-0.112 41	-0.180 36	-0.339 36	-0.225 71
ARWL-5A	0.137 41	0.028 42	0.042 41	0.002 41	-0.070 36	-0.141 36	-0.092 71
ARWL-5B	0.149 41	0.069 42	0.041 41	-0.040 41	-0.224 36	-0.199 36	-0.019 71
ARWL-7B	-0.221 41	-0.031 42	0.025 41	-0.135 41	-0.116 36	-0.335 36	-0.253 71
ARWL-7D	0.187 41	0.010 42	0.064 41	0.121 41	0.071 36	-0.066 36	-0.107 71
ARWL-9D	0.017 41	-0.143 42	0.133 41	-0.081 41	-0.085 36	-0.056 36	-0.050 71
ARWL-9E	0.021 41	-0.145 42	0.046 41	-0.151 41	-0.300 36	-0.209 36	-0.209 71
BRWL-16C	-0.074 41	0.017 42	-0.260 41	-0.131 41	0.417 36	0.103 36	0.092 71
BRWL-16D	-0.233 41	-0.016 42	-0.395 41	-0.197 41	-0.029 36	-0.246 36	-0.174 71
BRWL-19A	0.225 42	0.001 43	-0.017 42	0.152 42	0.251 37	0.223 37	0.080 72
BRWL-19B	0.194 42	0.198 43	0.235 42	0.303 42	0.040 37	0.175 37	0.039 72
BRWL-20A	0.273 42	0.068 43	0.202 42	0.142 42	0.144 37	0.097 37	0.244 72
BRWL-20B	0.230 42	0.093 43	-0.005 42	0.221 42	0.013 37	0.153 37	0.179 72

Note: each series was standardized with a 60-year spline function with a 50% frequency response

Bolded correlation coefficients are significant at $p < 0.05$

* Sampling size is indicated under each correlation coefficient

Table 3.6. Descriptive statistics for the $\delta^{13}\text{C}$, ring-width (RWL) and discrimination (Δ) *Thuja occidentalis* chronologies for each individual-site (A and B), both sites (AB) and regional ring-width (REG-RWL)

	A-$\delta^{13}\text{C}$	B-$\delta^{13}\text{C}$	AB-$\delta^{13}\text{C}$	A-RWL	B-RWL	AB-RWL	REG-RWL	AB-Δ
No. series	8	7	15	16	14	30	231	15
Time span	1681-2006	1650-2006	1650-2006	1676-2005	1542-2006	1542-2006	1519-2006	1650-2005
Mean¹	-22.10	-21.23	-21.69	0.61	0.39	0.51	0.60	14.98
Standard deviation¹	0.49	0.50	0.49	0.30	0.19	0.25	0.28	0.42
Median¹	-22.12	-21.06	-21.41	0.59	0.41	0.46	0.51	14.97
1st order autocorrelation²	0.28	0.31	0.30	0.46	0.55	0.49	0.42	0.51
PC-1 (%) variance³	65.7	62.3	50.0	55.3	53.0	40.8	34.0	49.5
EPS statistic³	0.83	0.80	0.86	0.87	0.71	0.85	0.96	0.85
Interseries correlation³	0.54	0.50	0.43	0.46	0.37	0.32	0.31	0.42

¹ calculated from untransformed data (raw data)

² calculated from the standardized chronology

³ calculated from the residual chronology for the common period 1736-1958

Note: The discrimination chronology was standardized using the horizontal line through the mean. All other chronologies were standardized with a 60-year spline function with a 50% frequency response

Table 3.7. Correlation matrix of the seven *Thuja occidentalis* residual chronologies for the common period 1681-2005

	A- $\delta^{13}\text{C}$	B- $\delta^{13}\text{C}$	AB- $\delta^{13}\text{C}$	A-RWL	B-RWL	AB-RWL	REG-RWL
A- $\delta^{13}\text{C}$	1						
B- $\delta^{13}\text{C}$	0.562	1					
AB- $\delta^{13}\text{C}$	0.881	0.853	1				
A-RWL	0.146	0.020	0.108	1			
B-RWL	0.035	-0.004	0.013	0.416	1		
AB-RWL	0.102	-0.005	0.059	0.827	0.829	1	
REG-RWL	0.101	0.015	0.070	0.809	0.719	0.918	1

Bolded correlation coefficients are significant at $p < 0.01$

4.0 General Conclusions

This study indicated that the distinct morphology of *T. occidentalis* scale-like leaves predisposed the former for enhanced water-use efficiency as observed in considerably more enriched $\delta^{13}\text{C}$ values relative to other tree species possessing broad- or needle-leaved morphologies published in the literature. The wood components within *T. occidentalis* wood tissue were compared and assessed for their suitability in dendroclimatology. Extractives, lignin and hemicelluloses each contain a unique isotopic signature which may distort the climate signal with their collective inclusion in tree-ring $\delta^{13}\text{C}$ analysis. Both extractive and lignin removal are recommended, however, hemicellulose removal may not be feasible where very narrow tree-rings are present as mean α -cellulose % yield was shown to be nearly half that of holocellulose. It is therefore, crucial to follow a consistent and replicable chemical extraction methodology, since incorporation of an isotope chronology derived from one wood fraction with that derived from a completely different fraction could introduce noise into the data set. Extraction to holo- or α -cellulose as standard dendroisotopic procedure would encourage the development of stable isotope networks and may allow greater insight into regional climate variability.

This is the first study to examine the inter-annual $\delta^{13}\text{C}$ – climate association of *T. occidentalis* trees. Previous studies have shown that *T. occidentalis* radial growth was sensitive to drought conditions (Archambault and Bergeron 1992b; Tardif and Stevenson 2001; Buckley et al. 2004). As expected, both *T. occidentalis* ring-width and $\delta^{13}\text{C}$ were sensitive to moisture stress in this study. Higher vapor pressure deficit during times of

drought causes a reduction in stomatal aperture which thereby results in more efficient utilization of pre-existing intercellular leaf CO₂ by the photosynthetic enzyme (RuBisCO). Drought conditions resulted in reduced radial growth along with $\delta^{13}\text{C}$ enrichment. This suggested that $\delta^{13}\text{C}$ variability is dominated by stomatal restrictions to photosynthesis. During the current summer, ring-width and $\delta^{13}\text{C}$ were negatively and positively associated with the CDC, respectively. Previous drought events were identified using both ring-width and tree-ring $\delta^{13}\text{C}$ chronologies. Sensitivity to moisture stress throughout the *T. occidentalis* chronologies were observed as periods of low radial growth and enriched tree-ring $\delta^{13}\text{C}$ values during the 1790s, 1840s, 1890s, 1930s and 1965-75. Interestingly, the ring-width chronology showed a greater correspondence than that of $\delta^{13}\text{C}$ to prolonged drought intervals as documented from tree-ring records and historical accounts. We suggest that the greater importance of climate conditions during the year prior to ring-formation could have resulted in the higher sensitivity of radial growth to extended drought periods.

In this study, *T. occidentalis* $\delta^{13}\text{C}$ provided standalone information from ring-width as shown by a near absence of association between these tree-ring parameters. Ring-width was negatively associated with summer drought and positively associated with November and December temperatures during the year prior to ring-formation. In the current growing season, *T. occidentalis* radial growth was associated with conditions during the spring and early summer (May and June maximum temperature as well as June and July precipitation) whereas, carbon assimilation was more indicative of overall summer temperatures (May, June and August maximum temperature). This indicated

that photosynthates continued to be deposited after a majority of radial growth had been completed in *T. occidentalis* trees growing at the northwestern limit of their distribution. The robust *T. occidentalis* ring-width and $\delta^{13}\text{C}$ chronologies may therefore, be used in tandem to infer past climatic variability.

5.0 Bibliography

Archambault, S. and Bergeron, Y. 1992a. Discovery of a living 900 year-old Northern White Cedar, *Thuja occidentalis*, in northwestern Québec. Canadian Field-Naturalist **106**(2): 192-195.

Archambault, S. and Bergeron, Y. 1992b. An 802-year tree-ring chronology from the Quebec boreal forest. Canadian Journal of Forest Research **22**: 674-682.

Barber, V., Juday, G. and Finney, R. 2000. Reduced growth of Alaska white spruce in the twentieth century from temperature-induced drought stress. Nature **405**: 668-672.

Berling, D.J. 1994. Predicting leaf gas exchange and $\delta^{13}\text{C}$ responses to the past 30 000 years of global environmental change. New Phytologist **128**: 425-433.

Benner, R., Marilyn, L., Fogel, E., Sprague, K and Hodson, R.E. 1987. Depletion of ^{13}C in lignin and its implications for stable isotope studies. Nature **329**(22): 708-710.

Bergeron, Y. and Debuc, M. 1989. Succession in the southern part of the Canadian boreal forest. Vegetatio **79**: 51-63.

Bert, D., Leavitt, S.W. and Dupouey, J-L. 1997. Variations of wood $\delta^{13}\text{C}$ and water-use efficiency of *Abies alba* during the last century. Ecology **78**(5): 1588-1596.

Boettger, T., Hiller, A., Gehre, M., Friedrich, M. and Kremenetski, C. 2002. Climate response of stable isotope variations in wood cellulose of pine (*Pinus sylvestris* L.) and their tree-ring width on the Kola Peninsula, North-Western Russia. *In* Study of environmental change using isotope techniques. International conference held in Vienna, 23-27 April 2001. International Atomic Energy Agency, Austria. pp. 252-262.

Borella, S., Leuenberger, M, Saurer, M. and Siegwolf, R. 1998. Reducing the uncertainties in $\delta^{13}\text{C}$ analysis of tree rings: pooling, milling, and cellulose extraction. *Journal of Geophysical Research* **103**(D16): 19519-19526.

Boutton, T.W., Archer, S.R. and Midwood, A.J. 1999. Stable isotopes in ecosystem science: structure, function and dynamics of a subtropical savanna. *Rapid Communications in Mass Spectrometry* **13**(13): 1263-1277.

Bowling, D.R., McDowell, N.G., Bond, B. J., Law, B.E. and Ehleringer, J.R. 2002. ^{13}C content of ecosystem respiration is linked to precipitation and vapor pressure deficit. *Oecologia* **131**: 113-124.

Bradley, R.S. 1999. *Paleoclimatology, reconstructing climates of the quaternary*. 2nd ed. Academic Press, San Diego, California.

Brooks, J.R., Flanagan, L.B., Buchmann, N. and Ehleringer, J.R. 1997. Carbon isotope composition of boreal plants: functional grouping of life forms. *Oecologia* **110**: 301-311.

Brooks, J.R., Flanagan, L.B. and Ehleringer, J.R. 1998. Responses of boreal conifers to climate fluctuations: indications from tree-ring widths and carbon isotope analyses. *Canadian Journal of Forest Research* **28**: 524-533.

Buckley, B.M., Wilson, R.J.S., Kelly, P.E., Larson, D.W. and Cook, E.R. 2004. Inferred summer precipitation for southern Ontario back to AD 610, as reconstructed from ring widths of *Thuja occidentalis*. *Canadian Journal of Forest Research* **34**(12): 2541-2553.

Buhay, W.M., Timsic, S., Blair, D., Reynolds, J., Jarvis, S., Petrash, D., Rempel, M. and Bailey, D. 2008. Riparian influences on carbon isotopic composition of tree rings in the Slave River Delta, Northwest Territories, Canada. *Chemical Geology* **252**: 9-20.

Bukata, A.R. and Kyser, T.K. 2007. Carbon and nitrogen isotope variations in tree-rings as records of perturbations in regional carbon and nitrogen cycles. *Environmental Science and Technology* **41**(4): 1331-1338.

Case, R.A. 2000. Dendrochronological investigations of precipitation and streamflow for the Canadian Prairies. Ph.D. Thesis, Department of Geography, University of California, Los Angeles.

- Collier, D.E. and Boyer, M.G. 1989. The water relations of *Thuja occidentalis* L. from two sites of contrasting moisture availability. *Botanical Gazette* **150**: 445-448.
- Coplen, T.B. 1995. Discontinuance of SMOW and PDB. *Nature* **373**: 285.
- Core, H.A., Cote, W.A. and Day, A.C. 1976. Wood structure and identification. Syracuse University Press, Syracuse, New York.
- Craig, H. 1954. Carbon-13 in plants and the relationship between carbon-13 and carbon-14 variations in nature. *Journal of Geology* **62**: 115-149.
- Cullen, L.E., Adams, M.A., Anderson, M.J. and Grierson, P.F. 2008. Analyses of $\delta^{13}\text{C}$ and $\delta^{18}\text{O}$ in tree rings of *Callitris columellaris* provide evidence of a change in stomatal control of photosynthesis in response to regional changes in climate. *Tree Physiology* **28**: 1525-1533.
- Curtis, J.D. 1946. Preliminary observations on northern white cedar in Maine. *Ecology* **27**: 23-36.
- Dawson, T.E. and Brooks, P.D. 2001. Fundamentals of stable isotope chemistry and measurement. *In* Stable isotope techniques in the study of biological processes and functioning of ecosystems. *Edited by* M. Unkovich, J. Pate, A. McNeill and D.J. Gibbs. Kluwer, Dordrecht. pp. 1-18.

Dawson, T.E., Mambelli, S., Plamboeck, A.H., Templer, P.H. and Tu, K.P. 2002. Stable isotopes in plant ecology. *Annual Review of Ecology and Systematics* **33**: 507-559.

Duquesnay, A., Bréda, N., Stievenard, M. and Dupouey, J.L. 1998. Changes of tree-ring $\delta^{13}\text{C}$ and water-use efficiency of beech (*Fagus sylvatica* L.) in north-eastern France during the past century. *Plant, Cell and Environment* **21**: 565-572.

Eamus, D. and Jarvis, P.G. 1989. The direct effects of increase in the global atmospheric CO_2 concentration on natural and commercial temperate trees and forests. *Advances in Ecological Research* **19**: 1-55.

Ehleringer, J.R. and Rundel, P.W. 1989. Stable isotopes: history, units and instrumentation. *In* *Stable isotopes in ecological research*. Edited by P.W. Rundel, J.R. Rundel and K.A. Nagy. Springer-Verlag, New York. pp. 1-16.

Ehleringer, J.R. and Cerling, T.E. 1995. Atmospheric CO_2 and the ratio of intercellular to ambient CO_2 concentrations in plants. *Tree Physiology* **15**: 105-111.

Evans, J.R., Sharkey, T.D., Berry, J.A. and Farquhar, G.D. 1986. Carbon isotope discrimination measured concurrently with gas exchange to investigate CO_2 diffusion in leaves of higher plants. *Australian Journal of Plant Physiology* **13**: 281-292.

Farquhar, G.D., O'Leary, M.H. and Berry, H.A. 1982. On the relationship between carbon isotope discrimination and intercellular carbon dioxide concentration in leaves. *Australian Journal of Plant Physiology* **9**: 121-137.

Farquhar, G.D., Hubick, K.T., Condon, A.G. and Richards, R.A. 1988. Carbon isotope fractionation and plant water-use efficiency. *Ecological Studies* **68**: 21-40.

Farquhar, G.D., Ehleringer, J.R. and Hubick, K.T. 1989. Carbon isotope discrimination and photosynthesis. *Annual Review of Plant Physiology and Plant Molecular Biology* **40**: 503-537.

Faure, G. and Mensing, T.M. 2005. *Isotopes: principles and applications*. John Wiley and Sons, Hoboken.

Feng, X. and Epstein, S. 1995. Carbon isotopes of trees from arid environments and implications for reconstructing atmospheric CO₂ concentration. *Geochimica et Cosmochimica Acta* **59**(12): 2599-2608.

Francey, R.J., Allison, C.E., Etheridge, D.M., Trudinger, C.M., Enting, I.G., Leuenberger, M., Langengelds, R.L., Michel, E. and Steele, L.P. 1999. A 1000-year high precision record of $\delta^{13}\text{C}$ in atmospheric CO₂. *Tellus* **51B**: 170-193.

Freyer, H.D. 1986. Interpretation of the northern hemispheric record of $^{13}\text{C}/^{12}\text{C}$ trends of atmospheric CO_2 in tree rings. *In Changing carbon cycle, a global analysis. Edited by J.R. Trabalka and D.E. Reichle. Springer-Verlag, New York, New York. pp.125-150.*

Fritts, H.C. 1976. Tree rings and climate. Academic Press, New York, NY.

Fry, B. and Arnold, C. 1982. Rapid $^{13}\text{C}/^{12}\text{C}$ turnover during growth of brown shrimp (*Penaeus aztecus*). *Oecologia* **54**: 200-204.

Gagen, M., McCarroll, D. and Edouard, J-L. 2004. Latewood width, maximum density and stable carbon isotope ratios of pine as palaeoclimate indicators in a dry sub-alpine environment in the southern French Alps. *Arctic, Antarctic and Alpine Research* **36**(2): 166-171.

Gagen, M., McCarroll, D. and Edouard, J-L. 2006. Combining ring width, density, and stable carbon isotope proxies to enhance the climate signal in tree-rings: an example from the southern French Alps. *Climate Change* **78**: 363-379.

Gagen, M., McCarroll, D., Loader, N.J., Robertson, I., Jalkanen, R. and Anchukaitis, K.J. 2007. Exorcising the 'segment length curse': summer temperature reconstruction since AD 1640 using non-detrended stable carbon isotope ratios from pine trees in northern Finland. *The Holocene* **17**(4): 435-446.

Gillon, J.S., Borland, A.M, Harwood, K.G., Roberts, A., Broadmeadow, M.S.J. and Griffiths, H. 1998. Carbon isotope discrimination in terrestrial plants: carboxylations and decarboxylations. *In* Stable isotopes: integration of biological, ecological and geochemical processes. *Edited by* H. Griffiths. Bios Scientific Publishers, Oxford, United Kingdom. pp. 111-128.

Gray, J. and Thompson, P. 1977. Climatic information from $^{18}\text{O}/^{16}\text{O}$ analysis of cellulose, lignin and whole wood from tree rings. *Nature* **270**: 708-709.

Gray, J. and Song, S.J. 1984. Climatic implications of the natural variations of D/H ratios in tree ring cellulose. *Earth and Planetary Science Letters* **70**: 129-138.

Guehl, J.-M., Fort, C. and Ferhi, A. 1995. Differential response of leaf conductance, carbon isotope discrimination and water-use efficiency to nitrogen deficiency in maritime pine and pedunculate oak plants. *New Phytologist* **131**: 149-157.

Habeck, J.R. 1958. White cedar ecotypes in Wisconsin. *Ecology* **39**: 457-463.

Hemming, D.L., Switsur, V.R., Waterhouse, J.S., Heaton, T.H.E. and Carter, A.H.C. 1998. Climate variation and the stable carbon isotope composition of tree ring cellulose: an intercomparison of *Quercus robur*, *Fagus sylvatica* and *Pinus silvestris*. *Tellus* **50B**: 25-33.

Hemming, D., Fritts, H., Leavitt, S.W., Wright, W., Long, A. and Shashkin, A. 2001.

Modelling tree-ring $\delta^{13}\text{C}$. *Dendrochronologia* **19**(1): 23-38.

Hoefs, J. 1987. Stable isotope geochemistry. 3rd Edition. Springer-Verlag, Berlin.

Hubick, K.T. and Farquhar, G.D. 1989. Carbon isotope discrimination and the ratio of carbon gained to water lost in barley cultivars. *Plant, Cell and Environment* **12**: 795-804.

Hubick, K.T., Farquhar, G.D. and Shorter, R. 1986. Correlation between water-use efficiency and carbon isotope discrimination in diverse peanut (*Arachis*) germplasm.

Australian Journal of Plant Physiology **13**: 803-816.

Hughes, M.K. 2002. Dendrochronology in climatology – the state of the art.

Dendrochronologia **20**: 95-116.

Johnston, W.F. 1990. Northern white-cedar (*Thuja occidentalis* L.). *In* *Silvics of North America*. Vol. 1. Conifers. Agriculture Handbook 654. *Edited by* R.M. Burns and B.H. Honkala. U.S. Department of Agriculture Forest Service. Washington, D.C.

Kelly, P.E. and Larson, D.W. 2007. *The Last Stand*. Natural Heritage Books. Toronto, Ontario.

Kelly, P.E., Cook, E.R. and Larson, D.W. 1994. A 1397-year tree-ring chronology of *Thuja occidentalis* from cliff faces of the Niagara Escarpment, southern Ontario, Canada. *Canadian Journal of Forest Research* **24**: 1049-1057.

Kendall, C. and McDonnell, J.J., eds. 1998. Isotope tracers in catchment hydrology. Elsevier Science, Amsterdam.

Kienast, F. and Luxmoore, R.J. 1988. Tree-ring analysis and conifer growth responses to increased atmospheric CO₂ levels. *Oecologia* **76**: 487-495.

Kirdyanov, A.V., Treydte, K.S., Nikolaev, A., Helle, G. and Schleser, G.H. 2008. Climate signals in tree-ring width, density and $\delta^{13}\text{C}$ from larches in Eastern Siberia (Russia). *Chemical Geology* **252**: 31-41.

Kloepfel, B.D., Gower, S.T., Treichel, I.W. and Kharuk, S. 1998. Foliar carbon isotope discrimination in *Larix* species and sympatric evergreen conifers: a global comparison. *Oecologia* **114**: 153-159.

Ko-Heinrichs, D. and Tardif, J. 2006. Ecology of northern-white cedar (*Thuja occidentalis* L.) stands at their limit of distribution in Manitoba, Canada [abstract]. 6th Annual Parks and Protected Areas Research Forum of Manitoba [online]. Available from <http://www.umanitoba.ca/outreach/pparfm/index.php?page=pubs> [accessed 7 January 2007].

Larson, D.W. and Kelly, P.E. 1991. The extent of old-growth *Thuja occidentalis* on cliffs of the Niagara Escarpment. *Canadian Journal of Botany* **69**: 1628-1636.

Larson, D.W. and Melville, L. 1996. Stability of wood anatomy of living and Holocene *Thuja occidentalis* L. derived from exposed and submerged portions of the Niagara Escarpment. *Quaternary Research* **45**: 210-215.

Leavitt, S.W. 1993a. Environmental information from $^{13}\text{C}/^{12}\text{C}$ ratios of wood. *In* Climate change in continental isotopic records. *Geophysical Monograph* **78**. *Edited by* P.K. Swart, K.C. Lohmann, J. McKenzie and S. Savin. American Geophysical Union, Washington. pp. 325-331.

Leavitt, S.W. 1993b. Seasonal $^{13}\text{C}/^{12}\text{C}$ changes in tree rings: species and site coherence, and a possible drought influence. *Canadian Journal of Forest Research* **23**: 210-218.

Leavitt, S.W. and Long, A. 1984. Sampling strategy for stable carbon isotope analysis of tree rings in pine. *Nature* **311**(13): 145-147.

Leavitt, S.W. and Long, A. 1988. Intertree variability of $\delta^{13}\text{C}$ in tree rings. *In* Stable isotopes in ecological research. *Edited by* P.W. Rundel, J.R. Ehleringer and K.A. Nagy. Springer-Verlag, New York. pp. 95-104.

Leavitt, S.W and Long, A. 1989. Drought indicated in carbon-13/carbon-12 ratios of southwestern tree rings. *Water Resources Bulletin* **25**(2): 341-347.

Leavitt, S.W., Chase, T.N., Rajagopalan, B., Lee, E., Lawrence, P.J. and Woodhouse, C.A. 2007. Southwestern U.S. drought maps from Pinyon tree-ring carbon isotopes. *Eos* **88**(4): 39-40.

Leuenberger, M., Borella, S., Stocker, T., Saurer, M., Siegwolf, R., Schweingruber, F. and Matyssek, R. 1998. Stable isotopes in tree rings as climate and stress indicators. Final Report NRP **31**, VDF, ETH Zurich.

Lipp, J., Trimborn, P., Fritz, P., Moser, H., Becker, B. and Frenzel, B. 1991. Stable isotopes in tree ring cellulose and climate change. *Tellus* **43B**: 322-330.

Loader, N.J., Robertson, I., Lücke, A. and Helle, G. 2002. Preparation of holocellulose from standard increment cores for stable carbon isotope analysis. *Swansea Geographer* **37**: 1-9.

Loader, N.J., Robertson, I. and McCarroll, D. 2003. Comparison of stable carbon isotope ratios in the whole wood, cellulose and lignin of oak tree-rings. *Palaeogeography, Palaeoclimatology, Palaeoecology* **196**: 395-407.

- Lorius, C., Jouzel, J., Ritz, C., Merlivat, L., Barkov, N.I., Korotkevich, Y.S. and Kotlyakov, V.M. 1985. A 150,000 year climate record from Antarctic ice. *Nature* **316**: 591-596.
- Long, A. 1982. Stable isotopes in tree rings. *In* *Climate from tree rings. Edited by* M.K. Hughes, P.M. Kelly, J.R. Pilcher and V.C. Lamarche Jr. Cambridge University Press, Cambridge. pp. 13-18.
- Macfarlane, C., Warren, C.R., Donald, A.W. and Adams, M.A. 1999. A rapid and simple method for processing wood to crude cellulose for analysis of stable carbon isotopes in tree rings. *Tree Physiology* **19**: 831-835.
- Marshall, J.D. and Monserud, R.A. 1996. Homeostatic gas-exchange parameters inferred from $^{13}\text{C}/^{12}\text{C}$ in tree rings of conifers. *Oecologia* **105**: 13-21.
- Maslin, M.A. and Swann, G.E.A. 2006. Isotopes in marine sediments. *In* *Developments in paleoenvironmental research vol. 10: isotopes in palaeoenvironmental research. Edited by* M.J. Leng. Springer, The Netherlands. pp. 227-273.
- Matthes-Sears, U. and Larson, D.W. 1991. Growth and physiology of *Thuja occidentalis* L. from cliffs and swamps: Is variation habitat or site specific? *Botanical Gazette* **152**: 500-508.

Mazany, T., Lerman, J.C. and Long, A. 1980. Carbon-13 in tree-ring cellulose as an indicator of past climates. *Nature* **287**: 432-435.

McCarroll, D. and Loader, N.J. 2006. Isotopes in tree rings. *In* Developments in paleoenvironmental research vol. 10: isotopes in palaeoenvironmental research. *Edited by* M.J. Leng. Springer, The Netherlands. pp. 67-106.

McCarroll, D. and Pawellek, F. 1998. Stable carbon isotope ratios of latewood cellulose in *Pinus sylvestris* from northern Finland: variability and signal strength. *The Holocene* **8**: 675-684.

McCarroll, D. and Pawellek, F. 2001. Stable carbon isotope ratios of *Pinus sylvestris* from northern Finland and the potential for extracting a climate signal from long Fennoscandian chronologies. *The Holocene* **11**(5): 517-526.

McCarroll, D., Jalkanen, R., Hicks, S., Tuovinen, M., Gagen, M., Pawellek, F., Eckstein, D., Schmitt, U., Autio, J. and Heikkinen, O. 2003. Multiproxy dendroclimatology: a pilot study in northern Finland. *The Holocene*: **13**(6): 829-838.

Melander, L. and Saunders, W.H. 1979. Reaction rates of isotopic molecules. John Wiley and Sons, New York.

Mitchell, A.K. and Hinckley, T.M. 1993. Effects of foliar nitrogen concentration on photosynthesis and water-use efficiency in Douglas-fir. *Tree Physiology* **12**: 403-411.

Mooney, H.A., Drake, B.G., Luxmoore, R.J., Oechel, W.C. and Pitelka, L.F. 1991. Predicting Ecosystem Responses to Elevated CO₂ Concentrations. *BioScience* **41**(2): 96-104.

Musselman, R.C., Lester, D.T. and Adams, M.S. 1975. Localized ecotypes of *Thuja occidentalis* L. in Wisconsin. *Ecology* **56**: 647-655.

Panek, J.A. and Waring, R.H. 1997. Stable carbon isotopes as indicators of limitations to forest growth imposed by climate stress. *Ecological Applications* **7**(3): 854-863.

Park, R. and Epstein, S. 1960. Carbon isotope fractionation during photosynthesis. *Geochimica et Cosmochimica Acta* **21**: 110-126.

Peterson, B.J. and Fry, B. 1987. Stable isotopes in ecosystem studies. *Annual Review of Ecology and Systematics* **18**: 293-320.

Peterson, B.J., Howarth, R.W. and Garritt, R.H. 1986. Sulfur and carbon isotopes as tracers of salt-marsh organic matter flow. *Ecology* **67**(4): 865-874.

Petrucci, R.H., Harwood, W.S. and Herring, G. 2002. General chemistry: principles and modern applications 8th ed. Prentice Hall. Upper Saddle River, New Jersey.

Pitelka, L.F. 1994. Ecosystem response to elevated CO₂. Trends in Ecology and Evolution 9(6): 204-207.

Polley, H.W., Johnson, H.B., Marino, B.D. and Mayeux, H.S. 1993. Increase in C3 plant water-use efficiency and biomass over Glacial to present CO₂ concentrations. Nature **361**: 61-64.

Raffalli-Delercq, G., Masson-Delmotte, V., Dupouey, J.L., Stievenard, M., Breda, N. and Moisselin, J.M. 2004. Reconstruction of summer droughts using tree-ring cellulose isotopes: a calibration study with living oaks from Brittany (western France). Tellus **56B**: 160-174.

Raven, J.A. and Farquhar, G. 1990. The influence of N metabolism and organic acid synthesis on the natural abundance of isotopes of carbon in plants. New Phytologist **116**: 505-529.

Robertson, I., Rolfe, J., Switsur, V.R., Carter, A.H.C., Hall, M.A., Barker, A.C., and Waterhouse, J.S. 1997a. Signal strength and climate relationships in ¹³C/¹²C ratios of tree ring cellulose from oak in southwest Finland. Geophysical Research Letters **24**(12): 1487-1490.

Robertson, I., Switsur, V.R., Carter, A.H.C., Barker, A.C., Waterhouse, J.S., Briffa, K.R. and Jones, P.D. 1997*b*. Signal strength and climate relationships in $^{13}\text{C}/^{12}\text{C}$ ratios of tree-ring cellulose from oak in east England. *Journal of Geophysical Research* **102**(D16): 19507-19516.

Saurer, M., Siegenthaler, U. and Schweingruber, F. 1995. The climate-carbon isotope relationship in tree rings and the significance of site conditions. *Tellus* **47B**: 320-330.

Saurer, M., Siegwolf, R.T.W. and Schweingruber, F.H. 2004. Carbon isotope discrimination indicates improving water-use efficiency of trees in northern Eurasia over the last 100 years. *Global Change Biology* **10**: 2109-2120.

Scheidegger, Y.M., Saurer, M., Bahn and Siegwolf, R. 2000. Linking stable oxygen and carbon isotopes with stomatal conductance and photosynthetic capacity: a conceptual model. *Oecologia* **125**: 350-357.

Schweingruber, F.H. 1996. *Tree rings and environment dendroecology*. Paul Haupt Publishers, Bern, Switzerland.

Scoggan, H.J. 1957. *Flora of Manitoba*. National Museum of Canada. Department of Northern Affairs and National Resources, Ottawa.

Sharp, Z. 2007. Principles of stable isotope geochemistry. Prentice Hall, New Jersey.

Sheppard, P.R. and Cook, E.R. 1988. Scientific value of trees in old-growth natural areas. *Natural Areas Journal* **8**: 7-11.

Simard, S., Morin, H. and Krause, C. 2008a. Natural and artificial defoliation impact on tree ring stable isotopes. TRACE conference April 27-30, Zakopane, Poland, **7**: 108-114.

Simard, S., Elhani, S., Morin, H., Krause, C. and Cherubini, P. 2008b. Carbon and oxygen stable isotopes from tree-rings to identify spruce budworm outbreaks in the boreal forest of Québec. *Chemical Geology* **252**: 80-87.

Sims, R.A., Kershaw, H.M. and Wickware, G.M. 1990. The autecology of major tree species in the north central region of Ontario. Ontario Ministry of Natural Resources Publication **5310**.

St. George, S. and Nielsen, E. 2001. Paleoclimatic potential of ring width and densitometric records from *Thuja occidentalis*, *Pinus strobus*, and *Pinus resinosa* in southeast Manitoba and northwest Ontario. *In* Climate extremes in southern Manitoba during the past millennium. *Edited by* S. St. George, T.W. Anderson, D. Forbes, C.F.M. Lewis, E. Nielsen, and L.H. Thorleifson. Final Report. Climate Change Action Fund, Environment Canada. pp. 24-32.

Sternberg, L.S.L. 1989. Oxygen and hydrogen isotope measurements in plant cellulose analysis. *In* Modern methods of plant analysis 10. *Edited by* H.F. Linskens and J.F. Jackson. Springer-Verlag, Berlin. pp. 89-99.

Stuiver, M. and Reimer, P. 1993. Extended ^{14}C data base and revised CALIB3.0 ^{14}C age calibration program. *Radiocarbon* 35: 215-230.

Tardif, J. and Stevenson, D. 2001. Radial growth-climate association of *Thuja occidentalis* L. at the northwestern limit of its distribution, Manitoba, Canada. *Dendrochronologia* 19(2): 179-187.

Tardif, J., Conciatori, F. and Leavitt, S. 2008. Tree rings, $\delta^{13}\text{C}$ and climate in *Picea glauca* growing near Churchill, subarctic Manitoba, Canada. *Chemical Geology* 252: 88-101.

Tieszen, L.L., Boutton, T.W., Tesdahl, K.G. and Slade, N.A. 1983. Fractionation and turnover of stable carbon isotopes in animal tissues: implications for $\delta^{13}\text{C}$ analysis of diet. *Oecologia* 57: 32-37.

Timell, T.E. 1967. Recent progress in the chemistry of wood hemicelluloses. *Wood Science and Technology* 1: 45-70.

Valentini, G.E., Scarascia Mugnozza, G.E. and Ehleringer, J.R. 1992. Hydrogen and carbon isotope ratios of selected species of a mediterranean macchia ecosystem.

Functional Ecology **6**: 627-631.

Ward, J.K., Dawson, T.E. and Ehleringer, J.R. 2002. Responses of *Acer negundo* genders to interannual differences in water availability determined from carbon isotope ratios of tree-ring cellulose. Tree Physiology **22**: 339-346.

Warren, C.R., McGraft, J.F. and Adams, M.A. 2001. Water availability and carbon isotope discrimination in conifers. Oecologia **127**: 476-486.

Waterhouse, J.S., Barker, A.C., Carter, A.H.C. Agafonov, L.I. and Loader, N.J. 2000. Stable carbon isotopes in Scots pine tree rings preserve a record of flow of the river Ob. Geophysical Research Letters. **27**(21): 3529-3532.

Welker, J.M., Wookey, P.A., Parsons, A.N., Press, M.C., Callaghan, T.V. and Lee, J.A. 1993. Leaf carbon isotope discrimination and vegetative responses of *Dryas octopetala* to temperature and water manipulations in a High Arctic polar semi-desert, Svalbard. Oecologia **95**: 463-469.

Wilson, A.T. and Grinsted, M.J. 1977. $^{12}\text{C}/^{13}\text{C}$ in cellulose and lignin as palaeothermometers. Nature **265**: 133-135.

Woodward, F.I. 1993. Plant responses to past concentrations of CO₂. *Vegetatio* **104/105**:
145-155.

Appendix 1

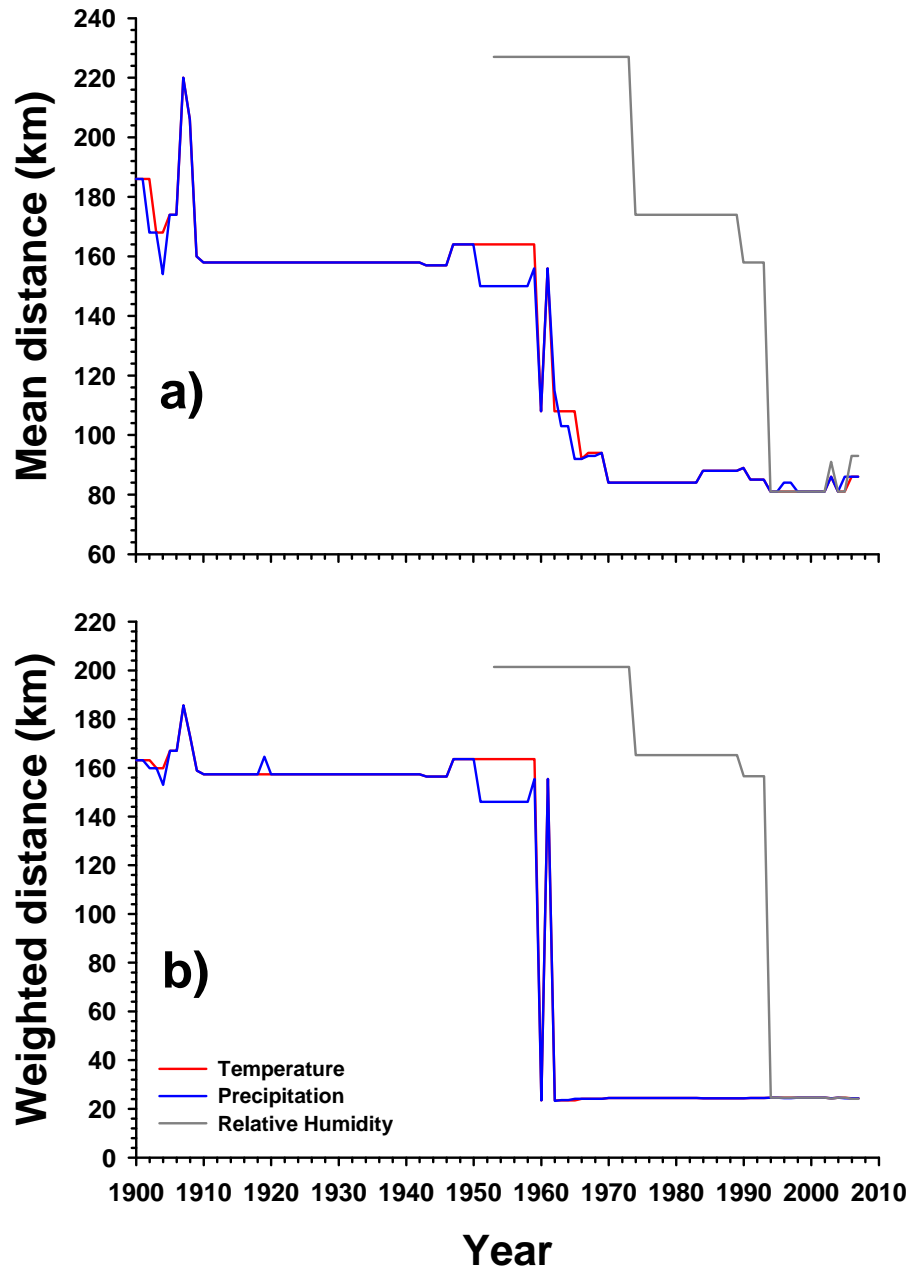


Figure A1.1. The a) mean distance and b) weighted distance of the three nearby meteorological stations at the mid-point of sites-A and -B from which the BioSIM climate data were interpolated. For each year, stations with available data that were closest to the mid-point were given more weight in interpolation of the climate data.

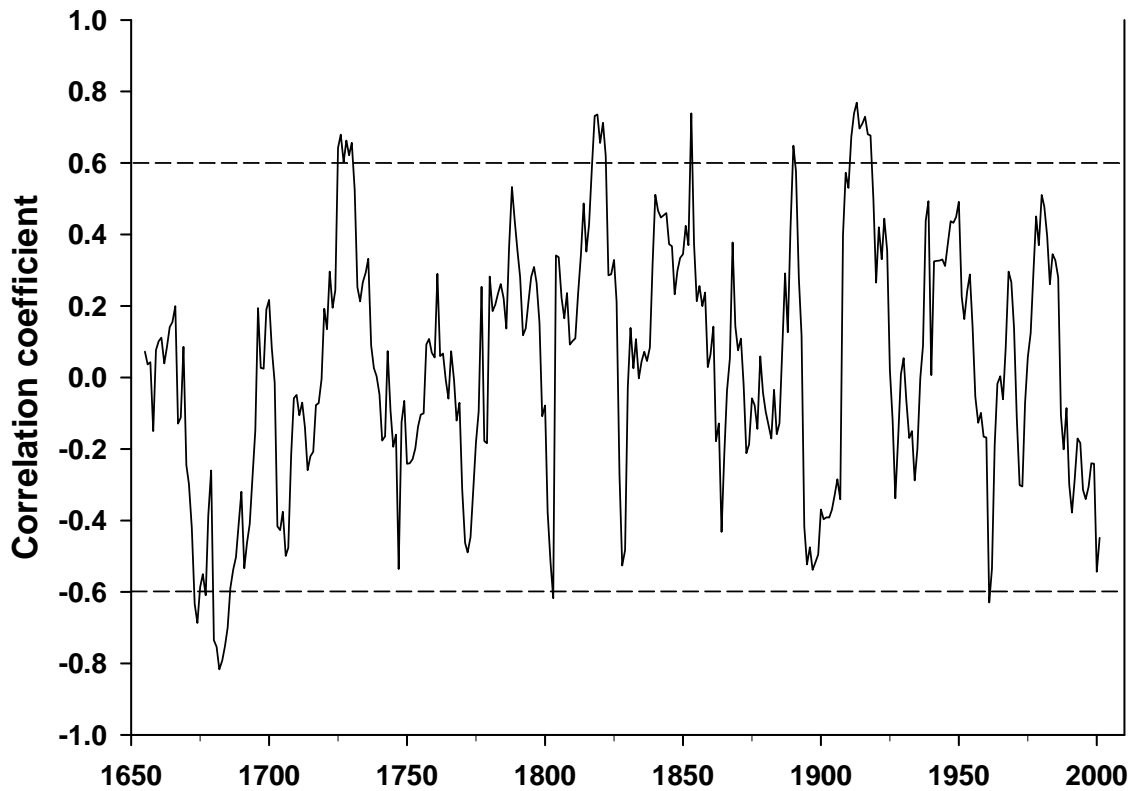


Figure A1.2. Eleven-year moving interval Pearson correlations between standard REG-RWL and AB- $\delta^{13}\text{C}$ chronologies whereby each successive segment advanced one year in time from 1650-2006. Each correlation was plotted as the median year of each period. The horizontal dashed lines indicate significant correlation coefficients at $p < 0.05$.

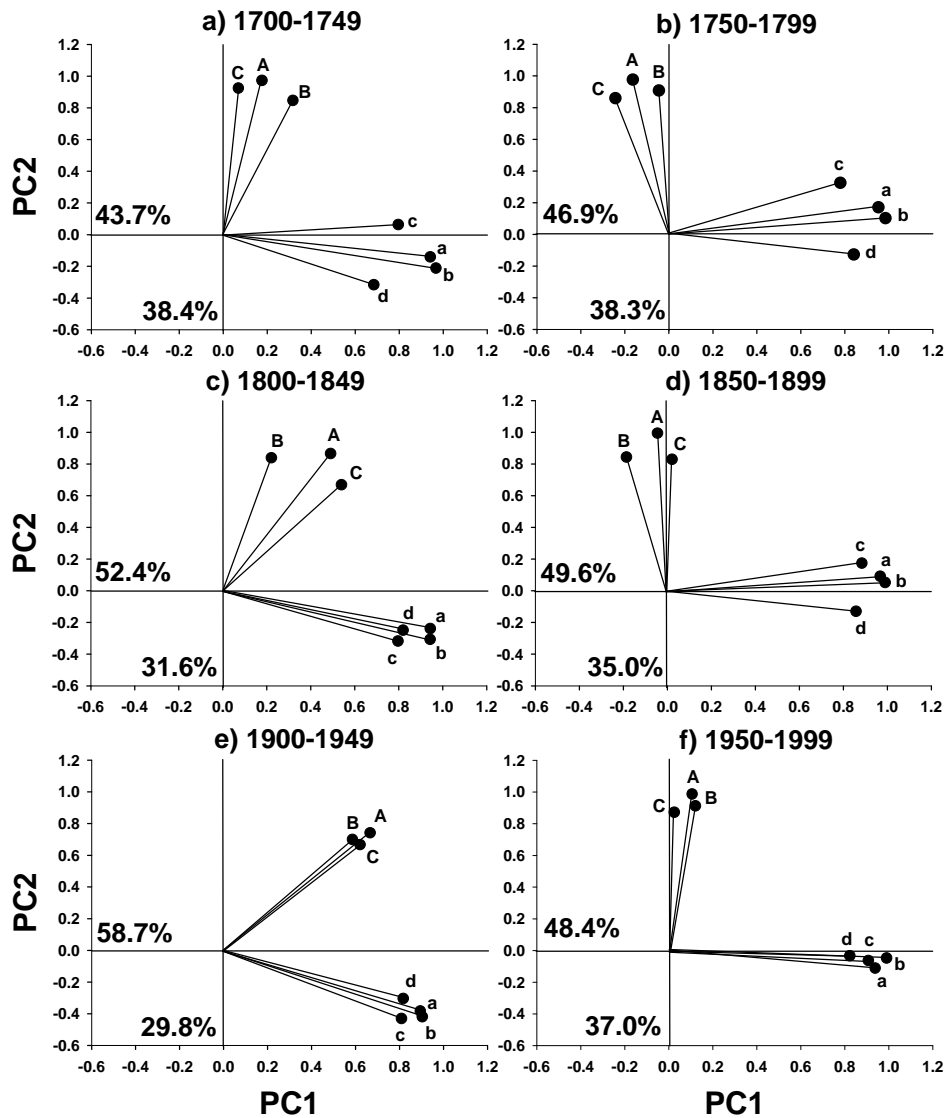


Figure A1.3. Principal components analyses (PCA) performed on correlation matrices conducted over six 50-year periods beginning in 1700 and ending in 1999 (a-f) and illustrating the relationships among the three *T. occidentalis* $\delta^{13}\text{C}$ residual chronologies (A; AB- $\delta^{13}\text{C}$, B; A- $\delta^{13}\text{C}$ and C; B- $\delta^{13}\text{C}$) and the four *T. occidentalis* ring-width residual chronologies (a; REG-RWL, b; AB-RWL, c; A-RWL and d; B-RWL). Percentages of variation explained by PC1 and PC2 are displayed for each PCA.

Table A1.1. Pearson correlation matrix between standardized *Thuja occidentalis* $\delta^{13}\text{C}$ series from dead trees at sites-A and -B*

	$\text{A}\delta^{13}\text{C-O}$	$\text{A}\delta^{13}\text{C-D}$	$\text{A}\delta^{13}\text{C-F}$	$\text{A}\delta^{13}\text{C-H}$	$\text{B}\delta^{13}\text{C-5}$	$\text{B}\delta^{13}\text{C-6}$	$\text{B}\delta^{13}\text{C-M}$	$\text{B}\delta^{13}\text{C-K}$
$\text{A}\delta^{13}\text{C-O}$	1.000 285							
$\text{A}\delta^{13}\text{C-D}$	0.615 285	1.000 308						
$\text{A}\delta^{13}\text{C-F}$	0.510 285	0.494 302	1.000 302					
$\text{A}\delta^{13}\text{C-H}$	0.546 278	0.505 278	0.491 278	1.000 278				
$\text{B}\delta^{13}\text{C-5}$	0.225 223	0.275 223	0.332 223	0.309 223	1.000 223			
$\text{B}\delta^{13}\text{C-6}$	0.415 285	0.309 308	0.268 302	0.361 278	0.506 223	1.000 356		
$\text{B}\delta^{13}\text{C-M}$	0.445 285	0.443 308	0.277 302	0.324 278	0.399 223	0.510 344	1.000 344	
$\text{B}\delta^{13}\text{C-K}$	0.350 285	0.328 308	0.349 302	0.229 278	0.480 223	0.449 345	0.370 344	1.000 345

Note: each series was standardized with a 60-year spline function with a 50% frequency response

Bolded correlation coefficients are significant at $p < 0.01$

* Sampling size is indicated under each correlation coefficient

Table A1.2. Pearson correlation matrix between standardized *Thuja occidentalis* $\delta^{13}\text{C}$ series from live trees at sites-A and -B*

	A $\delta^{13}\text{C}$ -4	A $\delta^{13}\text{C}$ -5	A $\delta^{13}\text{C}$ -7	A $\delta^{13}\text{C}$ -9	B $\delta^{13}\text{C}$ -16	B $\delta^{13}\text{C}$ -19	B $\delta^{13}\text{C}$ -20
A $\delta^{13}\text{C}$ -4	1.000 42						
A $\delta^{13}\text{C}$ -5	0.628 42	1.000 43					
A $\delta^{13}\text{C}$ -7	0.651 42	0.686 42	1.000 42				
A $\delta^{13}\text{C}$ -9	0.734 42	0.630 42	0.728 42	1.000 42			
B $\delta^{13}\text{C}$ -16	0.159 37	0.397 37	0.304 37	0.157 37	1.000 37		
B $\delta^{13}\text{C}$ -19	0.342 37	0.559 37	0.592 37	0.424 37	0.558 37	1.000 37	
B $\delta^{13}\text{C}$ -20	0.475 42	0.612 43	0.602 42	0.455 42	0.558 37	0.791 37	1.000 72

Note: each series was standardized with a 60-year spline function with a 50% frequency response

Bolded correlation coefficients are significant at $p < 0.05$

* Sampling size is indicated under each correlation coefficient

Appendix 2

Table A2.1. Matrix of Pearson correlation coefficients between the A- $\delta^{13}\text{C}$ chronology and mean monthly minimum temperature (Tmin), mean monthly maximum temperature (Tmax), total monthly precipitation (Precip), mean monthly average Canadian Drought Code values (CDC), mean monthly dew point temperature (Dewpt), mean monthly relative humidity (RH), total monthly radiation (Totrad) and total monthly number of frost days (Frost).

Month	Tmin	Tmax	Precip	CDC	Dewpt	RH	Totrad	Frost
M	-0.069	-0.113	-0.044	0.064	0.079	-0.010	-0.036	0.040
J	-0.034	-0.026	0.065	-0.030	-0.007	0.032	0.036	-0.039
J	-0.182	-0.087	0.043	-0.063	-0.132	-0.051	0.141	.
A	-0.055	-0.038	-0.022	0.000	-0.098	-0.029	0.076	-0.088
S	0.086	0.199	-0.128	0.042	0.126	-0.269	0.154	-0.026
O	-0.079	-0.178	-0.103	0.081	-0.231	0.162	-0.135	0.026
N	0.060	0.073	-0.115	0.107	-0.082	0.049	0.049	-0.019
D	0.153	0.188	-0.039	0.140	0.075	0.145	-0.034	0.125
j	0.135	0.138	-0.031	.	0.201	0.137	-0.094	0.182
f	0.025	0.050	-0.038	.	-0.030	-0.045	0.023	0.060
m	-0.070	-0.058	-0.076	-0.135	0.131	0.103	0.081	0.216
a	-0.083	-0.074	0.107	-0.114	-0.181	-0.030	-0.108	0.016
m	0.108	0.219	-0.131	-0.011	-0.114	-0.182	0.216	0.003
j	0.186	0.259	-0.125	0.207	-0.083	-0.139	-0.035	-0.155
j	-0.148	-0.106	-0.144	0.246	-0.363	-0.107	0.075	.
a	0.059	0.121	-0.095	0.173	0.009	-0.166	0.147	0.021
s	-0.082	-0.031	-0.150	0.224	-0.079	-0.067	-0.005	0.116
S	0.012	0.102	-0.242	0.244	-0.165	-0.156	0.062	0.072

Correlations with Dewpt and RH were conducted over the period 1953-2005. All other correlations were conducted over the period of 1900-2005 from May of the year prior to ring formation (large caps) to September of the year of ring formation (small caps). The seasonalized summer variable (S) included the current June, July, August and September months. Bolded correlation coefficients are significant at $p < 0.05$

Table A2.2. Matrix of Pearson correlation coefficients between the B- $\delta^{13}\text{C}$ chronology and mean monthly minimum temperature (Tmin), mean monthly maximum temperature (Tmax), total monthly precipitation (Precip), mean monthly average Canadian Drought Code values (CDC), mean monthly dew point temperature (Dewpt), mean monthly relative humidity (RH), total monthly radiation (Totrad) and total monthly number of frost days (Frost).

Month	Tmin	Tmax	Precip	CDC	Dewpt	RH	Totrad	Frost
M	-0.115	-0.115	-0.025	0.048	-0.071	-0.334	0.039	0.062
J	-0.058	-0.045	0.018	-0.049	-0.100	-0.155	-0.072	-0.053
J	-0.214	-0.196	0.181	-0.118	-0.182	-0.042	-0.001	.
A	0.062	-0.025	0.141	-0.151	-0.134	-0.037	-0.025	-0.072
S	0.048	0.084	-0.145	-0.103	-0.103	-0.428	0.112	0.126
O	-0.111	-0.176	-0.232	-0.006	-0.403	-0.084	-0.072	0.106
N	0.029	0.058	-0.078	0.066	-0.224	-0.093	0.037	0.067
D	0.084	0.108	0.011	0.077	-0.071	0.021	-0.147	0.221
j	0.115	0.142	-0.082	.	0.118	-0.026	-0.103	0.116
f	-0.166	-0.134	-0.045	.	-0.310	-0.208	-0.019	-0.013
m	-0.105	-0.146	-0.106	-0.117	0.012	0.067	-0.087	0.295
a	-0.099	-0.104	0.021	-0.066	-0.143	0.168	-0.057	0.094
m	0.010	0.090	-0.057	-0.060	-0.084	-0.168	0.144	0.038
j	0.308	0.389	-0.098	0.115	0.212	-0.181	-0.025	-0.235
j	0.055	0.044	-0.053	0.152	-0.220	-0.137	-0.116	.
a	0.251	0.270	-0.096	0.145	0.134	-0.222	0.031	0.013
s	0.182	0.186	-0.052	0.136	0.072	-0.204	0.038	-0.048
S	0.277	0.360	-0.144	0.160	0.095	-0.235	-0.034	-0.102

Correlations with Dewpt and RH were conducted over the period 1953-2005. All other correlations were conducted over the period of 1900-2005 from May of the year prior to ring formation (large caps) to September of the year of ring formation (small caps). The seasonalized summer variable (S) included the current June, July, August and September months. Bolded correlation coefficients are significant at $p < 0.05$

Table A2.3. Matrix of Pearson correlation coefficients between the AB- $\delta^{13}\text{C}$ chronology and mean monthly minimum temperature (Tmin), mean monthly maximum temperature (Tmax), total monthly precipitation (Precip), mean monthly average Canadian Drought Code values (CDC), mean monthly dew point temperature (Dewpt), mean monthly relative humidity (RH), total monthly radiation (Totrad) and total monthly number of frost days (Frost).

Month	Tmin	Tmax	Precip	CDC	Dewpt	RH	Totrad	Frost
M	-0.084	-0.127	-0.031	0.084	0.016	-0.145	-0.023	0.024
J	-0.043	-0.044	0.053	-0.040	-0.052	-0.033	-0.013	-0.055
J	-0.211	-0.149	0.110	-0.100	-0.174	-0.073	0.099	.
A	0.001	-0.044	0.068	-0.072	-0.138	-0.016	0.006	-0.088
S	0.088	0.168	-0.161	-0.027	0.045	-0.363	0.144	0.031
O	-0.093	-0.199	-0.178	0.054	-0.337	0.058	-0.138	0.063
N	0.054	0.065	-0.104	0.104	-0.155	-0.010	0.033	0.027
D	0.139	0.166	-0.028	0.130	-0.001	0.094	-0.099	0.188
j	0.144	0.158	-0.038	.	0.184	0.094	-0.115	0.161
f	-0.071	-0.041	-0.060	.	-0.165	-0.129	0.016	0.031
m	-0.113	-0.133	-0.084	-0.143	0.077	0.086	0.003	0.273
a	-0.122	-0.114	0.065	-0.120	-0.204	0.048	-0.080	0.079
m	0.083	0.194	-0.129	-0.033	-0.129	-0.216	0.219	0.012
j	0.280	0.353	-0.123	0.205	0.052	-0.153	-0.050	-0.220
j	-0.023	-0.007	-0.136	0.241	-0.306	-0.150	-0.012	.
a	0.170	0.216	-0.100	0.184	0.090	-0.198	0.110	0.012
s	0.069	0.096	-0.124	0.215	0.011	-0.116	0.008	0.022
S	0.175	0.267	-0.229	0.243	-0.031	-0.198	0.013	-0.033

Correlations with Dewpt and RH were conducted over the period 1953-2005. All other correlations were conducted over the period of 1900-2005 from May of the year prior to ring formation (large caps) to September of the year of ring formation (small caps). The seasonalized summer variable (S) included the current June, July, August and September months. Bolded correlation coefficients are significant at $p < 0.05$

Table A2.4. Matrix of Pearson correlation coefficients between the A-RWL chronology and mean monthly minimum temperature (Tmin), mean monthly maximum temperature (Tmax), total monthly precipitation (Precip), mean monthly average Canadian Drought Code values (CDC), mean monthly dew point temperature (Dewpt), mean monthly relative humidity (RH), total monthly radiation (Totrad) and total monthly number of frost days (Frost).

Month	Tmin	Tmax	Precip	CDC	Dewpt	RH	Totrad	Frost
M	-0.078	-0.176	0.260	-0.045	-0.006	0.090	-0.139	0.062
J	-0.036	-0.051	0.060	-0.236	-0.123	-0.052	0.071	0.044
J	-0.103	-0.125	0.046	-0.102	-0.097	-0.048	-0.164	.
A	-0.245	-0.307	0.142	-0.206	-0.119	0.189	-0.062	-0.015
S	-0.124	-0.110	0.086	-0.240	-0.081	0.204	0.013	0.102
O	-0.053	0.042	-0.045	-0.187	-0.303	-0.132	0.141	0.034
N	0.267	0.304	-0.237	-0.106	0.404	-0.149	-0.216	-0.012
D	0.268	0.290	-0.128	-0.018	0.278	-0.035	-0.223	-0.052
j	0.066	0.118	-0.086	.	0.199	-0.003	-0.280	0.028
f	0.038	0.025	-0.222	.	0.170	0.052	-0.241	-0.027
m	-0.120	-0.087	-0.305	0.114	0.090	-0.108	-0.015	0.046
a	0.144	0.263	-0.024	0.149	0.312	-0.153	-0.067	-0.279
m	0.191	0.282	-0.016	0.175	0.185	-0.215	-0.118	-0.166
j	-0.195	-0.234	0.255	-0.086	-0.127	0.120	-0.231	0.119
j	-0.022	0.045	0.184	-0.173	0.058	-0.058	0.011	.
a	-0.146	-0.200	0.113	-0.265	-0.092	0.048	-0.097	0.126
s	0.072	0.151	-0.114	-0.185	0.173	0.084	0.105	-0.033
S	-0.106	-0.098	0.225	-0.220	-0.002	0.069	-0.107	0.009

Correlations with Dewpt and RH were conducted over the period 1953-2005. All other correlations were conducted over the period of 1900-2005 from May of the year prior to ring formation (large caps) to September of the year of ring formation (small caps). The seasonalized summer variable (S) included the current June, July, August and September months. Bolded correlation coefficients are significant at $p < 0.05$

Table A2.5. Matrix of Pearson correlation coefficients between the B-RWL chronology and mean monthly minimum temperature (Tmin), mean monthly maximum temperature (Tmax), total monthly precipitation (Precip), mean monthly average Canadian Drought Code values (CDC), mean monthly dew point temperature (Dewpt), mean monthly relative humidity (RH), total monthly radiation (Totrad) and total monthly number of frost days (Frost).

Month	Tmin	Tmax	Precip	CDC	Dewpt	RH	Totrad	Frost
M	-0.111	-0.194	0.328	-0.173	-0.091	0.035	-0.111	0.124
J	-0.087	-0.063	0.008	-0.266	-0.072	-0.294	0.090	0.022
J	0.007	-0.014	-0.048	-0.068	-0.209	-0.286	-0.122	.
A	-0.119	-0.177	0.174	-0.140	-0.138	-0.110	-0.139	-0.056
S	-0.071	-0.139	0.193	-0.272	-0.368	-0.082	-0.061	0.060
O	-0.028	-0.002	-0.122	-0.252	-0.320	-0.184	0.125	0.033
N	0.170	0.179	-0.153	-0.167	0.111	0.051	-0.055	0.095
D	0.160	0.154	-0.188	-0.119	0.083	-0.167	-0.167	-0.048
j	0.112	0.130	-0.023	.	0.195	-0.050	-0.216	-0.025
f	0.062	0.014	-0.058	.	0.074	-0.086	-0.172	-0.076
m	-0.054	-0.035	-0.218	-0.059	0.015	-0.157	-0.001	0.042
a	0.086	0.145	0.065	0.007	0.310	-0.180	-0.042	-0.159
m	0.123	0.212	-0.073	0.092	0.196	-0.310	-0.058	-0.051
j	-0.182	-0.181	0.215	-0.069	-0.072	-0.060	-0.119	0.065
j	-0.022	-0.064	0.137	-0.189	-0.082	-0.020	-0.114	.
a	0.094	0.012	0.024	-0.174	0.106	-0.128	-0.063	0.009
s	0.031	0.071	-0.087	-0.065	-0.097	-0.156	0.092	0.006
S	-0.027	-0.061	0.148	-0.145	-0.052	-0.109	-0.095	0.023

Correlations with Dewpt and RH were conducted over the period 1953-2005. All other correlations were conducted over the period of 1900-2005 from May of the year prior to ring formation (large caps) to September of the year of ring formation (small caps). The seasonalized summer variable (S) included the current June, July, August and September months. Bolded correlation coefficients are significant at $p < 0.05$

Table A2.6. Matrix of Pearson correlation coefficients between the AB-RWL chronology and mean monthly minimum temperature (Tmin), mean monthly maximum temperature (Tmax), total monthly precipitation (Precip), mean monthly average Canadian Drought Code values (CDC), mean monthly dew point temperature (Dewpt), mean monthly relative humidity (RH), total monthly radiation (Totrad) and total monthly number of frost days (Frost).

Month	Tmin	Tmax	Precip	CDC	Dewpt	RH	Totrad	Frost
M	-0.085	-0.184	0.324	-0.108	-0.041	0.028	-0.145	0.096
J	-0.073	-0.073	0.063	-0.293	-0.147	-0.208	0.071	0.048
J	-0.074	-0.107	0.010	-0.112	-0.205	-0.188	-0.176	.
A	-0.219	-0.301	0.187	-0.217	-0.168	0.044	-0.131	-0.031
S	-0.112	-0.144	0.146	-0.302	-0.251	0.097	-0.038	0.084
O	-0.055	0.014	-0.097	-0.256	-0.380	-0.179	0.162	0.040
N	0.250	0.283	-0.238	-0.156	0.308	-0.075	-0.160	0.046
D	0.238	0.246	-0.184	-0.076	0.180	-0.142	-0.234	-0.042
j	0.094	0.132	-0.063	.	0.234	-0.031	-0.290	0.009
f	0.048	0.013	-0.177	.	0.147	-0.021	-0.240	-0.069
m	-0.077	-0.046	-0.315	0.046	0.098	-0.144	-0.016	0.033
a	0.149	0.240	0.033	0.090	0.372	-0.216	-0.094	-0.259
m	0.197	0.292	-0.044	0.152	0.252	-0.302	-0.107	-0.137
j	-0.221	-0.251	0.290	-0.103	-0.134	0.035	-0.206	0.117
j	-0.032	-0.023	0.216	-0.232	-0.018	-0.024	-0.054	.
a	-0.039	-0.117	0.066	-0.270	-0.017	-0.035	-0.084	0.085
s	0.056	0.125	-0.116	-0.155	0.050	-0.029	0.119	-0.026
S	-0.084	-0.105	0.233	-0.229	-0.047	-0.010	-0.112	0.012

Correlations with Dewpt and RH were conducted over the period 1953-2005. All other correlations were conducted over the period of 1900-2005 from May of the year prior to ring formation (large caps) to September of the year of ring formation (small caps). The seasonalized summer variable (S) included the current June, July, August and September months. Bolded correlation coefficients are significant at $p < 0.05$

Table A2.7. Matrix of Pearson correlation coefficients between the REG-RWL chronology and mean monthly minimum temperature (Tmin), mean monthly maximum temperature (Tmax), total monthly precipitation (Precip), mean monthly average Canadian Drought Code values (CDC), mean monthly dew point temperature (Dewpt), mean monthly relative humidity (RH), total monthly radiation (Totrad) and total monthly number of frost days (Frost).

Month	Tmin	Tmax	Precip	CDC	Dewpt	RH	Totrad	Frost
M	-0.023	-0.156	0.311	-0.074	-0.060	0.073	-0.197	0.020
J	-0.014	-0.034	0.056	-0.238	-0.072	-0.154	0.039	0.008
J	-0.055	-0.132	-0.023	-0.066	-0.172	-0.090	-0.227	.
A	-0.161	-0.264	0.186	-0.159	-0.132	0.061	-0.147	-0.047
S	-0.075	-0.127	0.108	-0.259	-0.269	0.053	-0.068	0.058
O	-0.039	0.038	-0.161	-0.188	-0.350	-0.282	0.164	0.049
N	0.287	0.304	-0.262	-0.061	0.337	-0.112	-0.234	0.040
D	0.242	0.239	-0.137	0.017	0.165	-0.160	-0.274	-0.083
j	0.085	0.125	-0.057	.	0.233	-0.058	-0.294	0.005
f	0.104	0.059	-0.183	.	0.218	0.001	-0.303	-0.119
m	-0.003	0.000	-0.270	0.036	0.155	-0.115	-0.068	-0.028
a	0.117	0.187	0.076	0.028	0.332	-0.219	-0.089	-0.195
m	0.197	0.270	-0.063	0.097	0.239	-0.242	-0.106	-0.138
j	-0.129	-0.205	0.345	-0.128	0.004	0.156	-0.274	0.075
j	0.072	0.040	0.194	-0.236	0.124	0.020	-0.090	.
a	-0.011	-0.118	0.096	-0.291	0.046	0.051	-0.114	0.079
s	0.074	0.084	-0.077	-0.185	0.090	0.063	0.059	-0.013
S	-0.003	-0.082	0.279	-0.252	0.089	0.104	-0.183	0.013

Correlations with Dewpt and RH were conducted over the period 1953-2005. All other correlations were conducted over the period of 1900-2005 from May of the year prior to ring formation (large caps) to September of the year of ring formation (small caps). The seasonalized summer variable (S) included the current June, July, August and September months. Bolded correlation coefficients are significant at $p < 0.05$

Table A2.8. Matrix of Pearson correlation coefficients between the PC1 scores and mean monthly minimum temperature (Tmin), mean monthly maximum temperature (Tmax), total monthly precipitation (Precip), mean monthly average Canadian Drought Code values (CDC), mean monthly dew point temperature (Dewpt), mean monthly relative humidity (RH), total monthly radiation (Totrad) and total monthly number of frost days (Frost).

Month	Tmin	Tmax	Precip	CDC	Dewpt	RH	Totrad	Frost
M	-0.095	-0.208	0.307	-0.089	-0.048	0.026	-0.155	0.087
J	-0.064	-0.066	0.059	-0.275	-0.123	-0.199	0.068	0.021
J	-0.102	-0.127	0.018	-0.110	-0.222	-0.178	-0.157	.
A	-0.193	-0.278	0.188	-0.200	-0.179	0.041	-0.118	-0.057
S	-0.081	-0.099	0.106	-0.280	-0.248	-0.012	-0.009	0.085
O	-0.065	-0.018	-0.145	-0.217	-0.438	-0.189	0.126	0.053
N	0.261	0.290	-0.252	-0.106	0.273	-0.076	-0.161	0.048
D	0.262	0.274	-0.170	-0.024	0.190	-0.111	-0.249	-0.020
j	0.121	0.162	-0.069	.	0.273	-0.017	-0.300	0.039
f	0.052	0.022	-0.174	.	0.127	-0.043	-0.244	-0.068
m	-0.085	-0.066	-0.305	0.005	0.117	-0.118	-0.022	0.080
a	0.106	0.194	0.055	0.047	0.310	-0.195	-0.095	-0.217
m	0.199	0.311	-0.075	0.126	0.206	-0.333	-0.056	-0.124
j	-0.134	-0.154	0.259	-0.059	-0.082	0.027	-0.221	0.054
j	-0.014	-0.010	0.163	-0.166	-0.057	-0.053	-0.064	.
a	0.007	-0.066	0.055	-0.220	0.028	-0.065	-0.068	0.080
s	0.067	0.125	-0.127	-0.107	0.053	-0.040	0.099	-0.007
S	-0.028	-0.041	0.181	-0.169	-0.020	-0.034	-0.123	0.013

Correlations with Dewpt and RH were conducted over the period 1953-2005. All other correlations were conducted over the period of 1900-2005 from May of the year prior to ring formation (large caps) to September of the year of ring formation (small caps). The seasonalized summer variable (S) included the current June, July, August and September months. Bolded correlation coefficients are significant at $p < 0.05$

Table A2.9. Matrix of Pearson correlation coefficients between the PC2 scores and mean monthly minimum temperature (Tmin), mean monthly maximum temperature (Tmax), total monthly precipitation (Precip), mean monthly average Canadian Drought Code values (CDC), mean monthly dew point temperature (Dewpt), mean monthly relative humidity (RH), total monthly radiation (Totrad) and total monthly number of frost days (Frost).

Month	Tmin	Tmax	Precip	CDC	Dewpt	RH	Totrad	Frost
M	-0.072	-0.072	-0.131	0.106	0.024	-0.177	0.038	0.019
J	-0.031	-0.025	0.036	0.038	-0.027	0.005	-0.037	-0.063
J	-0.203	-0.128	0.121	-0.074	-0.120	-0.011	0.139	.
A	0.057	0.039	0.011	-0.024	-0.089	-0.034	0.060	-0.077
S	0.109	0.204	-0.199	0.054	0.102	-0.380	0.162	0.024
O	-0.088	-0.205	-0.148	0.117	-0.244	0.109	-0.170	0.057
N	-0.021	-0.009	-0.041	0.139	-0.232	-0.001	0.090	0.012
D	0.070	0.099	0.031	0.144	-0.040	0.131	-0.031	0.208
j	0.114	0.118	-0.037	.	0.119	0.087	-0.030	0.165
f	-0.095	-0.052	-0.005	.	-0.209	-0.122	0.079	0.052
m	-0.085	-0.108	-0.013	-0.149	0.056	0.127	0.009	0.274
a	-0.145	-0.165	0.057	-0.126	-0.277	0.113	-0.066	0.131
m	0.020	0.101	-0.098	-0.075	-0.177	-0.122	0.237	0.054
j	0.332	0.423	-0.208	0.218	0.077	-0.179	0.021	-0.244
j	-0.043	-0.023	-0.177	0.295	-0.316	-0.133	0.006	.
a	0.173	0.245	-0.124	0.255	0.074	-0.196	0.132	-0.004
s	0.041	0.057	-0.088	0.249	-0.011	-0.124	-0.015	0.038
S	0.180	0.285	-0.287	0.296	-0.039	-0.204	0.054	-0.026

Correlations with Dewpt and RH were conducted over the period 1953-2005. All other correlations were conducted over the period of 1900-2005 from May of the year prior to ring formation (large caps) to September of the year of ring formation (small caps). The seasonalized summer variable (S) included the current June, July, August and September months. Bolded correlation coefficients are significant at $p < 0.05$

Table A2.10. Matrix of Pearson correlation coefficients between the AB- $\delta^{13}\text{C}$ scores and mean monthly minimum temperature (Tmin), mean monthly maximum temperature (Tmax), total monthly precipitation (Precip), mean monthly average Canadian Drought Code values (CDC), total monthly radiation (Totrad) and total monthly number of frost days (Frost) from 1900-1959.

Month	Tmin	Tmax	Precip	CDC	Totrad	Frost
M	-0.309	-0.344	0.148	-0.015	-0.122	0.164
J	-0.206	-0.093	-0.047	-0.141	0.132	0.000
J	-0.302	-0.100	0.076	-0.045	0.161	.
A	-0.099	-0.022	0.183	-0.071	-0.053	-0.098
S	-0.029	0.063	0.046	-0.186	0.037	0.091
O	-0.100	-0.052	-0.250	-0.056	0.087	0.088
N	0.209	0.271	-0.249	0.061	0.005	-0.012
D	0.306	0.348	-0.126	0.093	-0.109	.
j	0.172	0.237	0.080	.	-0.180	.
f	-0.055	-0.001	0.006	.	-0.059	0.049
m	-0.395	-0.328	-0.180	0.005	0.245	0.327
a	-0.055	0.081	-0.180	0.128	-0.014	-0.049
m	0.194	0.325	0.083	0.030	0.054	-0.107
j	0.326	0.474	-0.110	0.186	-0.011	-0.310
j	0.069	0.162	-0.080	0.211	-0.007	.
a	0.172	0.216	-0.094	0.172	-0.067	0.099
s	0.009	0.172	-0.183	0.247	0.186	0.037
S	0.212	0.392	-0.213	0.233	0.018	-0.031

Note: correlations were not calculated for RH and Dewpt since climate data for these variables were only available from 1953 onwards. Correlations were conducted from May of the year prior to ring formation (large caps) to September of the year of ring formation (small caps). The seasonalized summer variable (S) included the current June, July, August and September months. Bolded correlation coefficients are significant at $p < 0.05$

Table A2.11. Matrix of Pearson correlation coefficients between the AB- $\delta^{13}\text{C}$ scores and mean monthly minimum temperature (Tmin), mean monthly maximum temperature (Tmax), total monthly precipitation (Precip), mean monthly average Canadian Drought Code values (CDC), total monthly radiation (Totrad) and total monthly number of frost days (Frost) from 1960-2005.

Month	Tmin	Tmax	Precip	CDC	Totrad	Frost
M	0.137	0.098	-0.186	0.183	0.099	-0.134
J	0.129	0.023	0.113	0.076	-0.108	-0.104
J	-0.175	-0.194	0.118	-0.121	0.127	.
A	0.044	-0.067	-0.020	-0.044	0.134	-0.079
S	0.171	0.289	-0.404	0.138	0.365	-0.010
O	-0.124	-0.361	-0.149	0.212	-0.324	0.055
N	-0.114	-0.153	0.092	0.195	0.081	0.081
D	-0.020	-0.021	0.133	0.206	-0.048	0.263
j	0.096	0.061	-0.157	.	0.023	0.226
f	-0.136	-0.115	-0.147	.	0.148	0.018
m	0.116	0.038	0.028	-0.277	-0.208	0.225
a	-0.242	-0.320	0.283	-0.369	-0.108	0.239
m	-0.033	0.093	-0.283	-0.062	0.434	0.134
j	0.224	0.256	-0.152	0.260	-0.040	-0.112
j	-0.175	-0.182	-0.186	0.310	0.047	.
a	0.149	0.212	-0.117	0.240	0.393	-0.153
s	0.093	0.027	-0.077	0.228	-0.120	0.042
S	0.116	0.153	-0.280	0.310	0.148	0.000

Note: correlations were not calculated for RH and Dewpt since climate data for these variables were only available from 1953 onwards thereby restricting any comparison with the 1900-1959 period. Correlations were conducted from May of the year prior to ring formation (large caps) to September of the year of ring formation (small caps). The seasonalized summer variable (S) included the current June, July, August and September months. Bolded correlation coefficients are significant at $p < 0.05$

Table A2.12. Matrix of Pearson correlation coefficients between the REG-RWL scores and mean monthly minimum temperature (Tmin), mean monthly maximum temperature (Tmax), total monthly precipitation (Precip), mean monthly average Canadian Drought Code values (CDC), total monthly radiation (Totrad) and total monthly number of frost days (Frost) from 1900-1959.

Month	Tmin	Tmax	Precip	CDC	Totrad	Frost
M	-0.030	-0.168	0.308	-0.077	-0.155	-0.004
J	0.031	-0.070	0.115	-0.325	-0.051	0.019
J	-0.102	-0.188	0.106	-0.165	-0.271	.
A	-0.174	-0.393	0.273	-0.302	-0.166	-0.058
S	0.130	-0.025	0.217	-0.430	-0.009	0.021
O	0.113	0.097	-0.037	-0.358	0.005	-0.130
N	0.281	0.292	-0.330	-0.218	-0.227	-0.017
D	0.348	0.299	-0.163	-0.106	-0.373	.
j	0.030	0.040	-0.011	.	-0.403	.
f	-0.021	-0.053	-0.224	.	-0.302	-0.133
m	-0.176	-0.199	-0.185	-0.006	-0.122	0.137
a	-0.015	0.088	0.089	-0.109	-0.120	-0.186
m	0.134	0.225	-0.046	-0.015	-0.107	-0.035
j	-0.165	-0.171	0.145	-0.083	-0.185	0.064
j	0.079	0.002	0.160	-0.102	-0.157	.
a	0.044	-0.178	0.169	-0.223	-0.269	0.108
s	0.141	0.117	-0.204	-0.110	0.058	-0.021
S	0.022	-0.078	0.113	-0.153	-0.239	0.005

Note: correlations were not calculated for RH and Dewpt since climate data for these variables were only available from 1953 onwards. Correlations were conducted from May of the year prior to ring formation (large caps) to September of the year of ring formation (small caps). The seasonalized summer variable (S) included the current June, July, August and September months. Bolded correlation coefficients are significant at $p < 0.05$

Table A2.13. Matrix of Pearson correlation coefficients between the REG-RWL scores and mean monthly minimum temperature (Tmin), mean monthly maximum temperature (Tmax), total monthly precipitation (Precip), mean monthly average Canadian Drought Code values (CDC), total monthly radiation (Totrad) and total monthly number of frost days (Frost) from 1960-2005.

Month	Tmin	Tmax	Precip	CDC	Totrad	Frost
M	-0.010	-0.164	0.339	-0.091	-0.325	0.061
J	-0.074	0.010	0.008	-0.158	0.146	-0.024
J	0.047	-0.060	-0.117	0.019	-0.274	.
A	-0.142	-0.119	0.123	-0.017	-0.200	-0.034
S	-0.350	-0.284	-0.052	-0.087	-0.225	0.110
O	-0.291	-0.065	-0.288	0.024	0.398	0.315
N	0.308	0.326	-0.169	0.140	-0.269	0.107
D	0.122	0.160	-0.095	0.177	-0.245	-0.142
j	0.206	0.279	-0.162	.	-0.254	0.000
f	0.316	0.254	-0.131	.	-0.449	-0.106
m	0.277	0.286	-0.420	0.097	-0.076	-0.298
a	0.383	0.337	0.064	0.224	-0.103	-0.215
m	0.296	0.326	-0.070	0.209	-0.175	-0.294
j	-0.038	-0.278	0.603	-0.221	-0.575	0.081
j	0.098	0.084	0.260	-0.444	-0.078	.
a	-0.043	-0.047	0.044	-0.437	0.051	-0.015
s	0.032	0.032	0.130	-0.319	0.021	-0.030
S	0.013	-0.104	0.525	-0.446	-0.358	-0.007

Note: correlations were not calculated for RH and Dewpt since climate data for these variables were only available from 1953 onwards thereby restricting any comparison with the 1900-1959 period. Correlations were conducted from May of the year prior to ring formation (large caps) to September of the year of ring formation (small caps). The seasonalized summer variable (S) included the current June, July, August and September months. Bolded correlation coefficients are significant at $p < 0.05$

Appendix 3

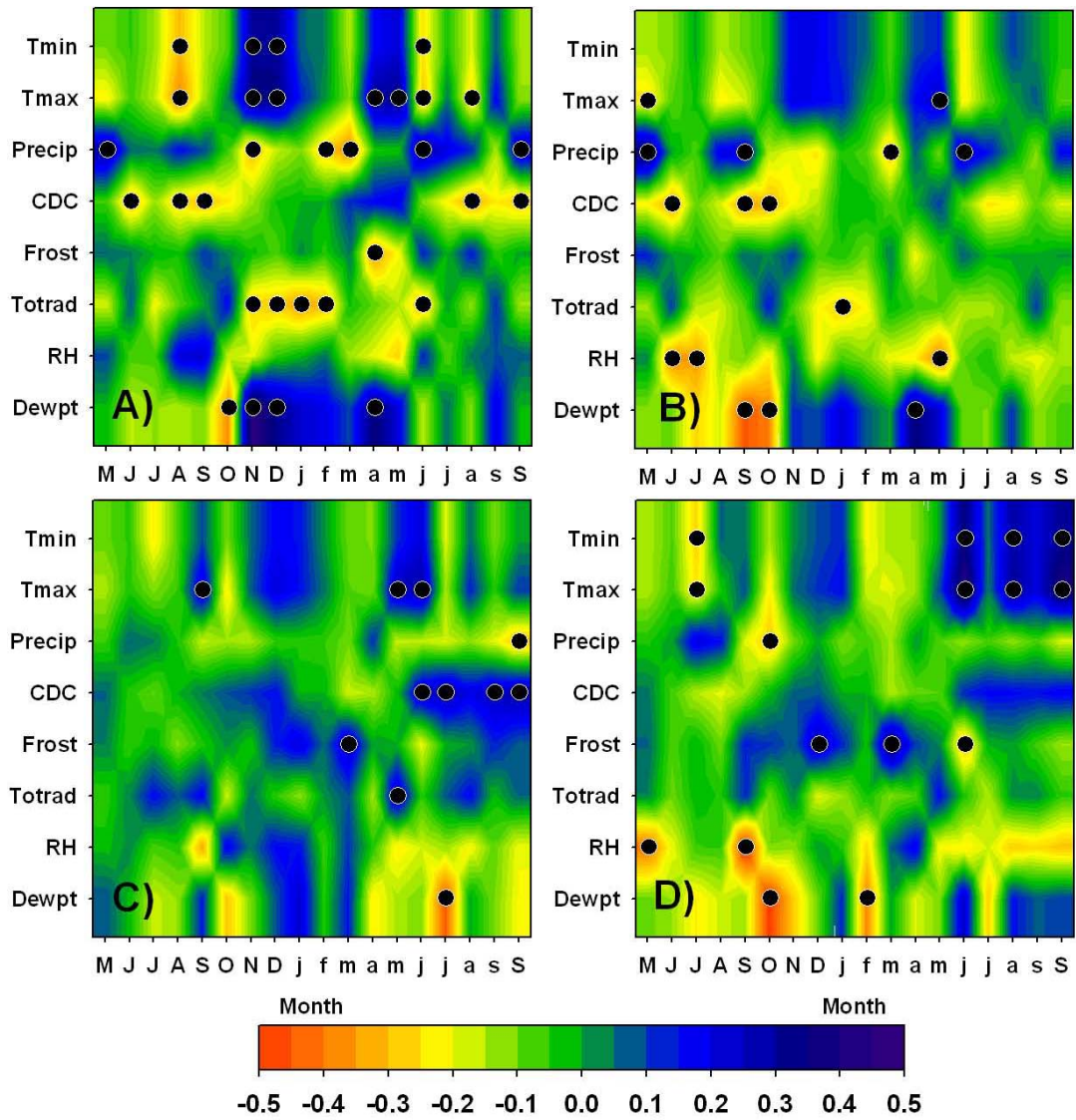


Figure A3.1.

Figure A3.1. Pearson correlation coefficients between A) A-RWL, B) B-RWL, C) A- $\delta^{13}\text{C}$ and D) B- $\delta^{13}\text{C}$ and monthly climate variables from May of the year prior to ring formation (large caps) to September of the year of ring formation (small caps). The seasonalized summer variable (S) included the current June, July, August and September months. From top to bottom, the climate variables included: mean monthly minimum temperature (Tmin), mean monthly maximum temperature (Tmax), total monthly precipitation (Precip), mean monthly average Canadian Drought Code values (CDC), total monthly frost days (Frost), total monthly radiation (Totrad), mean monthly relative humidity (RH) and mean monthly dew point temperature (Dewpt). All correlation coefficients that were significant at $p < 0.05$ are indicated by black dots. The period of analysis was 1953-2005 for RH and Dewpt and 1900-2005 for all other climate variables.

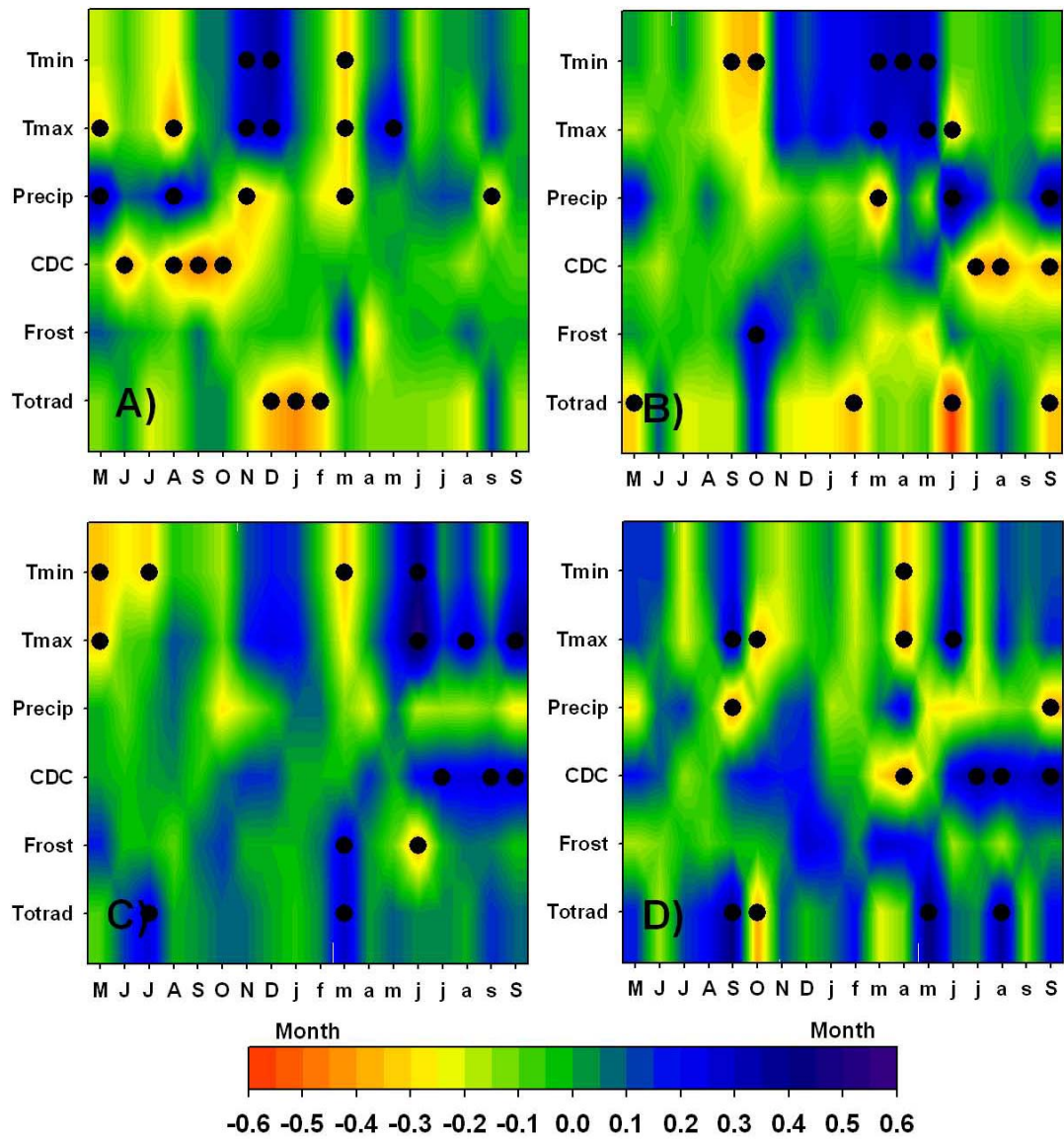


Figure A3.2.

Figure A3.2. Pearson correlation coefficients between PC1 (*top panel*) A) during 1900-1959 and B) during 1960-2005 and PC2 (*bottom panel*) C) during 1900-1959 and D) during 1960-2005 and monthly climate variables from May of the year prior to ring formation (large caps) to September of the year of ring formation (small caps). The seasonalized summer variable (S) included the current June, July, August and September months. From top to bottom, the climate variables included: mean monthly minimum temperature (Tmin), mean monthly maximum temperature (Tmax), total monthly precipitation (Precip), mean monthly average Canadian Drought Code values (CDC), total monthly frost days (Frost) and total monthly radiation (Totrad). All correlation coefficients that were significant at $p < 0.05$ are indicated by black dots.